

SURFACE FUNCTIONALIZATION OF SBA - 15 PARTICLES FOR  
AMOXICILLIN DELIVERY

A THESIS SUBMITTED TO  
THE GRADUATE SCHOOL OF NATURAL AND APPLIED SCIENCES  
OF  
MIDDLE EAST TECHNICAL UNIVERSITY

BY

FİLİZ F. SEVİMLİ

IN PARTIAL FULFILLMENT OF THE REQUIREMENTS  
FOR  
THE DEGREE OF MASTER OF SCIENCE  
IN  
CHEMISTRY

SEPTEMBER 2011

Approval of the thesis:

**SURFACE FUNCTIONALIZATION OF SBA - 15 PARTICLES FOR  
AMOXICILLIN DELIVERY**

submitted by **FİLİZ F. SEVİMLİ** in partial fulfillment of the requirements for the degree of **Master of Science in Chemistry Department, Middle East Technical University** by,

Prof. Dr. Canan Özgen  
Dean, Graduate School of **Natural and Applied Sciences**

\_\_\_\_\_

Prof. Dr. İlker Özkan  
Head of Department, **Chemistry**

\_\_\_\_\_

Assoc. Prof. Dr. Ayşen Yılmaz  
Supervisor, **Chemistry Department, METU**

\_\_\_\_\_

**Examining Committee Members:**

Prof. Dr. Ceyhan Kayran  
Chemistry Dept., METU

\_\_\_\_\_

Assoc. Prof. Dr. Ayşen Yılmaz  
Chemistry Dept., METU

\_\_\_\_\_

Assist. Prof. Dr. Emren Nalbant Esentürk  
Chemistry Dept., METU

\_\_\_\_\_

Assist. Prof. Dr. İrem Erel  
Chemistry Dept., METU

\_\_\_\_\_

Prof. Dr. Leyla Yıldırım  
Physical Engineering Dept., Hacettepe University

\_\_\_\_\_

**Date:** \_\_\_\_\_

**I hereby declare that all information in this document has been obtained and presented in accordance with academic rules and ethical conduct. I also declare that, as required by these rules and conduct, I have fully cited and referenced all material and results that are not original to this work.**

Name, Last name:

Signature:

## **ABSTRACT**

### **SURFACE FUNCTIONALIZATION OF SBA - 15 PARTICLES FOR AMOXICILLIN DELIVERY**

Sevimli, Filiz F.

M.Sc., Department of Chemistry

Supervisor: Assoc. Prof. Dr. Ayşen Yılmaz

September 2011, 93 pages

There are several studies in order to control drug delivery, decrease the toxicity of drugs and also for novel biomedical applications. It is necessary to be able to control the release of the drug within the body by using drug delivery systems. Mesoporous silica compounds have only been discovered twenty years ago and they have already attracted many researchers to study these materials for several applications. SBA-15 particles have a highly ordered regular structure and are a good matrix for guest-host applications. The aim of this study is to be able to address whether the surface functionalization of SBA - 15 samples would improve the loading of a drug into these particles. The synthesized SBA-15 particles were surface functionalized by post- grafting synthesis method in order to be used as carrier materials for drug delivery. Amoxicillin was used as a model drug. These mesoporous materials have been characterized using X-ray diffraction (XRD), small-angle X-ray spectroscopy (SAXS),

fourier-transform infrared spectroscopy (FTIR), transmission electron microscopy (TEM), N<sub>2</sub> adsorption/ desorption, solid-state silicon nuclear magnetic resonance (Si-NMR), high-performance liquid chromatography (HPLC), ultra-violet (UV) spectroscopy, elemental and thermo gravimetric analysis (TGA). The effect of concentration difference and the type of alkoxysilanes used for the functionalization have been discussed in terms of loading amoxicillin and controlling the delivery. Drug delivery systems have many further applications that still need to be investigated in areas such as neurosciences, cancer and biomedical engineering.

**Key words:** Mesoporous SBA - 15 materials, controlled drug delivery, surface functionalization, alkoxysilane and amoxicillin.

## ÖZ

### AMOKSİSİLİNİN SBA - 15 PARÇACIKLARINA TUTUKLANMASI İÇİN YÜZEY AKTİFLEME ÇALIŞMALARI

Sevimli, Filiz F.

Yüksek Lisans, Kimya Bölümü

Tez Yöneticisi: Doç. Dr. Ayşen Yılmaz

Eylül 2011, 93 sayfa

İlaç tutuklanmasını kontrol edebilmek, ilaçların toksitelerini azaltmak ve yeni biyomedikal uygulamalar için birçok araştırma yapılmaktadır. Bu nedenle de ilaç iletim sistemlerini kullanarak ilaçların vücut içerisindeki salınımını kontrol etmek gerekmektedir. Mezogözenekli silika bileşikler yalnızca yirmi yıl önce keşfedilmiş olup farklı alanlarda kullanımı için şimdiden birçok araştırmacının ilgisini çekmiştir. SBA-15 parçacıklarının oldukça düzgün bir şekli, büyük gözenek boyutları ve düzgün matrisi vardır. Buradaki asıl amacımız yüzey aktiflenmesi sonrası bu malzemelere ilaç yüklenmesinin artırıcı bir etkisi olup olmadığı sorusuna cevap bulabilmektir. İlaç tutuklanmasında taşıyıcı materyaller olarak kullanabilmek için sentezlenen SBA-15 parçacıklarının yüzeyleri sentez sonrası metodu ile aktiflenmiştir. Model ilaç olarak amoksisilin kullanılmıştır. Mezogözenekli bu materyallerin karakterizasyonu X-ışınları difraksiyonu (XRD), küçük - açı X-ışınları saçılması (SAXS),

fourier-transform kızılötesi (FTIR), geçirmeli elektron mikroskopisi (TEM), N<sub>2</sub>-adsorpsiyon/desorpsiyon, katı - hal silikon nükleer manyetik rezonans (Si-NMR), yüksek performans sıvı kromatografisi (HPLC), ultra-viyole (UV) spektroskopisi, elementel ve thermo gravimetrik analiz (TGA) yapılmıştır. Yüzey aktiflenmesinde kullanılan alkoksisilan türlerinin ve konsantrasyon değişiminin etkisi ilaç yüklenmesi ve salınımı açısından araştırılmıştır. İlaç tutuklanma sistemlerinin nörobilimler, kanser ve biyomedikal mühendisliği gibi birçok alanda uygulanabilmesi için daha fazla araştırmanın yapılması gerekmektedir.

**Anahtar kelimeler:** Mezogözenekli SBA - 15 malzemeler, kontrollü ilaç salınımı, yüzey aktiflenmesi, alkoksisilan ve amoksisilin.

*Dedicated to my dear parents for their love and support*

## ACKNOWLEDGMENTS

The author would like to express her gratitude to her supervisor Assoc. Prof. Dr. Ayşen Yılmaz for her guidance, suggestions and support throughout her graduate studies.

The author would also like to thank Assist. Prof. Dr. Önder Metin, Dr. Merve İçli Özkut, Dr. Yusuf Nur, Dr. Olcay Mert and Merve Şendur for their suggestions and assistance in certain analyses.

In addition, the assistance of the workers at the Central Laboratory has also been gratefully acknowledged.

Also, the author would like to express her gratitude to Prof. Dr. Leyla Yıldırım and Prof. Dr. Semra İde.

Especially, the author would like thank her family for their love and support throughout both her undergraduate and graduate studies.

This study was funded by METU with the Grant No: BAP - 07 - 02 - 2011 - 101.

## TABLE OF CONTENTS

<b>ABSTRACT</b> .....	iv
<b>ÖZ</b> .....	vi
<b>ACKNOWLEDGMENTS</b> .....	ix
<b>TABLE OF CONTENTS</b> .....	x
<b>LIST OF ABBREVIATIONS</b> .....	xiv
<b>LIST OF FIGURES</b> .....	xvii
<b>LIST OF TABLES</b> .....	xxii
<b>CHAPTERS</b> .....	1
<b>1. INTRODUCTION TO MESOPOROUS MATERIALS</b> .....	1
<b>1. 1. HISTORY</b> .....	1
<b>1. 2. TYPES</b> .....	2
<b>1. 2. 1. M41S</b> .....	2
<b>1. 2. 1. 1. MCM - 41</b> .....	3
<b>1. 2. 1. 2. MCM - 48</b> .....	4
<b>1. 2. 2. SBA</b> .....	4
<b>1. 2. 2. 1. SBA - 15</b> .....	5
<b>1. 2. 3. APPLICATIONS</b> .....	5
<b>1. 3. SYNTHESIS</b> .....	6

<b>1. 4. SURFACE FUNCTIONALIZATION</b> .....	6
<b>1. 4. 1. ONE - POT (CO - CONDENSATION)</b> .....	6
<b>1. 4. 2. POST - GRAFTING (SILYLATION)</b> .....	7
<b>1. 4. 3. ADVANTAGES &amp; DISADVANTAGES</b> .....	7
<b>2. CONTROLLED DRUG DELIVERY</b> .....	9
<b>2. 1. DRUG ABSORPTION</b> .....	10
<b>2. 2. DRUG DELIVERY SYSTEMS</b> .....	11
<b>2. 2. 1. POLYMERIC DRUG DELIVERY SYSTEMS</b> .....	12
<b>2. 2. 2. INORGANIC / ORGANIC HYBRID DRUG DELIVERY SYSTEMS</b> .....	13
<b>2. 2. 3. ADVANTAGES &amp; DISADVANTAGES</b> .....	13
<b>2. 3. ANTIBIOTICS</b> .....	14
<b>2. 3. 1. PENICILLINS</b> .....	15
<b>2. 4. AMOXICILLIN</b> .....	16
<b>2. 4. 1. STRUCTURE</b> .....	16
<b>2. 4. 2. EFFECT &amp; MECHANISM</b> .....	17
<b>2. 4. 3. DISEASES</b> .....	17
<b>3. EXPERIMENTAL</b> .....	18
<b>3. 1. SYNTHESIS OF SBA - 15 PARTICLES</b> .....	18
<b>3. 2. SURFACE FUNCTIONALIZATION</b> .....	20
<b>3. 3. AMOXICILLIN LOADING</b> .....	23

<b>3. 4. AMOXICILLIN RELEASE</b> .....	23
<b>4. CHARACTERIZATION</b> .....	25
<b>4. 1. X - RAY DIFFRACTION (XRD)</b> .....	25
<b>4. 2. SMALL - ANGLE X - RAY SCATTERING (SAXS)</b> .....	25
<b>4. 3. ELEMENTAL ANALYSIS</b> .....	26
<b>4. 4 .THERMOGRAVIMETRIC ANALYSIS (TGA)</b> .....	26
<b>4. 5. FOURIER - TRANSFORM INRFA - RED (FTIR)</b> .....	26
<b>4. 6. NITROGEN - SORPTION</b> .....	26
<b>4. 7. TRANSMISSION ELECTROM MICROSCOPY (TEM)</b> .....	26
<b>4. 8. SOLID - STATE <sup>29</sup>Si - MAS - NMR</b> .....	27
<b>4. 9. UV - VIS SPECTROSCOPY</b> .....	27
<b>4. 10. HIGH PERFORMANCE LIQUID CHROMATOGRAPHY</b> .....	27
<b>5. RESULTS AND DISCUSSION</b> .....	28
<b>5. 1. POWDER PATTERNS OF SBA – 15 SAMPLES</b> .....	28
<b>5. 2. SMALL - ANGLE X - RAY SCATTERING (SAXS)</b> .....	32
<b>5. 2. 1. UNIT CELL PARAMETERS AND d - SPACING VALUES</b> .....	32
<b>5. 2. 2. COMPARISON OF FUNCTIONALIZED SAMPLES</b> .....	35
<b>5. 3. ELEMENTAL ANALYSIS</b> .....	38
<b>5. 4. THERMOGRAVIMETRIC ANALYSIS (TGA)</b> .....	40
<b>5. 4. 1. CALCULATIONS</b> .....	40

<b>5. 5. FTIR SPECTRA</b> .....	42
<b>5. 5. 1. PURE AND FUNCTIONALIZED SBA - 15 SAMPLES</b> .....	42
<b>5. 5. 2. AMOXICILLIN LOADED SBA - 15 SAMPLES</b> .....	44
<b>5. 6. N<sub>2</sub> - ADSORPTION - DESORPTION ANALYSIS</b> .....	47
<b>5. 6. 1. SURFACE CHARACTERIZATION (BET ISOTHERMS)</b> .....	47
<b>5. 6. 2. PORE SIZE DISTRIBUTION (BJH METHOD)</b> .....	54
<b>5. 7. TEM MICROGRAPHS</b> .....	57
<b>5. 8. SOLID - STATE <sup>29</sup> Si - MAS - NMR SPECTRA</b> .....	62
<b>5. 9. UV ANALYSIS</b> .....	65
<b>5. 9. 1. AMOXICILLIN LOADING</b> .....	65
<b>5. 9. 2. AMOXICILLIN RELEASE</b> .....	68
<b>5. 10. HPLC ANALYSIS</b> .....	70
<b>6. CONCLUSION</b> .....	72
<b>REFERENCES</b> .....	76
<b>APPENDIX</b> .....	85
<b>A. CHROMATOGRAMS (HPLC ANALYSIS)</b> .....	85

## LIST OF ABBREVIATIONS

<b>A:</b> Absorbance	<b>IV:</b> intravenous
<b>b:</b> path length	<b>FTIR:</b> Fourier-transform infra-red
<b>c:</b> concentration	<b>GI:</b> Gastrointestinal tract
<b><math>\epsilon</math>:</b> molar absorptivity coefficient	<b>HCl:</b> hydrochloric acid
<b>Å:</b> Angstrom	<b>HPLC:</b> High - performance liquid chromatography
<b>d:</b> the distance between adjacent crystal planes	<b>KBr:</b> potassium bromide
<b>q:</b> scattering vector	<b>MAS:</b> Magic - angle spinning
<b><math>\lambda</math>:</b> wavelength of X - rays	<b>MCM:</b> Mobil Composite Materials
<b>APTES:</b> (3 - aminopropyl) triethoxy silane	<b>MPTMS:</b> mercaptopropyl trimethoxy silane
<b>BET:</b> Brunauer - Emmett - Teller	<b>M41S:</b> mesoporous silica family
<b>BJH:</b> Barrett - Joyner - Halenda	<b>N<sub>2</sub>:</b> nitrogen
<b>CHCl<sub>3</sub>:</b> chloroform	<b>NH<sub>3</sub>:</b> ammonia
<b>CO<sub>2</sub>:</b> carbon dioxide	<b>NIR:</b> Near infra - red
<b>CP:</b> Cross - polarization	<b>NMR:</b> Nuclear magnetic resonance
<b>d - H<sub>2</sub>O:</b> distilled water	<b>NO<sub>x</sub>:</b> nitrogen oxide
<b>DDS:</b> drug delivery system	<b>PBS:</b> Phosphate buffer saline
<b>EtOH:</b> ethanol	
<b>IM:</b> intramuscular	

**PEG:** polyethylene glycol

**PEO:** polyethylene oxide

**Pluronic - 123:** nonionic triblock  
copolymer (EO)<sub>20</sub>(PO)<sub>70</sub>(EO)<sub>20</sub>

**PPO:** polypropylene oxide

**SAXS:** Small - angle X- ray Scattering

**SBA:** Santa Barbara Amorphous

**SiO<sub>2</sub>:** silicon oxide (silica)

**SO<sub>y</sub>:** sulfur oxide

**TEOS:** tetraethyl orthosilicate

**TEM:** Transmission electron microscopy

**TEMS:** triethoxymethyl silane

**TGA:** Thermogravimetric analysis

**UV:** Ultra - violet

**VIS:** Visible

**XRD:** X-ray Diffraction

**SBA - 15 samples:**

**SBA - 15 - 1A:** amine functionalized  
sample by using 1 ml of APTES (**1A**)

**SBA - 15 - 2A:** amine functionalized  
sample by using 2 ml of APTES (**2A**)

**SBA - 15 - 4A:** amine functionalized  
sample by using 4 ml of APTES (**4A**)

**SBA - 15 - 1M:** thiol functionalized  
sample by using 1 ml of MPTMS (**1M**)

**SBA - 15 - 2M:** thiol functionalized  
sample by using 2 ml of MPTMS (**2M**)

**SBA - 15 - 4M:** thiol functionalized  
sample by using 4 ml of MPTMS (**4M**)

**1A - x:** amoxicillin loaded SBA - 15 - 1A  
(**1Ax**)

**2A - x:** amoxicillin loaded SBA - 15 - 2A  
(**2Ax**)

**4A - x:** amoxicillin loaded SBA - 15 - 4A  
(**4Ax**)

**1M - x:** amoxicillin loaded SBA - 15 - 1M  
(**1Mx**)

**2M - x:** amoxicillin loaded SBA - 15 - 2M  
(**2Mx**)

**4M - x:** amoxicillin loaded SBA - 15 - 4M  
(**4Mx**)

**SBA - 15 - 1T:** methyl functionalized sample by using 1 ml of TEMS (**1T**)

**SBA - 15 - 2T:** methyl functionalized sample by using 2 ml of TEMS (**2T**)

**SBA - 15 - 4T:** methyl functionalized sample by using 4 ml of TEMS (**4T**)

**1T - x:** amoxicillin loaded SBA - 15 - 1T (**1Tx**)

**2T - x:** amoxicillin loaded SBA - 15 - 2T (**2Tx**)

**4T - x:** amoxicillin loaded SBA - 15 - 4T (**4Tx**)

## LIST OF FIGURES

### FIGURES

<b>Figure 1:</b> The statistical analysis on recent publications of silica - based ordered mesoporous materials as drug delivery systems.....	2
<b>Figure 2:</b> The main differences in terms of pore size, synthesis and structure of MCM and SBA type of mesoporous materials.....	3
<b>Figure 3:</b> The synthesis procedure of MCM type of mesoporous materials.....	4
<b>Figure 4:</b> The synthesis scheme of SBA - 15 mesoporous materials.....	5
<b>Figure 5:</b> The release profile of conventional drug forms and controlled drug delivery systems.....	9
<b>Figure 6:</b> The drug plasma concentration vs. time in conventional therapies compared to the release profile of controlled drug delivery systems.....	11
<b>Figure 7:</b> The three - dimensional structure of amoxicillin.....	16
<b>Figure 8:</b> Synthesis scheme of SBA - 15 particles.....	19
<b>Figure 9:</b> Surface functionalization of SBA - 15 materials using organotriethoxysilanes by post - grafting synthesis method.....	21
<b>Figure 10:</b> The structures of the samples after the surface functionalization by post - grafting synthesis using APTES (a), MPTMS (b) and TEMS.....	22
<b>Figure 11:</b> Powder patterns of amine functionalized SBA - 15 samples.....	29

<b>Figure 12:</b> Powder patterns of thiol functionalized SBA - 15 samples .....	29
<b>Figure 13:</b> Powder patterns of methyl functionalized SBA -15 samples.....	30
<b>Figure 14:</b> Powder pattern of amoxicillin loaded amine functionalized samples .....	30
<b>Figure 15:</b> Powder pattern of amoxicillin loaded thiol functionalized samples.....	31
<b>Figure 16:</b> Powder pattern of amoxicillin loaded methyl functionalized samples.....	31
<b>Figure 17:</b> SAXS pattern of pure and amine functionalized SBA - 15 samples .....	35
<b>Figure 18:</b> SAXS pattern of pure and thiol functionalized SBA - 15 samples.....	36
<b>Figure 19:</b> SAXS pattern of pure and methyl functionalized SBA - 15 samples.....	37
<b>Figure 20:</b> % Weight loss of SBA – 15 samples after functionalization.....	40
<b>Figure 21:</b> FTIR spectra of pure silica and amine functionalized samples.....	42
<b>Figure 22:</b> FTIR spectra of pure silica and thiol functionalized samples .....	43
<b>Figure 23:</b> FTIR spectra of pure silica and methyl functionalized samples.....	43
<b>Figure 24:</b> FTIR spectra of amoxicillin loaded and 1 ml functionalized SBA - 15 samples.....	44
<b>Figure 25:</b> FTIR spectra of amoxicillin loaded amine functionalized SBA - 15 samples.....	45
<b>Figure 26:</b> FTIR spectra of amoxicillin loaded thiol functionalized SBA - 15 samples.....	45
<b>Figure 27:</b> FTIR spectra of amoxicillin loaded methyl functionalized SBA - 15 samples.....	46
<b>Figure 28:</b> BET isotherms of pure and amine functionalized SBA - 15 samples.....	47
<b>Figure 29:</b> BET isotherms of pure and thiol functionalized SBA - 15 samples.....	48

<b>Figure 30:</b> BET isotherms of pure and methyl functionalized SBA - 15 samples .....	49
<b>Figure 31:</b> BET isotherms of amoxicillin loaded pure and amine functionalized SBA - 15 samples .....	49
<b>Figure 32:</b> BET isotherms of amoxicillin loaded pure and thiol functionalized SBA - 15 samples.....	50
<b>Figure 33:</b> BET isotherms of amoxicillin loaded pure and methyl functionalized SBA - 15 samples.....	50
<b>Figure 34:</b> Pore size distribution of pure and amine functionalized SBA - 15 samples.....	54
<b>Figure 35:</b> Pore size distribution of pure and thiol functionalized SBA - 15 samples.....	54
<b>Figure 36:</b> Pore size distribution of pure and methyl functionalized SBA - 15 samples.....	55
<b>Figure 37:</b> Pore size distribution of amoxicillin loaded pure and amine functionalized SBA - 15 samples.....	55
<b>Figure 38:</b> Pore size distribution of amoxicillin loaded pure and thiol functionalized SBA - 15 samples.....	56
<b>Figure 39:</b> Pore size distribution of amoxicillin loaded pure and methyl functionalized SBA - 15 samples.....	56
<b>Figure 40:</b> TEM micrographs of pure SBA - 15 sample.....	57
<b>Figure 41:</b> TEM images of SBA - 15 - 1A.....	57

<b>Figure 42:</b> TEM images of SBA - 15 - 2A.....	58
<b>Figure 43:</b> TEM micrographs of SBA - 15 - 4A.....	58
<b>Figure 44:</b> TEM micrographs of SBA - 15 - 1M.....	59
<b>Figure 45:</b> TEM micrographs of SBA – 15 - 2M.....	59
<b>Figure 46:</b> TEM micrographs of SBA - 15 - 4M.....	60
<b>Figure 47:</b> TEM micrographs of SBA - 15 - 1T.....	60
<b>Figure 48:</b> TEM micrographs of SBA -15 - 2T.....	61
<b>Figure 49:</b> TEM micrographs of SBA - 15 - 4T.....	61
<b>Figure 50:</b> <sup>29</sup> Si - MAS - NMR spectra of the pure and 1 ml functionalized samples.....	62
<b>Figure 51:</b> Profile of amoxicillin loaded amine functionalized samples.....	66
<b>Figure 52:</b> Profile of amoxicillin loaded thiol functionalized samples.....	67
<b>Figure 53:</b> Profile of amoxicillin loaded methyl functionalized samples.....	67
<b>Figure 54:</b> Amoxicillin release profile of pure and amine functionalized samples.....	68
<b>Figure 55:</b> Amoxicillin release profile of pure and thiol functionalized samples.....	69
<b>Figure 56:</b> Amoxicillin release profile of pure and methyl functionalized samples.....	69
<b>Figure 57:</b> Amoxicillin release (in mg) from samples pure SBA - 15, 1A, 1M and 1T.....	70
<b>Figure 58:</b> Amoxicillin release of pure SBA - 15 after 5 minutes.....	85
<b>Figure 59:</b> Amoxicillin release of pure SBA - 15 after 15 minutes.....	85
<b>Figure 60:</b> Amoxicillin release of pure SBA - 15 after 30 minutes.....	86
<b>Figure 61:</b> Amoxicillin release of pure SBA - 15 after 60 minutes.....	86

<b>Figure 62:</b> Amoxicillin release of pure SBA - 15 after 120 minutes.....	86
<b>Figure 63:</b> Amoxicillin release of pure SBA - 15 after 180 minutes.....	87
<b>Figure 64:</b> Amoxicillin release of SBA - 15 - 1A after 5 minutes.....	87
<b>Figure 65:</b> Amoxicillin release of SBA - 15 - 1A after 15 minutes.....	87
<b>Figure 66:</b> Amoxicillin release of SBA - 15 - 1A after 30 minutes.....	88
<b>Figure 67:</b> Amoxicillin release of SBA - 15 - 1A after 60 minutes.....	88
<b>Figure 68:</b> Amoxicillin release of SBA - 15 - 1A after 120 minutes.....	88
<b>Figure 69:</b> Amoxicillin release of SBA - 15 - 1A after 180 minutes.....	89
<b>Figure 70:</b> Amoxicillin release of SBA - 15 - 1M after 5 minutes.....	89
<b>Figure 71:</b> Amoxicillin release of SBA - 15 - 1M after 15 minutes.....	89
<b>Figure 72:</b> Amoxicillin release of SBA - 15 - 1M after 30 minutes.....	90
<b>Figure 73:</b> Amoxicillin release of SBA - 15 - 1M after 60 minutes.....	90
<b>Figure 74:</b> Amoxicillin release of SBA - 15 - 1M after 120 minutes.....	90
<b>Figure 75:</b> Amoxicillin release of SBA - 15 - 1M after 180 minutes.....	91
<b>Figure 76:</b> Amoxicillin release of SBA - 15 - 1T after 5 minutes.....	91
<b>Figure 77:</b> Amoxicillin release of SBA - 15 - 1T after 15 minutes.....	91
<b>Figure 78:</b> Amoxicillin release of SBA - 15 - 1T after 30 minutes.....	92
<b>Figure 79:</b> Amoxicillin release of SBA - 15 - 1T after 60 minutes.....	92
<b>Figure 80:</b> Amoxicillin release of SBA - 15 - 1T after 120 minutes.....	92
<b>Figure 81:</b> Amoxicillin release of SBA - 15 - 1T after 180 minutes.....	93

## LIST OF TABLES

### TABLES

<b>Table 1:</b> Precursors used for the synthesis of SBA - 15 particles.....	19
<b>Table 2:</b> The amount of the chemicals used for the functionalization of SBA - 15 samples.....	20
<b>Table 3:</b> The amount of chemicals used for the amoxicillin loading of SBA - 15 samples.....	23
<b>Table 4:</b> Amount of the chemicals used for the preparation of PBS.....	24
<b>Table 5:</b> Amount of the chemicals used for the preparation of the mobile phase.....	24
<b>Table 6:</b> d - spacing, unit cell parameter and q values of pure and functionalized SBA - 15 samples.....	33
<b>Table 7:</b> d - spacing values of functionalized and amoxicillin loaded SBA - 15 samples.....	34
<b>Table 8:</b> Elemental composition of functionalized SBA - 15 samples in terms of % C, % H, %N and % S.....	38
<b>Table 9:</b> Elemental composition of 1 ml alkoxysilane functionalized SBA - 15 samples loaded with amoxicillin.....	39
<b>Table 10:</b> The pore size data of the pure and functionalized samples before and after amoxicillin loading.....	51

<b>Table 11:</b> The pore volume data of the pure and functionalized samples before and after amoxicillin loading.....	52
<b>Table 12:</b> The surface area data of the pure and functionalized samples before and after amoxicillin loading.....	53
<b>Table 13:</b> Amount of amoxicillin used to prepare standard solutions.....	65
<b>Table 14:</b> % Weight of amoxicillin loaded to SBA - 15 samples.....	65
<b>Table 15:</b> The change in peak area of the chromatograms within 3 hours of amoxicillin release.....	71
<b>Table 16:</b> The change in peak height of the chromatograms within 3 hours of amoxicillin release.....	71

## CHAPTER 1

### INTRODUCTION TO MESOPOROUS MATERIALS

The pore sizes of materials are important in differentiating the type of porous materials. The materials with pore sizes smaller than 2 nm are defined as microporous materials, while the ones with pore sizes larger than 50 nm are defined as macroporous materials. The main interest in this study is the type called as mesoporous materials which possess pores in the size range of 2 and 50 nm [1].

#### 1. 1. HISTORY

The most commonly known porous materials are microporous zeolites with uniform pore sizes and good stability. It is possible to incorporate heteroelements within the structure of these materials. Therefore, they are widely applied in many areas such as catalysis, sorption and membrane separation. However, their application is limited due to their small pore size and so it was necessary to find a new kind of material with larger pores. In the early 1990s, a new type of material, M41S family of ordered mesoporous silicas have been first reported. Since then, many researchers have been interested in the synthesis and possible applications of these new type of advanced mesoporous materials. Especially, after year 2003, the number of reports published about mesoporous materials has increased (Figure - 1) [2, 3].

The synthesis of ordered mesoporous materials by surfactant - templated sol-gel process was reported in 1992 by the Mobil researchers. These materials have attracted many researchers because of their unique properties; highly ordered structure, uniform pore size and high thermal stability. Furthermore, mesoporous materials are potential candidates that could be used in many areas such as catalysis, sensors, separation and sorption. However, these type of materials were not proposed as drug delivery systems until 2001. An intensive research is still ongoing in order to improve their application in controlled drug delivery [4 - 7].

One of the most important questions is that whether the inner core of the pores of the mesoporous silica are filled with the drug or it is anchored to the outer surface.

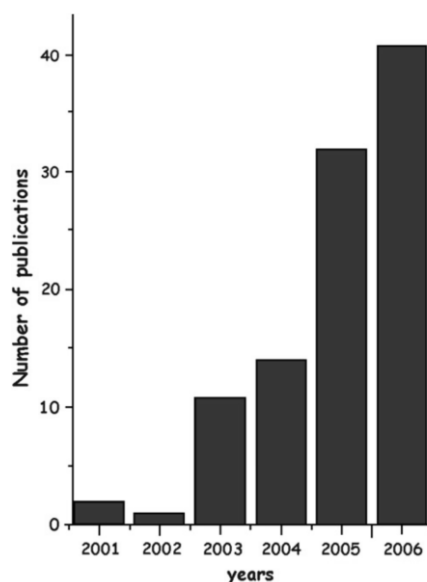


**Figure - 1: The statistical analysis on recent publications of silica - based ordered mesoporous materials as drug delivery systems (the results from Web of Science) [3].**

## **1. 2. TYPES**

### **1. 2. 1. M41S**

M41S - type of silica materials are the first reported mesoporous materials which were discovered by Kresge and coworkers. Self-assembling surfactants were used as structure - directing agents to form silica materials. M41S is the name of the family of several types of MCM (Mobil Composition of Matter) materials. The number after the acronym MCM is used in order to distinguish the different types. Three of them are mostly important: cubic MCM - 48, hexagonal MCM - 41 and lamellar MCM - 50. The pore walls of these materials contain amorphous silica; however, their pores are uniformly distributed in a highly ordered structure. In order to prepare these type of materials either quaternary ammonium salts or gemini salts are used. The main factors affecting the synthesis of these type of materials are the temperature, the hydrogel composition, the type and length of the surfactant, the alkalinity and time [2].

In order to easily distinguish the type of mesoporous materials the main properties such as pore size, structure, synthesis conditions and type of surfactants have been given below in Figure - 2.

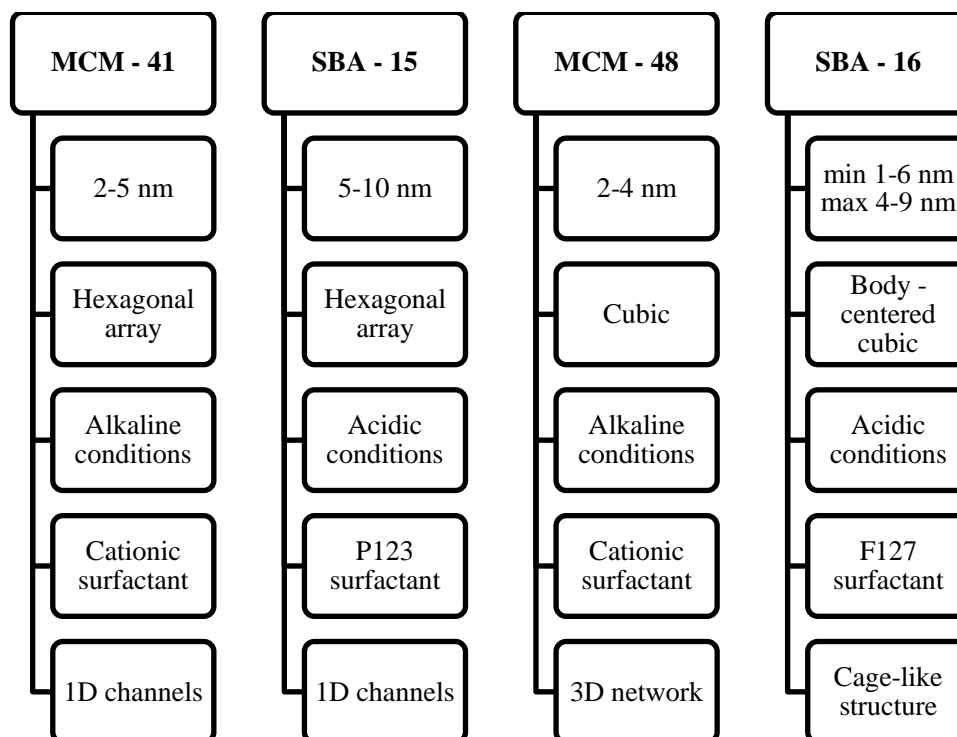


**Figure - 2: The main differences in terms of pore size, synthesis and structure of MCM and SBA type of mesoporous materials [2, 8, 9].**

### 1. 2. 1. 1. MCM - 41

The mostly studied type of mesoporous silica is MCM - 41. In consequence of its simple synthesis, it is applied in areas such as catalysis and sorption. The pore - blocking effect of MCM - 41 type of materials is negligible. MCM - 41 possesses a hexagonal, amorphous and uniformly distributed array of channels. Therefore, it shows reflections only at low  $2\theta$  degree angles. The thickness of the pore walls is effective on the hydrothermal and chemical stability. Due to their thin pore walls (1 - 1.5 nm) poor stability is observed and so there have been investigations in order to improve these properties [2].

### 1. 2. 1. 2. MCM - 48

In order to synthesize MCM - 48 type of materials the surfactant to silica ratio must be higher than 1. MCM - 48 shows similar pore size and surface properties like MCM - 41. In comparison to MCM - 41, it is less studied due to its synthesis route and poor stability. Its chemical and hydrothermal stability are both low in comparison to MCM - 41. As a result of its amorphous nature only a broad band is observed at low  $2\theta$  angles as well. The most important characteristic of these materials is their cubic and three - dimensional structure. In addition, these materials are advantageous in areas such as catalysis and separation technology compared to the one - dimensional MCM - 41 type of silica [2]. The synthesis scheme of MCM - 41 and MCM - 48 type of mesoporous materials has been illustrated in Figure - 3.

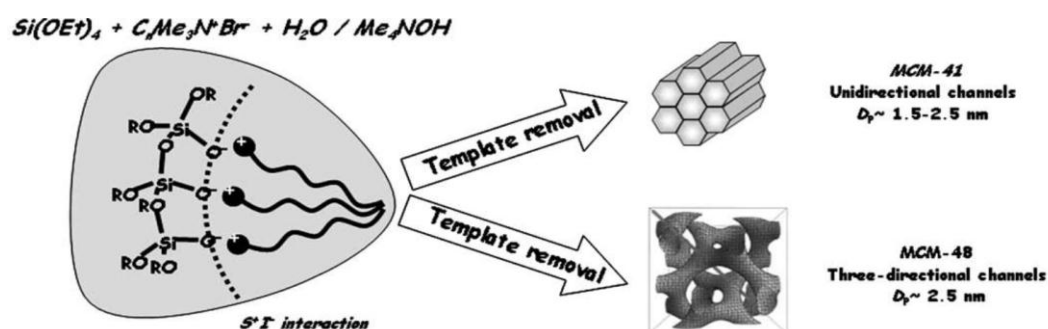


Figure - 3: The synthesis procedure of MCM type of mesoporous materials [10].

### 1. 2. 2. SBA

In order to prepare silica with larger pore sizes different structure directing agents have been investigated. Thus, non - ionic triblock copolymers have been used instead of cationic surfactants. As a result, by using these surfactants under acidic conditions a new type of highly ordered mesoporous silica has been discovered in 1998 by Stucky and coworkers. In the literature, there are several reports about the different type of SBA materials. SBA - 15 is used in many different applications because of its unique properties [2, 11].

### 1. 2. 2. 1. SBA - 15

SBA - 15 is a two - dimensional, hexagonal and amorphous type of silica. It consists of micropores and mesopores within its uniformly distributed mesoporous structure. The pore walls of these type of materials are thick compared to other type of mesoporous silica (3 - 6 nm). Therefore, these materials show high hydrothermal stability. The nature of the pores, micropores or mesopores, mostly depend on the synthesis conditions. The micropores are originated from the polyethylene oxide blocks (PEO) of the surfactant while the mesopores arise from the polypropylene oxide blocks (PPO). In addition, the lengths of these two blocks affect the pore wall thickness, amount of the micropores and mesopores. It is possible to obtain straight or short channels by changing certain parameters (pH, temperature, swelling agents etc.). Many researchers are investigating SBA - 15 materials because the synthesis is fast and rather inexpensive. SBA - 15 materials are applied in several areas such as controlled drug delivery, catalysis, immobilization of enzymes and photoluminescence. The synthesis scheme of SBA - 15 materials is also given in Figure - 4 [2, 11].

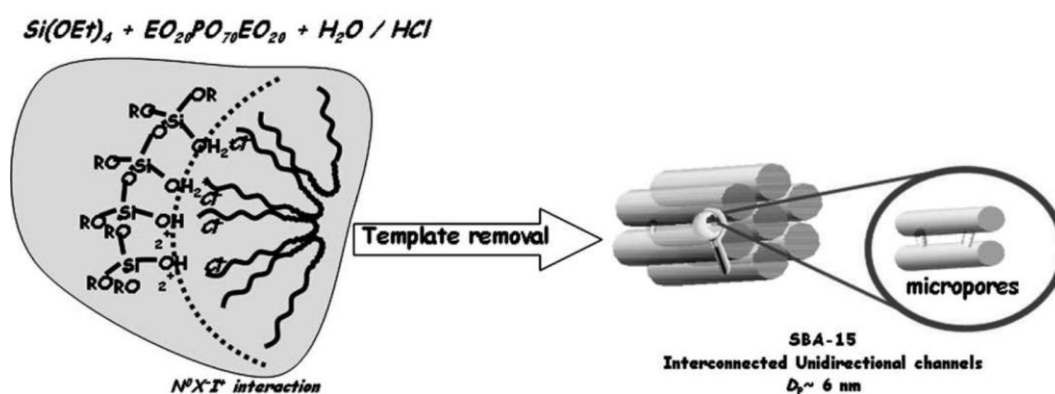


Figure - 4: The synthesis scheme of SBA – 15 mesoporous materials [10].

### 1. 2. 3. APPLICATIONS

Mesoporous materials have several applications due to their unique characteristics. Since the discovery of these materials they have been applied to areas such as catalysis and sorption. Nowadays, after modification and in combination with other type of materials, they are used as contrast agents in magnetic resonance imaging [12]. Recently, silica – based mesoporous

materials are studied in order to be applied in biomedicine as biomarkers, enzyme supporters and biosensors [13]. The mesopores of silica materials are tunable and so the pore sizes could be optimized preserving the narrow size distribution depending on the size of the active agent. Therefore, these materials are ideal matrices for certain applications such as drug immobilization and controlled release. In fact, recently there have been many studies regarding immobilization and release of active agents using these type of materials as carriers [14]. In addition, there are widely studied to be used as carriers of drug delivery systems for sustained or prolonged delivery. Furthermore, they have been applied to scaffolds for bone tissue regeneration. Also, after immobilization of an antibiotic within the carrier they have been used as a scaffold in bone repair [15]. These materials are used for bone tissue regeneration because of their potential host - guest applications, biocompatibility and bioerodible nature [16].

### **1. 3. SYNTHESIS**

The studies have been continuing on since the past ten years in order to prepare materials within the nano size which could be applied in various fields. In comparison to microporous zeolites, these materials contain more active sites that could be accessed. In addition to their unique characteristics also their acid strength could be tuned. Several inorganic mesoporous materials have been discovered using different organic templates as precursors [17]. Besides using other synthesis methods it is possible to obtain the same type of mesoporous material by only changing the surfactant or other parameters such as chemical ratios, additives, temperature, time and pH [2].

### **1. 4. SURFACE FUNCTIONALIZATION**

The methods of surface functionalization could be classified as one - pot synthesis and post – grafting:

#### **1. 4. 1. ONE - POT SYNTHESIS (CO - CONDENSATION)**

This type of synthesis route is also called the direct functionalization process which is based on the co-condensation of the silica source with an organotrialkoxysilane ( $R'-Si(OR)_3$ ). It could be completed under acidic, alkaline or neutral medium depending on the type of the

mesoporous material being synthesized. The organosilane is used to achieve two purposes: The first one is to contribute to the silica network while the second one is the substitution of the silanol groups on the backbone with the functional groups of the organosilane. It is necessary to remove the surfactant template in order to obtain a pure solid. This could be completed in two different ways; either calcination or chemical extraction. The method is chosen depending on the nature of the organic groups, surfactant and the process being followed [11, 18].

#### **1. 4. 2. POST - GRAFTING (SILYLATION)**

The first step is to synthesize silica using the same method as in the co - condensation method followed by the removal of the surfactant. In the second step, the free silanol groups on the surface react with the organosilane. And so, the silanol groups are replaced with the organic functional groups. The number of active sites, the nature of the organosilane and the reactivity of the silanol groups affect the efficiency of the grafting. In general, the post - synthesis is completed in the presence of a non - polar solvent with an excess amount of organosilane. The improvements in this area have lead to higher efficiency of exchange of functional groups. One of these developments is the surfactant - silyl exchange process which the organosilanes are either introduced as solvents or as a mixture with ethanol. It is completed in acidic medium where both the surface modification and substitution with different functional groups take place [11, 19].

#### **1. 4. 3. ADVANTAGES & DISADVANTAGES**

In general, grafting agents such as organo - alkoxy silane, - chlorosilane and - silazane are used in the post - synthesis route while organoalkoxy silanes are used for the one - pot synthesis. In both methods large functional groups are chosen such as amine derivatives, chloro, iodo, alkyl groups, urea and polymer precursors. Multifunctionalization is the main advantage of both of these processes. It is possible to prepare bifunctional ordered mesoporous materials by combining the two methods. The importance of multifunctionalization has been revealed by selective post-grafting. Two strategies have been developed: The first one is based on grafting the external surface and then the internal surface of the pores while the second one is the selective grafting of micropores and mesopores of SBA - 15 type of silica [20].

It is necessary to functionalize the surface of the pore walls of a mesoporous material for certain applications such as controlled drug delivery. In most cases, the hybrid drug delivery systems require surface functionalization prior to the drug loading process. The type of functionalization is chosen according to chemical nature of the drug. It might be possible to promote the loading of a hydrophobic drug into the silica - based mesoporous material by functionalization. In general, drugs are loaded into the mesoporous matrix by adsorption from an organic solution. Functional groups such as carboxyl and amine are especially important for drug delivery, providing stronger attraction between the adsorbent and adsorbate. In addition, these bondings can be optimized for better immobilization through covalent linkages. The most widely reported organic group used for the functionalization is amine groups. It is especially used to improve host - guest interactions between the mesoporous material and the drug with phosphonate and carboxylate groups. Chemically modifying the pore walls of the mesoporous materials using functionalization in order to host guest molecules such as biomolecules is an effective way to control the adsorption and release. Mesoporous silica matrixes weakly interact with guest molecules via Van der Waals forces or hydrogen bonds due to the silanol groups present on the pore walls. However, the interactions between the organic - inorganic hybrid materials are generally hydrophilic - hydrophobic interactions, electrostatic attractive forces or electronic interactions. And so, surface functionalization would improve the interactions between the matrix and the drug. As a consequence, the hydrophobic drug could easily penetrate into the silica matrix via diffusion [11, 14].

The degree of functionalization depends on the method used for surface functionalization. The one - pot synthesis method is limited; the grafting takes place during the synthesis which means that the inner and outer surfaces of the pores are both grafted. And so, an ordered structure would not be obtained due to the defect sites resulting from the synthesis. Also, co - condensation usually involve large volumes of organosilanes. Therefore, it would also be quite expensive. In contrast, by using the post - grafting method, only the outer surface would be functionalized which a higher degree of functionalization could be achieved. The synthesized material would possess an ordered structure. In comparison to the one - pot synthesis approach, the material synthesized by post - grafting method would be more stable [11, 21].

## CHAPTER 2

### CONTROLLED DRUG DELIVERY

The controlled release of a drug in oral dosage form could be classified as either prolonged or sustained release. Sustained release is the type of form which a predetermined amount of drug is rapidly released into the gastrointestinal tract (GI). This fraction (loading dose) is the amount of drug necessary for the pharmacological response. Then, the remaining fraction (maintenance dose) is released rapidly as necessary to keep the activity of the drug at maximum level constant for a longer time interval rather than the estimated time from the usual dosage of the drug. In the prolonged release, however, the constant drug level could not be maintained. The duration of the pharmacological response is only extended. Therefore, it is much more difficult to prepare a drug delivery system for sustained release [22]. The sustained release profile and the conventional release are given in Figure - 5.

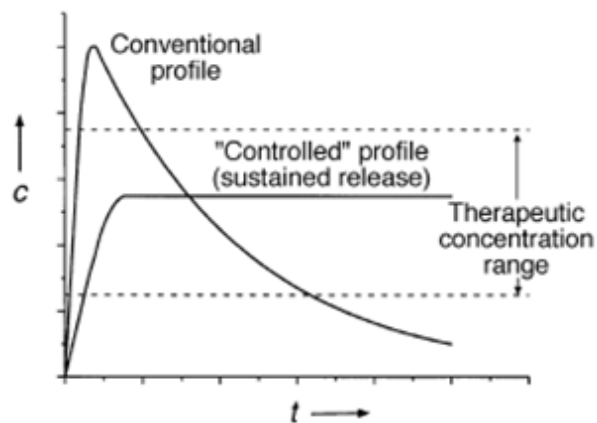


**Figure - 5: The release profile of conventional drug forms and controlled drug delivery systems [23].**

## 2. 1. DRUG ABSORPTION

The passage of a drug from the site of administration through to the plasma is defined as absorption. And so, it is necessary to consider the absorption of a drug for all routes except for intravenous administration. The main routes of administration could be classified as oral, sublingual, rectal, cutaneous, inhalation and injection [24].

**a. Oral administration:** A diversity of drugs are consumed orally. In most of the cases these drugs show little absorption passing from the stomach and the absorption is completed when it reaches the pyloric sphincter [24].

**b. Sublingual administration:** In some cases, a rapid response of the drug is needed; because of its instability or rapid metabolism. Therefore, this route is used and the drug is absorbed directly from the oral cavity. Also, it is necessary to provide that the drug administered by using this route does not taste horrible. In fact, the drug absorbed this way directly passes into the systemic circulation and the first pass effect is eliminated. However, it could not be used for drugs with high molecular weight [24].

**c. Rectal administration:** It is used for drugs that cause gastric irritation and that require to provide a local effect. These type of drugs are absorbed from the rectum and mostly by - pass the liver. Thus, it is useful for drugs that are rapidly inactivated by the liver [25].

**d. Cutaneous administration:** The main reason of this administration is the treatments that require a local effect on the skin such as topically - applied steroids [25].

**e. Inhalation:** It is useful for the administration of volatile and gaseous anaesthetic agents. The type of drugs that are used to be effective on the lungs are also given this way [25].

**f. Injection (intravenous, intrathecal, intramuscular and subcutaneous):** Intravenous injection is the most rapid and certain route. Also, the uncertainties of absorption are avoided. Intrathecal injection is based on injecting the drug into the subarachnoid space. It is used for certain situations such as the treatment of meningitis. Intramuscular or subcutaneous injections of drugs provide a faster response than the oral administration. The intramuscular injection is based on the direct injection of the drug into the muscle tissues. In subcutaneous injection the drug is injected under the skin tissues (subcutis) [25].

The drug - body interactions could be divided into pharmacodynamic and pharmacokinetic processes. The pharmacodynamic processes are the actions of the drug on the body while the pharmacokinetic processes are the actions of the body (enzymes) on the drug. The pharmacokinetic processes play an important role for the selection of the administration route. There are many important factors that need to be considered such as the interactions between the drug and receptor, the duration of the drug action and the available binding sites. In order to reach the effective concentration, the drug must be absorbed into the blood after administration and distributed to the site of action. The permeation of a drug could proceed as in the following: aqueous diffusion, lipid diffusion, special carriers, endocytosis and exocytosis. After the drug shows its effect, it must be metabolically inactivated and eliminated from the body [26].

## 2. 2. DRUG DELIVERY SYSTEMS

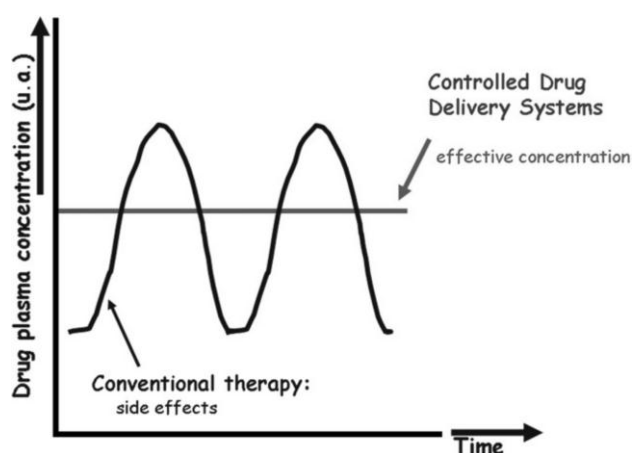


**Figure - 6: The drug plasma concentration vs. time in conventional therapies compared to the release profile of controlled drug delivery systems [3]**

As a result of the improvements in the pharmaceutical area many drugs have been studied in order to prepare drug delivery systems and to control their delivery. In comparison to conventional drug dosages it is possible to change the pharmacokinetics of a drug and also to control its delivery by using drug delivery systems. As it is indicated in Figure - 6, the usage

of traditional dosage causes side effects which could be altered by using controlled drug delivery systems. Therefore, the potential toxic effect of the drug and the degradation could be prevented. Also, the drug dosage and its frequency could be adjusted [27]. Nowadays, the studies are focused on to prepare mesoporous silicas as drug carriers with high loading efficiency and to be able to either control or sustain the release of the drug. There are several studies which a diversity of drugs have been used (ibuprofen, vitamin B1, gentamicin etc.). As it has been reported in earlier studies it is possible to adjust the drug release rate by modifying the pore size, structure and surface with organic groups [28].

In order to prepare a drug delivery system for sustained release many factors must be considered such as the route of drug administration, the type of therapy (acute or chronic), the disease, the type of drug delivery system and the properties of the drug. The drug behavior within the body and in the drug delivery system is also crucial. In addition, the physiochemical properties of the drug affect the performance of the release. These properties could be classified as the dosage, solubility, partition coefficient, stability, size, protein binding and pKa [29].

There are some potential advantages of controlled drug delivery. The first one is to avoid patient compliance problems which are based on the psychological and physical condition of the patient. The patient might forget to take the drug at a necessary time interval or might not follow the treatment and so, the therapy would be ineffective. The second advantage is related to economical reasons. Less amount of drug would be used and therefore the synthesis and preparation of a drug would be less expensive. Finally, by controlling the conditions and minimizing the side effects the efficiency of the treatment could be improved [30].

## **2. 2. 1. POLYMERIC DRUG DELIVERY SYSTEMS**

Biocompatibility, tissue specificity and capacity of drug loading are important characteristics that are required for materials to be used as carriers. Also, these materials must be properly designed to avoid premature release from the host. Polymers have been used as carriers in drug delivery systems for many years. However, there are some limitations such as the

premature degradation of the therapeutic agent, destruction of the polymeric system, poor chemical and thermal stability, non - homogeneous dispersion of the drug and rapid excretion through the system. Therefore, mesoporous materials are promising drug carriers due to their unique properties [31, 32].

## **2. 2. 2. INORGANIC / ORGANIC HYBRID DRUG DELIVERY SYSTEMS**

Silica is a unique molecule with great adsorptive characteristics which is able to encapsulate different types of molecules within its pores. Ordered mesoporous silica is being studied in order to prepare carriers of drug molecules by tuning the pore size and dimensions. Up to now, SBA - 15, MCM - 41, MCM - 48 and the derivatives of these mesoporous silicas have been used in order to encapsulate drugs for controlled release. The release of the drug molecules depend on the pore size of the mesostructured silica which results in either a prolonged or immediate release. Also, it is possible to chemically modify the surface of the walls of the mesoporous silica to control the drug release by tuning the pore diameter or using nanocaps [27, 33].

## **2. 2. 3. ADVANTAGES & DISADVANTAGES**

Controlled release based on stimuli – responsive systems have become an interesting subject for researchers due to their applicability in areas such as drug and gene delivery. Particularly, surface functionalized and capped mesoporous silica is reported as an efficient system with the advantage of zero premature release. In the past two decades, different type of materials such as silica, hydroxyapatite, self - assembled multilayers and hydrogel nanoparticles have been studied in order to use them as drug delivery systems. Amorphous bioceramics with high stability and porosity could be obtained using sol - gel method. In addition, it is possible to obtain different forms of shapes of silica - based materials (spherical particles, fibers and films). The biocompatibility of mesoporous materials, both in vitro and in vivo applications, has been reported recently. In addition, these materials have been tested on animals through intravenous administration (IV) which also indicate the potential. The porosity of these particles makes it possible to host the guest molecules both within the channels and on the surface which is especially useful for codelivery applications. In fact, these could be used to overcome the problems in traditional therapy [14, 27, 34].

One of the recent improvements in nanobiotechnology is the usage of mesoporous silica materials for targeted drug delivery as carriers. Although, there are some drawbacks of these systems such as the protection of the active agent until the target is reached. Therefore, stimuli - responsive systems were prepared by many researchers. Previously, materials such as gold nanoparticles, quantum dots, iron oxide nanoparticles and dendrimers have been used as caps to prevent leakage of the active agent from the pores. Also, there have been studies in order to carry genes and hydrophobic anticancer drugs. In terms of surface functionalization, many different functional groups (thiol, amino, phosphonate and carboxyl) and large molecules (phospholipids, polyethylene glycol (PEG) and block copolymers) have been used to develop the dispersibility of silica [35, 36].

It is possible to incorporate the active agent in this case the drug by different methods. The method which the drug is directly incorporated during the synthesis is mostly used because it is completed in only one step. Although, the drug loading efficiency might be low due the poor solubility of the drug and possible phase separation. The amount of drug incorporated into the silica network and its release rate depends on the porosity of the samples. Furthermore, the active agent might be entrapped within the pores and it might not be released. Therefore, it is difficult to tune the necessary parameters for each application. Direct compression, wet granulation or mechanical mixing could also be used for the drug loading process. Also, the active agent might not be homogeneously distributed and it might not be reproducible. In order to prevent these kinds of situations, the drug must be incorporated by adsorption from solution onto the silica network and the solvent must be evaporated afterwards. If the drug is poorly soluble the most certain solution would be post - impregnation. In particular, it is a convenient approach to load drugs into porous materials. Also, the amount of the drug could be adjusted. The most important problem regarding the drug immobilization is that the solvent could be remaining. Therefore, the solvent must be carefully chosen for better adsorption. It is most likely that the release of the drug could be controlled if there is not any drug entrapped within the pores [14].

### **2. 3. ANTIBIOTICS**

Beta - lactam antibiotics are one of the most commonly used type of antimicrobial agents due to their safeness and broad antibacterial spectrum. This group of antibiotics is either used

in oral or parenteral forms. There are very few reports indicating minor significant interaction of this type of antibiotic agents with other drugs. The interaction of these drugs could be classified as major, moderate or minor. The major case of interaction is the type which might potentially threaten the life of the patient. The moderate type is the one which are less harmful while minor interactions are the less effective type. These types of therapeutic agents have a similar mechanism of action on the body such as the inhibition of some enzymes in the cell wall of the bacteria. In addition, all of these  $\beta$  - lactams are in - effective on certain organisms. Although, the high dosage of these type of antibiotics might cause seizures.  $\beta$  - lactam antibiotics can be classified as penicillins, cephalosporins, carbapenems and monobactams[37]. In this study, the main interest is amoxicillin which is a penicillin - like antibiotic.

### **2. 3. 1. PENICILLINS**

One of the most common and oldest type of antimicrobial agent is penicillin. Penicillin has been discovered by Alexander Fleming in 1929 while its crystal state was isolated in 1940. It belongs to the group of  $\beta$  - lactam antibiotics. It is the first natural antibiotic used in order to treat infections caused of bacteria. And so, the year of isolation could also be noted as the birth of the science of antibiotics. Since then, new type of substances which could be obtained from various microorganisms, plants and animals have been investigated to be used as antibiotics. The discovery of penicillin is therefore very important for the developments in areas such as biology, medicine and chemistry. Also, it was found to be a very effective chemotherapeutic agent. This new compound was prepared by biological synthesis using microorganisms [37, 38, 39].

The half - lives of penicillins are less than two hours which makes it necessary to increase the dosage. These therapeutic agents show poor absorption even if the drug is consumed orally. The only minor side effect that has been reported related to the usage of these types of drugs is immunologic sensitization. As a result of the sensitization the patients could not use this type of antibiotics. Therefore, it was necessary to discover new type of antibiotics which any bacteria could be resistant. In other words, the spectrum of effectiveness of penicillin became narrower after its discovery [37, 39].

Penicillin G and V are the active agents. This class of penicillins have short half-lives and so frequent dosing or continuous infusion is necessary. However, they differ in formulations and the frequency is very important. It is mainly used in the treatment of syphilis and susceptible streptococcal infections like pharyngitis and endocarditis [37].

It is much more difficult to cover the gram-negative area of the spectrum. Aminopenicillins are more hydrophilic and can pass through the channel of some gram - negative organisms [37].

## 2. 4. AMOXICILLIN

### 2. 4. 1. STRUCTURE

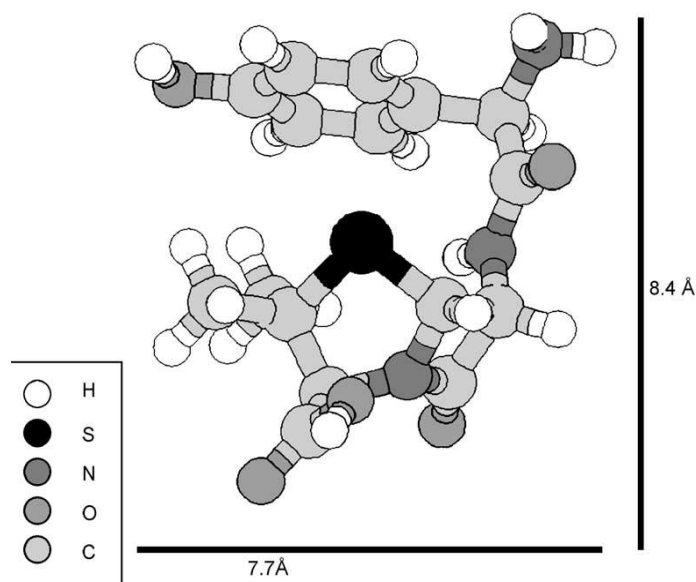


**Figure - 7: The three - dimensional structure of amoxicillin with interatomic distance**

((2S, 5R, 6R) - 6 - [(2R) - 2 - Amino - 2 - (4 - hydroxyphenyl) acetyl amino] - 3, 3 - dimethyl - 7- oxo - 4 - thia - 1 - azabicyclo [3.2.0] heptanes - 2 - carboxylic acid) [40].

The interatomic distances of amoxicillin are indicated in Figure - 7. The values reveal that amoxicillin is small enough to pass through the pores of SBA - 15 materials which consist of pores within the range of 5 - 10 nm. Amoxicillin has been used in only a few studies regarding drug delivery systems using mesoporous materials.

#### **2. 4. 2. EFFECT & MECHANISM**

The adverse effect of oral uptake of aminopenicillins is mainly diarrhea. The main active agents of these type of drugs are ampicillin and amoxicillin. Amoxicillin is bioavailable, its dosage frequency is lower and it is much more tolerated. Therefore, it is a better choice to give amoxicillin orally [37]. It is reported that the half - life of amoxicillin is 1.7 hours and that 86 % of the orally consumed amoxicillin would be excreted in urine [41]. The release rate, amount of the drug and the host of the drug delivery system play an important role in the control of the release within the target area. Therefore, the physical properties, bioactivity and release of the drug must be considered for both in vivo and in vitro studies [42].

#### **2. 4. 3. DISEASES**

Aminopenicillins are effective on infections of susceptible gram - negative rods. Amoxicillin is one of the penicillin like antibiotics which is hydrophilic. It is most commonly used in the treatment of the upper respiratory tract such as strep throat and bronchitis. Also, it is used to treat bone disorders, lung, skin and ear infections. In addition, it is used before surgeries and by dentists to prevent future infections and also for the treatment of certain bacterial (*Helicobacter pylori*) infections like pneumonia [39, 43, 44].

It is known that it is difficult to maintain the plasma concentration of amoxicillin at a certain level for a prolonged delivery. Therefore, only a few studies have been reported which the amoxicillin release has been extended. Recently, there are only a couple of studies which mesoporous silica is used as the carrier of amoxicillin for controlled delivery. In fact, there is only one article published about amoxicillin delivery using SBA - 15 materials. However, there are no studies concerning functionalized SBA - 15 samples as carriers of amoxicillin for controlled drug delivery [40]. In addition, the main type of surface functionalization reported about SBA - 15 materials is amine functionalization.

In other words, the purpose of this thesis was to determine the effect of amine, thiol and methyl functionalization on amoxicillin delivery. Besides, the effect of the concentration difference on the surface functionalization process and the drug delivery was also studied.

## CHAPTER 3

### EXPERIMENTAL

#### 3. 1. SYNTHESIS OF SBA-15 PARTICLES

The weighed Pluronic 123 triblock copolymer (structure directing agent) was dissolved in the prepared HCl solution (37 %). The solution was stirred at ambient temperature for 75 minutes until it became colorless. Then, the temperature was raised to 40°C. TEOS was used as the silica source and so it was added very slowly. The solution was stirred for 24 hours using a magnetic stirrer at this temperature.

The next day the solution was transferred into a Teflon bottle. The bottle was placed into the oven adjusted to 90°C. It was kept at this temperature for 48 hours (aging). The obtained solution contained two phases (white precipitate and clear solution). Then it was washed with 150 ml of water, filtered and left to dry at room temperature. The following day, the precipitate obtained was placed into the oven adjusted to 60°C and it was dried at this temperature for one day.

Later on the solid was placed into the muffle oven inside of a crucible. The ramp rate was 5°C/ min. After it reached 400°C it was kept an hour at this temperature, then it was heated till 600°C with the same ramp rate and it was kept at this temperature for 5 hours (calcination). The previously reported synthesis was followed [45].

The amounts of the chemicals used in the synthesis procedure are given in Table - 1. In addition, all of the chemicals were used without further purification.

**Table - 1: Precursors used for the synthesis of SBA - 15 particles**

Chemicals	m(g) or V(ml)	Brand	d (g/ml)	MW (g/mole)
Pluronic 123	4 g	Aldrich	1.02	5800
HCl	19.5 ml	Sigma - Aldrich	1.20	36.46
H <sub>2</sub> O	130 ml	-	1.00	18.00
TEOS	9.46 ml	Aldrich	0.93	208.33

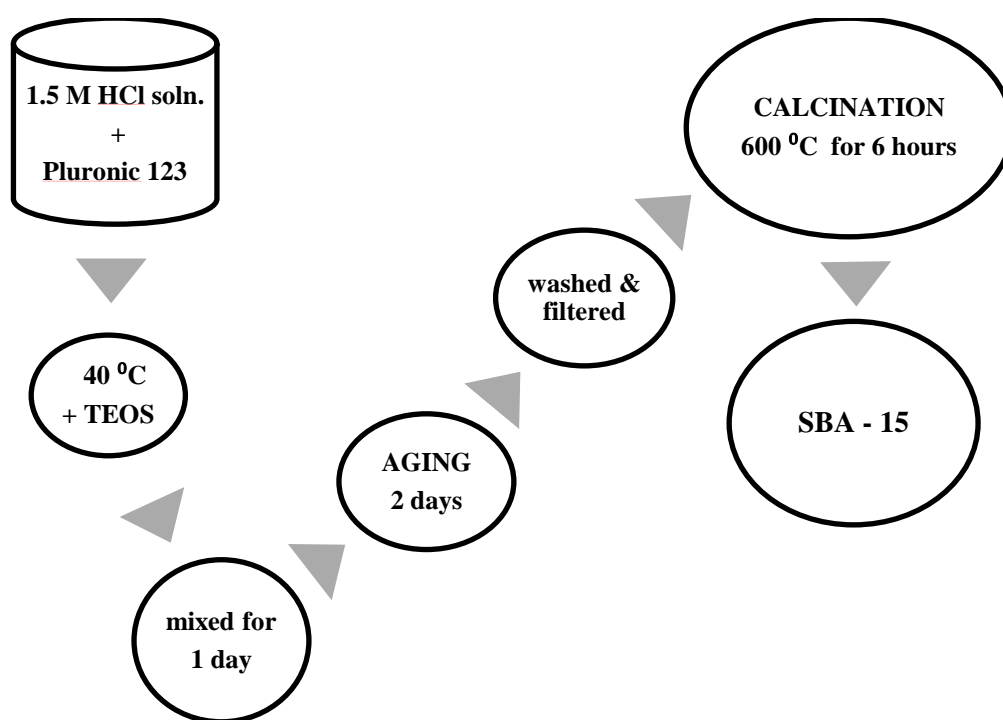


**Figure - 8: Synthesis scheme of SBA - 15 particles**

The synthesis procedure of SBA - 15 particles is also illustrated in the figure above. Therefore, the synthesis of these particles is completed in approximately 6 days.

### 3. 2. SURFACE FUNCTIONALIZATION

The surfaces of the synthesized SBA-15 particles were functionalized using APTES, MPTMS and TEMS. Three different concentrations were prepared for each type of alkoxy silane: 1 g SBA - 15: 1 ml alkoxy silane (1:1), 1 g SBA - 15: 2 ml alkoxy silane (1:2) and 1 g SBA - 15: 4 ml alkoxy silane (1:4). The temperature was increased up to 70°C and the solution began to boil. However, it has been reported that the functionalization process was completed at 80 °C in 12 hours [31]. Therefore, the temperature was adjusted to 50°C ( $\pm 5^\circ\text{C}$ ) and solution was stirred for 6 hours at this temperature. Then, it was washed with distilled water, filtered and kept in the furnace at 60°C for it to dry over the night. The thiol and methyl functionalization were also completed following the same process. The amounts of the precursors used during the functionalization have been given in Table - 2. All of the chemicals used for the functionalization process were purchased from Sigma - Aldrich.

**Table - 2: The amount of the chemicals used for the functionalization of SBA - 15 samples**

Chemicals	m(g) or V(ml)	n (mole)	d (g/ml)	MW (g/mole)
EtOH	50 ml	0.8563	0.789	46.07
SiO <sub>2</sub>	1 g	0.0167	-	60.00
APTES	1 ml	0.0043	0.946	221.37
	2 ml	0.0086		
	4 ml	0.0171		
MPTMS	1 ml	0.0054	1.057	196.34
	2 ml	0.0108		
	4 ml	0.0215		
TEMS	1 ml	0.0050	0.895	178.30
	2 ml	0.0100		
	4 ml	0.0200		

The aim of the surface functionalization is to replace the silanol groups present in the pure sample with other organic functional groups by using alkoxy silanes. The samples were functionalized after synthesizing SBA - 15 particles (post - grafting synthesis). The preparation scheme is illustrated in Figure - 9.

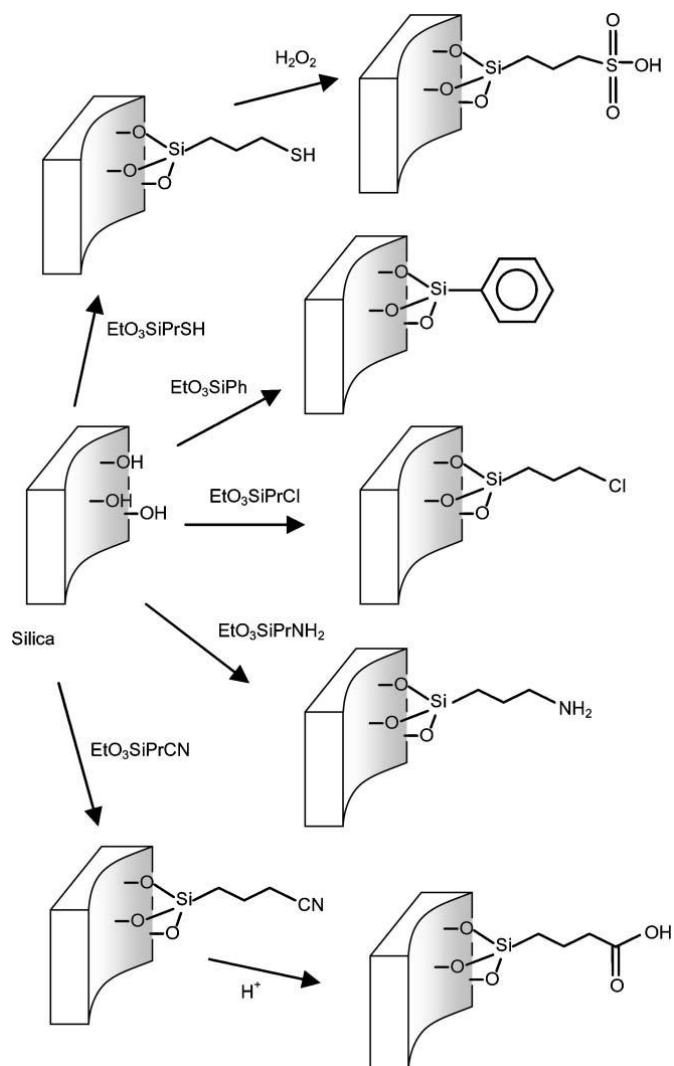


**Figure - 9: Surface functionalization of SBA - 15 materials using organotriethoxysilanes by post - grafting synthesis method [8].**

The expected structures of the samples after the surface functionalization process are given in Figure - 10. Also, the structures of the alkoxysilanes used during the preparation are established as well.

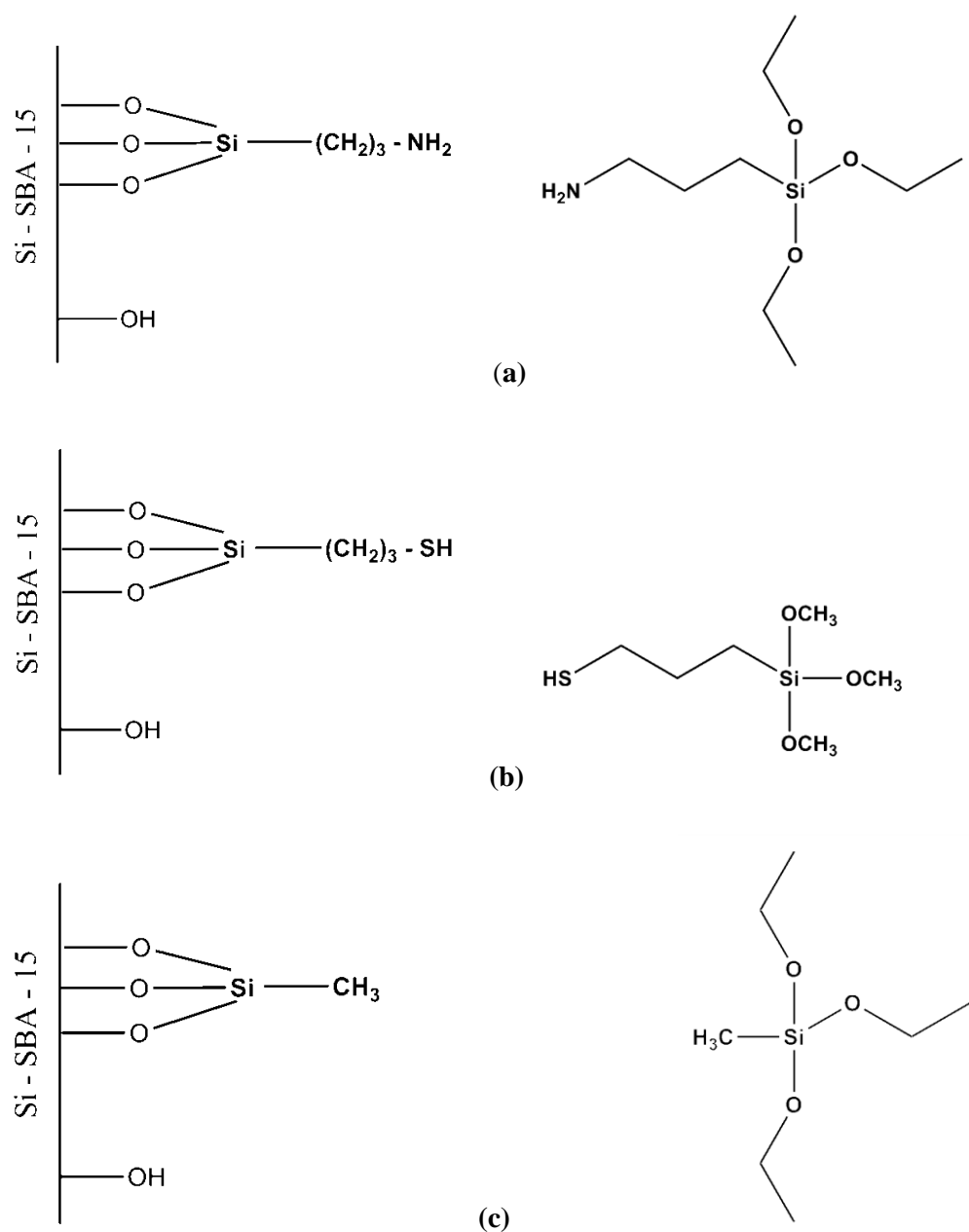


**Figure - 10: The structures of the samples after the surface functionalization by post-grafting synthesis using APTES (a), MPTMS (b) and TEMS (c).**

### 3. 3. AMOXICILLIN LOADING

The amoxicillin used during the experiments was purchased from Sigma. 3 mg/ml of amoxicillin solution was prepared using 33 ml of distilled water and 0.1 g of amoxicillin. Then 0.1 g of SBA - 15 was added into the solution and mixed for 3 days at ambient temperature using an incubator (120 rpm) [28, 40].

Amoxicillin loading was monitored using Cary 5000 UV/VIS/NIR Spectrophotometer. The wavelength was set between 200 and 800 nm. The loading of amoxicillin was completed in 3 days. Therefore, the concentration change was measured in different time intervals: 4 hours, 8 hours, 12 hours, 24 hours, 48 hours and 72 hours. The amount of amoxicillin loaded was calculated using the absorbance values obtained at 272 nm. The absorption peak observed at this wavelength is attributed to amoxicillin.

**Table - 3: The amount of chemicals used for the amoxicillin loading of SBA – 15 samples**

Chemicals	m(g) or V(ml)	n (mole)	d (g/ml)	MW (g/mole)
Amoxicillin	0.1 g	0.00027	-	365.4
SiO <sub>2</sub>	0.1 g	0.00167	-	60.0
H <sub>2</sub> O	33 ml	1.83000	1.0	18.0

### 3. 4. AMOXICILLIN RELEASE

The amoxicillin release was determined using two different analyses:

#### a. UV analysis:

Initially, the phosphate buffer solution (pH: 7.4) was prepared for the release experiments. Then the SBA - 15 samples loaded with amoxicillin (0.01g) were added to the solution (10 ml). Each of the prepared solutions were mixed at 37 °C in order to simulate the body temperature.

The amount of amoxicillin released from the silica particles was calculated according to the concentration change within 6 hours. Distilled water was used as the reference for each measurement. The measurements were completed within 30 minutes, 1 hour, 2 hours, 4 hours and 6 hours [31, 46].

#### **b. HPLC analysis:**

The amoxicillin loaded samples (0.01 g) were added to the phosphate buffer solution (33 ml) and were also mixed at 37 °C for 3 hours. 23 % of methanol solution was prepared as the mobile phase (Table - 4). Waters reverse-phased column was used during the analysis. The measurements were completed at 254 nm. The difference in the peak area was used in order to calculate the percentage of the amoxicillin released in PBS [40].

#### **Preparation of PBS (Phosphate buffer solution)**

In order to prepare the phosphate buffer solution two different phosphate salts were used:  $K_2HPO_4$  and  $KH_2PO_4$  (Table - 5). The pH of the prepared solution was adjusted to 7.4 to simulate the pH of the intestine.

**Table - 4: Amount of the chemicals used for the preparation of PBS**

PBS	m(g) or V(ml)	Brand	d (g/ml)	MW (g/mole)
$K_2HPO_4$	13.97 g	Riedel - Haën	2.44	178.30
$KH_2PO_4$	2.69 g	Merck	2.34	136.02
$H_2O$	1 L	-	1.00	18.00

**Table - 5: Amount of the chemicals used for the preparation of the mobile phase**

Mobile Phase	m(g) or V(ml)	Brand	d (g/ml)	MW (g/mole)
MeOH	300 ml	Sigma - Aldrich	0.79	32.04
$KH_2PO_4$	1.77 g	Merck	2.34	136.02
$H_2O$	1 L	-	1.00	18.00

## CHAPTER 4

### CHARACTERIZATION

#### 4. 1. X-RAY DIFFRACTION (XRD)

Powder XRD patterns of the samples were recorded under ambient conditions at  $0.9 - 8^\circ$  ( $2\theta$ ) with the resolution of  $0.05^\circ$  by using Rigaku X-ray Diffractometer with a Miniflex goniometer which was operated at 30 kV and 15 mA. The source of the X-ray radiation was Cu K $\alpha$  ( $\lambda = 1.54\text{\AA}$ ). The scanning mode was selected as continuous scanning. The powder patterns of interest given in the thesis are within the range between  $1.5$  and  $4^\circ$  ( $2\theta$ ).

#### 4. 2. SMALL - ANGLE X - RAY SCATTERING (SAXS)

The SAXS analysis was completed at the Physical Engineering Department, Faculty of Engineering, Hacettepe University by Prof. Dr. Leyla Yıldırım and Prof. Dr. Semra İde. The small angle X-ray scattering experiments were done by using a Hecus system with Kratky geometry (Hecus X-ray systems, Graz, Austria SWAXS). The X-ray collimation of the system is line - collimation and the source of the X-ray tube is copper ( $\lambda = 1,54\text{\AA}$ ). The X-ray power source was operated at 2 kW (50 kV and 40 mA). Position sensitive two linear detectors consisting 1024 channels were used for the measurements. The distance between the channels were  $54\ \mu\text{m}$  while the distance between the sample and the detector was 27.9 cm. The scattering patterns between 0.04 and  $0.550\ \text{\AA}$  were used as the SAXS results. All of the scattering patterns were obtained within 30 minutes at room temperature. In order to avoid instrumental errors during the analysis such as poor detection, the SAXS patterns were obtained at higher  $2\theta$  degree angles for each of the samples.

### **4. 3. ELEMENTAL ANALYSIS**

The samples were analyzed at the Central Laboratory (METU) using CHNS-932 (LECO) elemental analyzer to obtain information about the percentages of the carbon, hydrogen, nitrogen and sulfur present within each sample. The measurements were completed twice to obtain adequate results.

### **4. 4. THERMOGRAVIMETRIC ANALYSIS (TGA)**

The thermogravimetric analysis was completed by using Pyris1 Thermogravimetric Analyzer (Perkin Elmer) at the Central Laboratory. The measurements were completed under air atmosphere at temperatures between 25 and 700 °C with the heating rate of 10 °C/ min.

### **4. 5. FOURIER - TRANSFORM INFRA - RED SPECTROSCOPY (FTIR)**

The IR spectra of the samples were recorded with Varian 1000 FTIR (Scimitar FTS 1000) in the range of 400 and 4000  $\text{cm}^{-1}$ . Each sample was characterized before and after the loading of amoxicillin. The FTIR spectra were obtained at room temperature from KBr pellets.

### **4. 6. NITROGEN - SORPTION**

The  $\text{N}_2$  adsorption - desorption measurements were completed using Quantachrome Autosorb-6 at the Central Laboratory (METU). Prior to the measurement each sample was outgassed at 200 °C for 16 hours. The specific surface areas were calculated using multiple point Brunauer - Emmett - Teller (BET) method. The pore size distributions were calculated using desorption branches of the isotherms by Barrett - Joyner - Halenda (BJH) method.

### **4. 7. TRANSMISSION ELECTRON MICROSCOPY (TEM)**

The instrument used for the TEM analysis was JEOL JEM 2100F STEM. The analysis was completed at the Central Laboratory (METU). JEOL JEM 2100F Field Emission Gun was used during the experiments. The pure samples were operated at 80 kV and after functionalization the samples were analyzed at 200kV. Two measurements of the pore distances are obtained for each sample and the scale bar of all of the micrographs is 50 nm.

#### **4. 8. SOLID STATE <sup>29</sup>Si MAS - NMR**

The results were obtained using High Power Solid State 300 MHz Bruker Superconducting FT.NMR Spectrometer. The spin rate was adjusted to 8500 Hz. 4 mm MAS 1H/BB was used as probe and CHCl<sub>3</sub> was used as solvent. The measurements were completed within 16 hours. These analyses were also completed at the Central Laboratory (METU).

#### **4. 9. UV - VIS SPECTROSCOPY**

CARY 5000 UV - VIS - NIR Spectrophotometer was used in order to obtain information about the concentration change of amoxicillin for both the loading process and the release.

#### **4. 10. HIGH – PERFORMANCE LIQUID CHROMATOGRAPHY (HPLC)**

Thermo Separation Products AS3000 Spectra System was used as the HPLC Autosampler while the detector was the UV1000 Spectra System. The measurements were completed at room temperature. The mobile phase was a buffer solution of 0.01 M KH<sub>2</sub>PO<sub>4</sub> in 23 % methanol solution. The injection volume was 20 μL and the flow rate was adjusted to 0.1 ml/min. Waters reversed - phase column (WAT086344) was used for the HPLC analysis. The effluent was monitored at 254 nm.

## CHAPTER 5

### RESULTS AND DISCUSSION

#### 5. 1. POWDER PATTERNS OF SBA - 15 SAMPLES

The powder XRD patterns of all of the samples prior to drug loading are given in Figure- 11, Figure - 12 and Figure- 13. In order establish the effect of the concentration difference each powder pattern consists of samples with same type of functionalization. Moreover, the other three patterns (Figure 14 - 16) are obtained after the amoxicillin loading process. The mesostructure of each sample is remained after functionalization according to the diffraction peaks being present after the post-grafting process. SBA - 15 type of mesoporous materials exhibit a very intense diffraction peak between  $2\theta = 0.9$  and  $1.05$  degrees. The other two diffraction peaks are observed at between  $2\theta = 1.8$  and  $2$  degrees. The diffraction peaks are assigned to the planes as (100), (110) and (200). However, it is not possible to observe the most intense peak (100) within these powder patterns due to instrumental limitations while the less intense peaks (110) and (200) are present. These indexes are the main characteristic of the well - defined hexagonal structure. Furthermore, the honeycomb structure of the samples is established by the TEM micrographs as well. In accordance with the XRD patterns of SBA - 15 materials published by several authors, it has been established that these materials are hexagonally ordered with the space group  $p6mm$ . The diffraction peaks were only observed at low angles as expected. Prior to calcinations, the most intense peak (100) reflects the  $d$  - spacing value of  $104 \text{ \AA}$  depending on the first reported SBA - 15 material. Also, this peak corresponds to a large unit cell parameter of  $120 \text{ \AA}$ . After the calcination process, the XRD pattern indicates that the sample is still thermally stable. However, the  $d$  - spacing value and unit cell parameter related to the diffraction peak (100) change; the values  $95.7 \text{ \AA}$  and  $110 \text{ \AA}$  are obtained, respectively [2, 45, 47, 48].

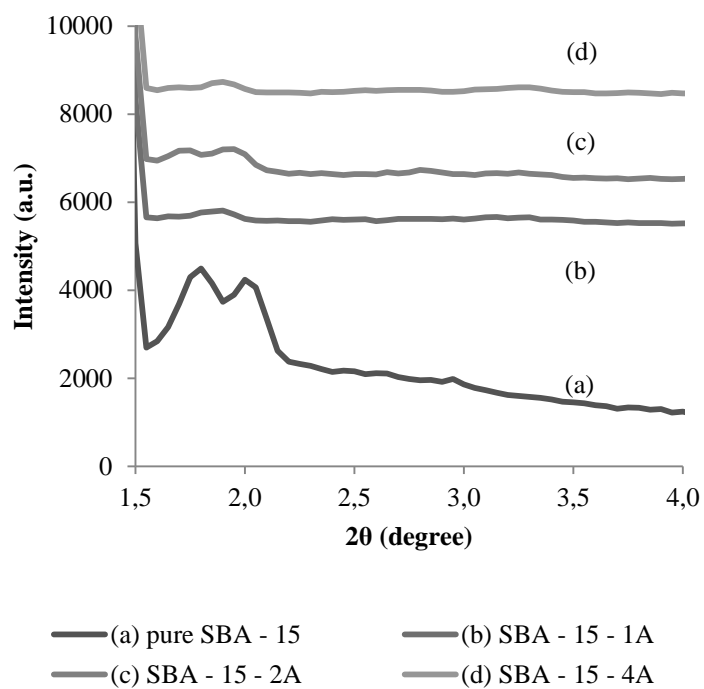


Figure - 11: Powder patterns of amine functionalized SBA – 15 samples

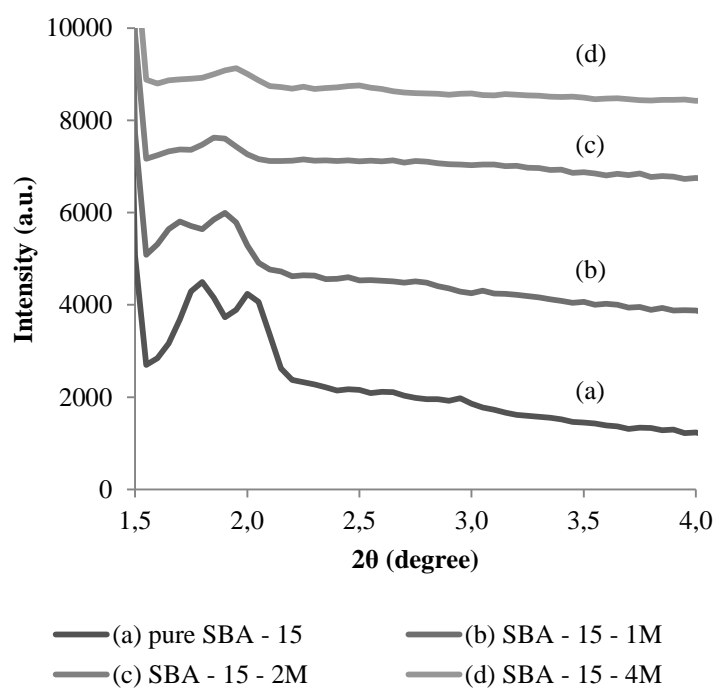


Figure - 12: Powder patterns of thiol functionalized SBA - 15 samples

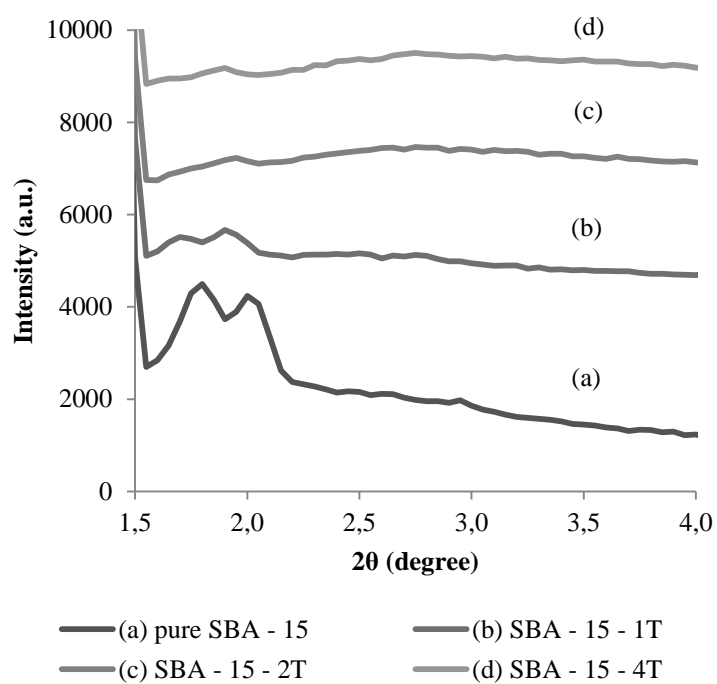


Figure - 13: Powder patterns of methyl functionalized SBA - 15 samples

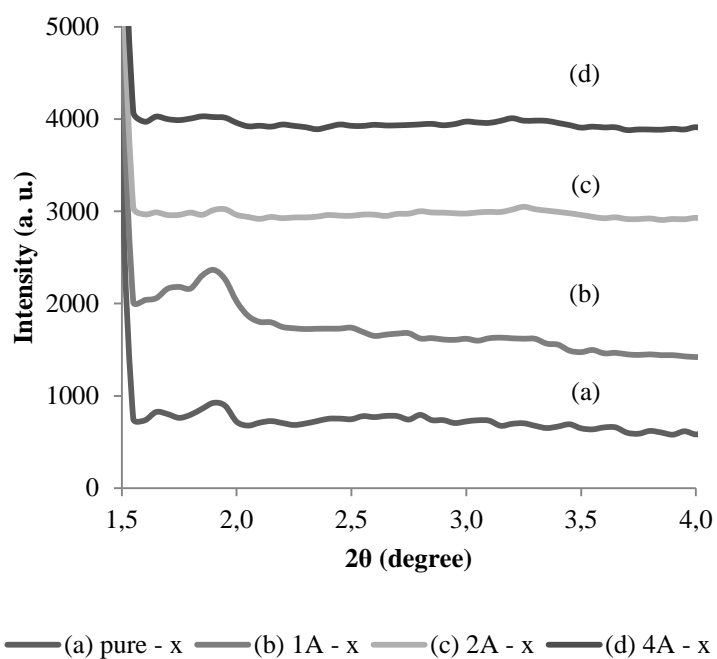
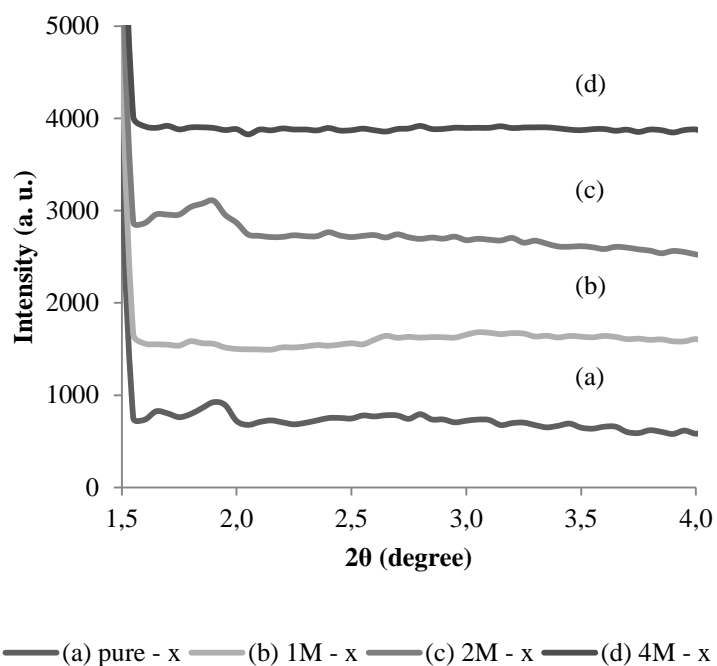
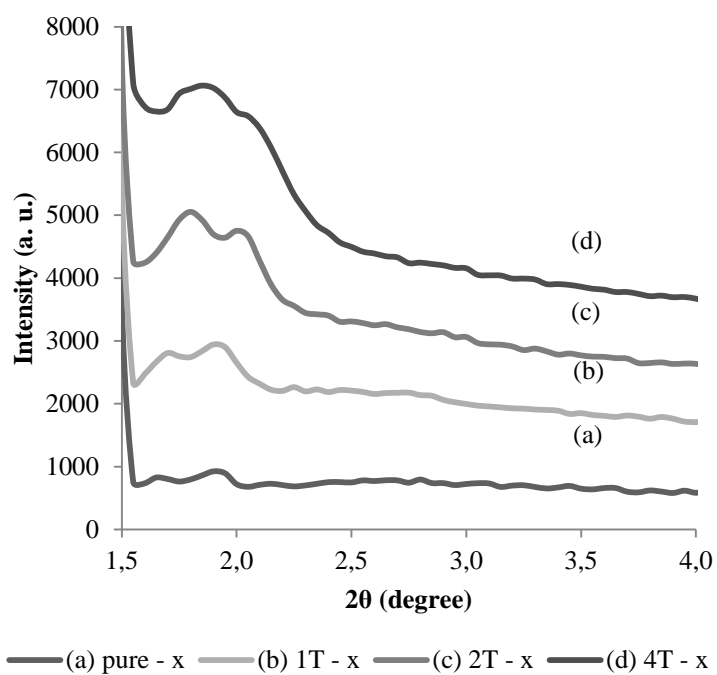


Figure - 14: Powder pattern of amoxicillin loaded amine functionalized samples



**Figure - 15: Powder pattern of amoxicillin loaded thiol functionalized samples**



**Figure - 16: Powder pattern of amoxicillin loaded methyl functionalized samples**

As a result, all of the powder patterns are similar. The less intense peaks are present in each pattern even after the samples are functionalized and loaded with amoxicillin. Therefore, the hexagonal structure is maintained after all of the applications. In other words, the samples are structurally stable even after the functionalization and amoxicillin loading.

## **5. 2. SMALL - ANGLE X - RAY SCATTERING (SAXS)**

As it could be observed in the SAXS patterns each sample has three diffraction peaks. The obtained SAXS patterns are similar to the patterns in the literature. The d - spacing values related to each peak have been calculated by using the Bragg law ( $\lambda=2d.\sin\theta\{1\}$  and  $q=4\pi.\sin\theta/\lambda\{2\}$ ). The hexagonal crystal structure has been proven by indexing the experimental d - spacing values using the program 3DVIEW. The space group could not be identified by using only three diffraction peaks. Therefore, p6mm space group in 2D - hexagonal indexing has been used because this space group is observed for similar structures in the literature. The most intense peak is the peak indexed as (100) while the other two peaks ((110) and (200)) are less intense [49]. The same types of functionalized samples have been shown in the same graph in order to understand the effect of the concentration difference within the samples.

### **5. 2. 1. UNIT CELL PARAMETERS AND d - SPACING VALUES**

The unit cell parameters, d - spacing and q - values are shown in Table - 6. In addition, the d - spacing values calculated using the powder XRD analysis results are given for comparison. The d - spacing values calculated from the diffraction peaks of the SAXS patterns are quite similar even after the functionalization processes. Also, it could be stated that the value of the pure sample (10.7 nm) is parallel to the published articles (9.8 nm). Furthermore, the unit cell parameter of the pure sample is 12.4 nm which is higher than the values obtained by other researchers (10.8 nm). After the functionalization the value is expected to become smaller due to the interactions. The unit cell parameters of the amine functionalized samples are between 11.9 and 12.2 nm while in the literature the value is reported as 10.4 nm. And so, the results are as expected [2, 16].

**Table - 6: d - spacing, unit cell parameter and q values of pure and functionalized SBA - 15 samples**

Sample	(hkl)	d (Å) - XRD	d (Å) - SAXS	q (1/ Å)	a (Å)
Pure SBA - 15	(100)	-	107.28	$5.86 \times 10^{-2}$	123.88
	(110)	49.00	62.03	$1.01 \times 10^{-1}$	
	(200)	44.18	53.65	$1.17 \times 10^{-1}$	
SBA - 15 - 1A	(100)	-	105.85	$5.94 \times 10^{-2}$	122.23
	(110)	53.55	61.55	$1.02 \times 10^{-1}$	
	(200)	46.50	53.29	$1.18 \times 10^{-1}$	
SBA - 15 - 2A	(100)	-	103.11	$6.09 \times 10^{-2}$	119.06
	(110)	51.97	59.49	$1.05 \times 10^{-1}$	
	(200)	45.31	51.57	$1.22 \times 10^{-1}$	
SBA - 15 - 4A	(100)	-	105.85	$5.94 \times 10^{-2}$	122.22
	(110)	51.97	61.08	$1.03 \times 10^{-1}$	
	(200)	46.50	52.94	$1.19 \times 10^{-1}$	
SBA - 15 - 1M	(100)	-	108.75	$5.78 \times 10^{-2}$	125.58
	(110)	51.97	63.02	$9.97 \times 10^{-1}$	
	(200)	46.50	54.39	$1.16 \times 10^{-1}$	
SBA - 15 - 2M	(100)	-	108.75	$5.78 \times 10^{-2}$	125.57
	(110)	53.55	62.52	$1.00 \times 10^{-1}$	
	(200)	47.75	54.02	$1.16 \times 10^{-1}$	
SBA - 15 - 4M	(100)	-	107.28	$5.86 \times 10^{-2}$	123.88
	(110)	51.97	62.03	$1.01 \times 10^{-1}$	
	(200)	45.31	53.65	$1.17 \times 10^{-1}$	
SBA - 15 - 1T	(100)	-	107.28	$5.86 \times 10^{-2}$	123.87
	(110)	51.97	62.03	$1.01 \times 10^{-1}$	
	(200)	46.50	53.65	$1.17 \times 10^{-1}$	
SBA - 15 - 2T	(100)	-	100.5	$6.25 \times 10^{-2}$	116.05
	(110)	51.97	58.39	$1.08 \times 10^{-1}$	
	(200)	45.31	50.58	$1.24 \times 10^{-1}$	
SBA - 15 - 4T	(100)	-	104.46	$6.01 \times 10^{-2}$	120.62
	(110)	53.55	60.61	$1.04 \times 10^{-1}$	
	(200)	46.50	52.59	$1.19 \times 10^{-1}$	

In Table - 7, the d - spacing values of the pure and functionalized samples are given in order to compare the values before and after the amoxicillin loading. According to the only article published about using SBA - 15 materials for amoxicillin delivery, the d - spacing values are

expected to increase after the drug loading process [40]. Moreover, an increase is observed in some samples while the others are the same after functionalization. Therefore, the expected change in the d - spacing values could not be observed because of instrumental limitations. The slit width is rather narrow and could not be changed. Also, the sample - detector distance could not be altered.

**Table - 7: d - spacing values of functionalized and amoxicillin loaded SBA - 15 samples**

Sample	(hkl)	d (Å)	Sample	(hkl)	d (Å)
Pure SBA - 15	(100)	-	Pure - x	(100)	-
	(110)	49.00		(110)	53.55
	(200)	44.18		(200)	46.50
SBA - 15 - 1A	(100)	-	1A - x	(100)	-
	(110)	53.55		(110)	50.49
	(200)	46.50		(200)	46.50
SBA - 15 - 2A	(100)	-	2A - x	(100)	-
	(110)	51.97		(110)	53.55
	(200)	45.31		(200)	46.50
SBA - 15 - 4A	(100)	-	4A - x	(100)	-
	(110)	51.97		(110)	53.55
	(200)	46.50		(200)	46.50
SBA - 15 - 1M	(100)	-	1M - x	(100)	-
	(110)	51.97		(110)	-
	(200)	46.50		(200)	47.75
SBA - 15 - 2M	(100)	-	2M - x	(100)	-
	(110)	53.55		(110)	53.55
	(200)	47.75		(200)	46.50
SBA - 15 - 4M	(100)	-	4M - x	(100)	-
	(110)	51.97		(110)	51.97
	(200)	45.31		(200)	47.75
SBA - 15 - 1T	(100)	-	1T - x	(100)	-
	(110)	51.97		(110)	51.97
	(200)	46.50		(200)	46.50
SBA - 15 - 2T	(100)	-	2T - x	(100)	-
	(110)	51.97		(110)	49.00
	(200)	45.31		(200)	44.18
SBA - 15 - 4T	(100)	-	4T - x	(100)	-
	(110)	53.55		(110)	-
	(200)	46.50		(200)	47.75

## 5. 2. 2. COMPARISON OF FUNCTIONALIZED SAMPLES

The powder pattern (Figure - 17) indicates that even after functionalization the samples preserve the less intense peaks. Although, the sample 2A is rather less intense than the sample 1A it still possesses the necessary peaks. The samples show similar arrangement while the only difference is their intensity. Due to the decrease in intensity (scattering power) and slight change in the position of the peaks it could be revealed that the functionalization of amine groups is successful. Furthermore, the amine groups are attached to the mesopore channels and the samples were grafted by these functional groups within their pores. Also, as a result of the elemental analysis it could be established that the optimum efficiency is 85 % which corresponds to the sample 1A (refer to Table - 8). And so, the sample 4A is less functionalized and its intensity is rather high than the other samples. In addition, the d - spacing (100) of the functionalized samples is smaller compared to the pure sample. Thus, the strong interaction of amine groups and the hydrophilic surfactant results in a decrease of d - spacing values due to the grafting within the channels of the porous structure [28].

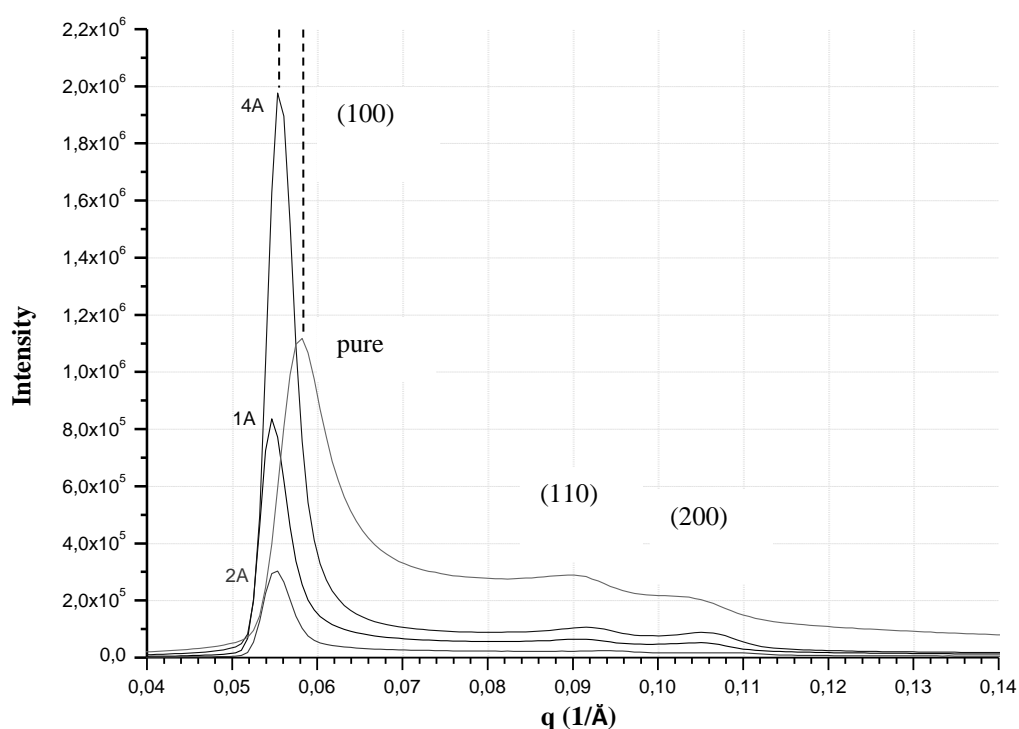
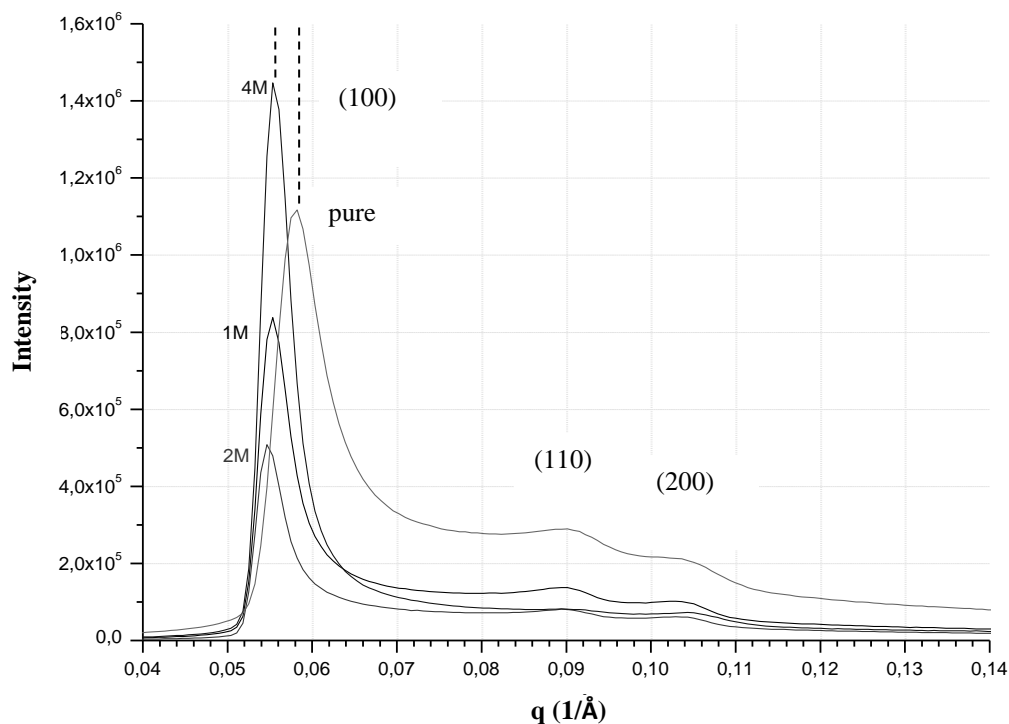


Figure - 17: SAXS pattern of pure and amine functionalized SBA – 15 samples



**Figure - 18: SAXS pattern of pure and thiol functionalized SBA – 15 samples**

Figure - 18 also shows a similar pattern, the d - spacing of the functionalized samples are smaller than the pure sample. The optimum functionalized sample is the sample 1M according to the pattern. However, the elemental analysis results show that 4M is the best functionalized sample due to its higher efficiency (refer to Table - 8). This might be due to several reasons: i) the highest functionalization might disrupt the ordered structure, ii) the outer surface of the pores might be grafted instead of the internal surface. Thus, the organic group would not attach to the pores because of its weak interaction and the d - spacing would not be lower. According to the table, the d - spacing values are similar to the pure sample. Therefore, the optimum functionalized sample is the sample 1M in this case as well [28].

The SAXS pattern of the methyl functionalized samples is quite different than the other two figures. The elemental analysis results established that the most efficient sample is 1T (23 %) while sample 2T (22.3 %) is quite similar as well (refer to Table - 8). According to the SAXS pattern, the intensity of sample 2T is rather low and the peaks (110) and (200) could not be detected. Thus, it could be said that the sample is grafted within the pores and that the hexagonal ordered structure is corrupted. In comparison to the other samples, sample 1T is promising; it preserves the peaks and the d - spacing value is the same as the pure sample. Although, its efficiency of functionalization was also quite low, this sample might be grafted on the outer surface by substitution of silanol groups with methyl groups.

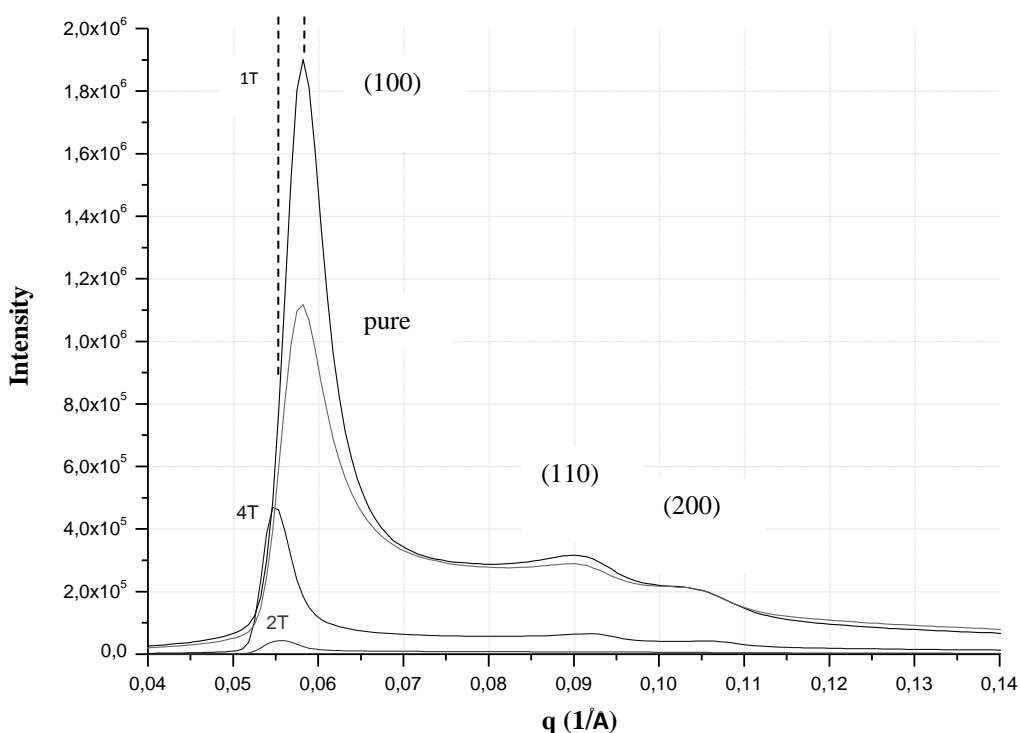


**Figure - 19: SAXS pattern of pure and methyl functionalized SBA – 15 samples**

In conclusion, the optimum sample for each type of functionalization is the 1 ml functionalized samples (1A, 1M and 1T). The hexagonal ordered structure could be preserved even after the silanol groups are substituted with other type of organic functional groups.

### 5. 3. ELEMENTAL ANALYSIS

The results of the elemental analysis reveal that the functionalization of certain samples is successful in terms of the efficiency. According to table, the most efficient functionalized sample is 1A with 85 % efficiency. Furthermore, between the thiol functionalized samples 4M with 62.3 % is the best choice for functionalization. In addition, the sample 1T is the most efficient sample of the methyl functionalized samples with 23 %. In comparison of the samples within the same type of functionalization the 1 ml functionalized samples are not the samples with the highest efficiency of functionalization. However, in account of all of the analyses, the samples 1A, 1M and 1T are the most promising samples for amoxicillin delivery.

**Table - 8: Elemental composition of functionalized SBA - 15 samples in terms of % C, % H, % N and % S**

<b>SAMPLE</b>	<b>% C</b>	<b>% H</b>	<b>% N</b>	<b>% S</b>	<b>EXPECTED</b>	<b>% EFFICIENCY</b>
<b>SBA - 15 - 1A</b>	7.45	2.43	2.61	-	3.07 % N	<b>85.0 %</b>
<b>SBA - 15 - 2A</b>	6.07	2.09	2.08	-	4.14 % N	<b>50.3 %</b>
<b>SBA - 15 - 4A</b>	7.06	2.42	2.45	-	5.00 % N	<b>49.0 %</b>
<b>SBA - 15 - 1M</b>	3.33	1.78	-	2.29	8.38 % S	<b>27.3 %</b>
<b>SBA - 15 - 2M</b>	5.67	1.97	-	4.16	11.06 % S	<b>37.6 %</b>
<b>SBA - 15 - 4M</b>	11.41	2.68	-	8.21	13.18 % S	<b>62.3 %</b>
<b>SBA - 15 - 1T</b>	0.73	1.50	-	-	3.18 % C	<b>23.0 %</b>
<b>SBA - 15 - 2T</b>	0.96	1.44	-	-	4.32 % C	<b>22.3 %</b>
<b>SBA - 15 - 4T</b>	0.68	1.33	-	-	5.26 % C	<b>13.0 %</b>

The elemental composition of the samples pure - x, 1A - x, 1M - x and 1T - x have been obtained by elemental analysis. The carbon, hydrogen, nitrogen and sulfur percentages within each of the samples have been obtained. The elemental composition of the pure sample establishes that the loaded amoxicillin is rather too low to be identified. As it is indicated in the table, the elemental composition of 1T - x is not quite different than the unloaded sample which is given in Table - 9. Also, it is possible to calculate the amount of amoxicillin loaded within the pure sample and 1T, by using other techniques such as UV spectroscopy. According to the table, the sample 1A - x was loaded with 19.1 % of the amoxicillin within its structure while the sample 1M - x was loaded with 25.5 % of amoxicillin. The values show consistence to the results of amoxicillin loading obtained from the UV analysis (refer to Table - 17). The amount of amoxicillin added into each sample is low and so it might not be detected as in the cases of the pure and methyl functionalized samples. Also, the calculations are only based on the nitrogen and sulfur percentages. In addition, the loading process is completed in aqueous phase while the results of the elemental composition are obtained from the solid samples after the filtration process. In fact, there might be some amoxicillin lost during the filtration. Although, there is an increase in the composition of each of the elements as it is expected.

**Table - 9: Elemental composition of 1 ml alkoxysilane functionalized SBA - 15 samples loaded with amoxicillin (%C, %H, %N and %S)**

<b>SAMPLE</b>	<b>% C</b>	<b>% H</b>	<b>% N</b>	<b>% S</b>	<b>EXPECTED</b>	<b>% EFFICIENCY</b>
<b>Pure - x</b>	2.46	1.68	-	-	-	-
<b>1A - x</b>	11.68	2.66	2.99	1.20	15.66 % N	<b>19.1 %</b>
<b>1M - x</b>	6.76	2.25	0.61	2.98	11.67 % S	<b>25.5 %</b>
<b>1T - x</b>	1.75	1.65	-	-	-	-

## 5. 4. THERMOGRAVIMETRIC ANALYSIS (TGA)

The loss in weight of each sample is mainly based on the weight loss due to the formation of oxides and gases such as CO<sub>2</sub>, NH<sub>3</sub>, N<sub>2</sub>, NO<sub>x</sub>, SO<sub>y</sub> and H<sub>2</sub>O. Therefore, the calculations are done taking in account the type of alkoxy silane used for the functionalization process of each sample. The calculated values are based on the assumption that certain gases are formed during the analysis. However, it is possible to gain information about the chemical formula of the gas using TGA + FTIR. And so, the exact weight loss could be determined.

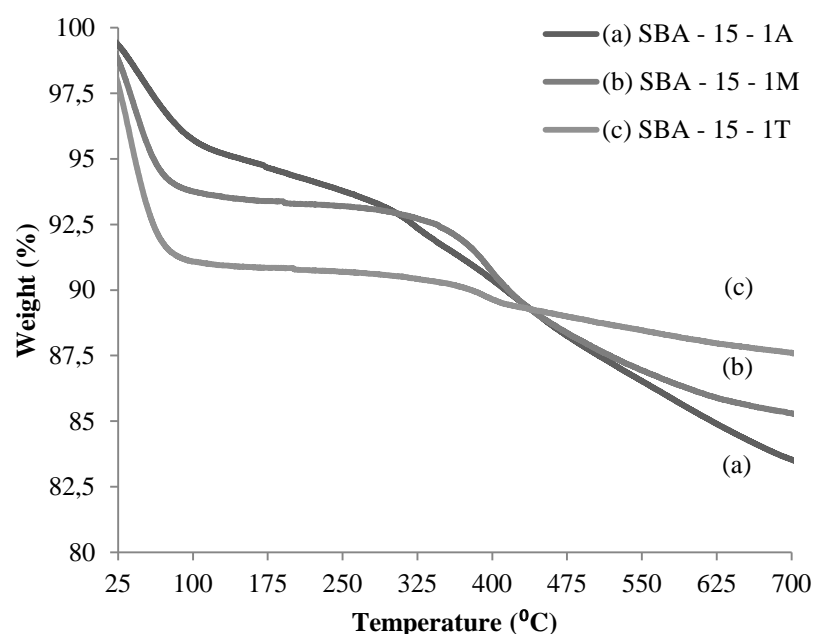


**Figure - 20: % Weight loss of SBA – 15 samples after functionalization**

**(SBA - 15 - 1A: 16.4 %, SBA - 15 - 1M: 14.6 % and SBA - 15 - 1T: 12.3 %)**

### 5. 4. 1. CALCULATIONS

#### SBA - 15 - 1A

1 g SBA - 15 + 0.946 g APTES = 1.946 g SBA - 15 - 1A (expected)

$$0.00427 \text{ moles} \times (44 \text{ g/mole CO}_2 + 17 \text{ g/mole NH}_3 + 18 \text{ g/mole H}_2\text{O}) = 0.3373 \text{ g loss}$$

$$0.34 \text{ g} \rightarrow 17.33 \% \text{ weight loss (expected result)}$$

$$0.32 \text{ g} \rightarrow 16.37 \% \text{ weight loss (experimental result)}$$

The efficiency of the functionalization has been calculated by using the results obtained from the elemental analysis and the expected values. Therefore, 85 % of the sample was functionalized and so, the experimental value is lower than the expected value.

### **SBA - 15 - 1M**

$$1 \text{ g SBA - 15} + 1.057 \text{ g MPTMS} = 2.057 \text{ g SBA - 15 - 1M (expected)}$$

$$0.00538 \text{ moles} \times (44 \text{ g/mole CO}_2 + 18 \text{ g/mole H}_2\text{O}) = 0.3336 \text{ g loss}$$

$$0.33 \text{ g} \rightarrow 16.22 \% \text{ weight loss (expected result)}$$

$$0.30 \text{ g} \rightarrow 14.59 \% \text{ weight loss (experimental result)}$$

According to the results of the elemental analysis only 27.3 % of the sample was functionalized. The experimental percentage weight loss is less than the expected value due to the low efficiency.

### **SBA - 15 - 1T**

$$1 \text{ g SBA - 15} + 0.895 \text{ g APTES} = 1.895 \text{ g SBA - 15 - 1T (expected)}$$

$$0.005 \text{ moles} \times (44 \text{ g/mole CO}_2 + 18 \text{ g/mole H}_2\text{O}) = 0.31 \text{ g loss}$$

$$0.31 \text{ g} \rightarrow 16.36 \% \text{ weight loss (expected result)}$$

$$0.23 \text{ g} \rightarrow 12.29 \% \text{ weight loss (experimental result)}$$

The efficiency of functionalization is 23 % which is rather low in comparison to the 1 ml functionalized samples. The % weight loss is also smaller than the expected value because of the low efficiency.

## 5. 5. FTIR SPECTRA

### 5. 5. 1. PURE AND FUNCTIONALIZED SBA - 15 SAMPLES

The functionalized samples have a similar FTIR spectrum; however, there is a slight difference in comparison to the pure silica sample. The asymmetric  $\text{NH}_2$  bending is observed at  $1602\text{ cm}^{-1}$ . Thus, the peak at  $1600\text{ cm}^{-1}$  which is divided into two other peaks indicates that an amine group is present as it is expected. It is known that IR adsorption bands related to the stretching vibrational mode of the silanol groups present on the surface are observed in the range  $3740 - 3500\text{ cm}^{-1}$ . The NH stretching generally is observed as a broad band at  $3380 - 3310\text{ cm}^{-1}$ . In addition, the silanol groups which remain from the calcination process (hydroxyl groups on the silica surface) also appear as a broad band at  $3500 - 3000\text{ cm}^{-1}$ . Therefore, it is no possible to distinguish these absorption bands and so, the asymmetric  $\text{NH}_2$  bending becomes important in understanding whether an amine group is present or not [47].

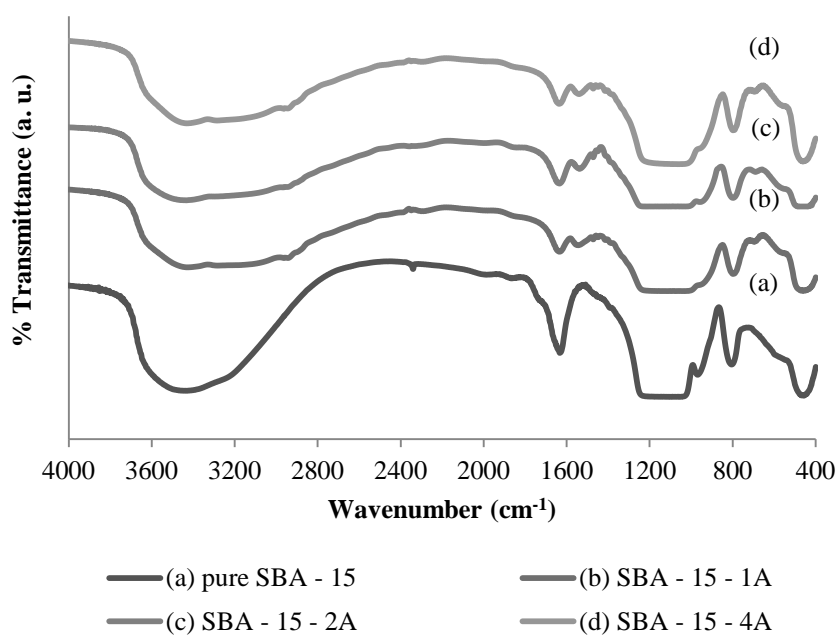
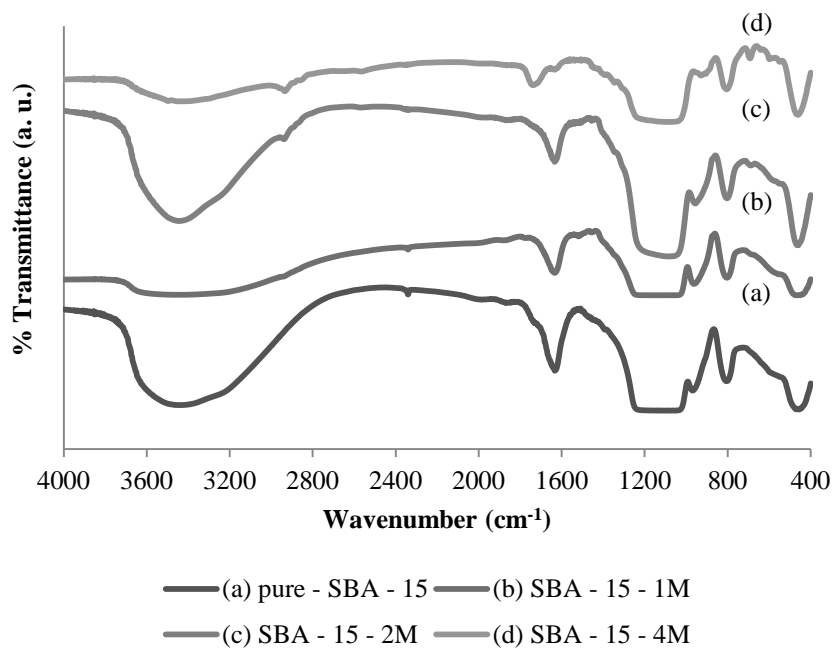
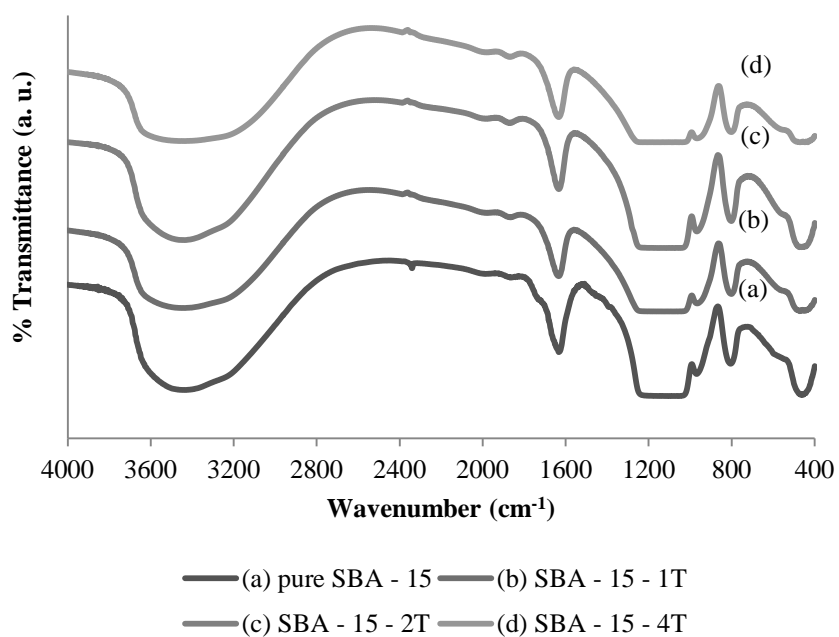


Figure - 21: FTIR spectra of pure silica and amine functionalized samples



**Figure - 22: FTIR spectra of pure silica and thiol functionalized samples**



**Figure - 23: FTIR spectra of pure silica and methyl functionalized samples**

The FTIR spectrum establishes that the broad band related to the silanol groups at the range between  $3800 - 2800 \text{ cm}^{-1}$  is quite different after functionalization with thiol groups while the methyl functionalized samples are similar to each other. The reason of this is due to the functionalization efficiency of the samples. The maximum efficiency of the methyl functionalized samples is 23 % while for thiol functionalized samples it is 62.3 %. As a result, the destruction of the band indicates the success of grafting.

### 5. 5. 2. AMOXICILLIN LOADED SBA - 15 SAMPLES

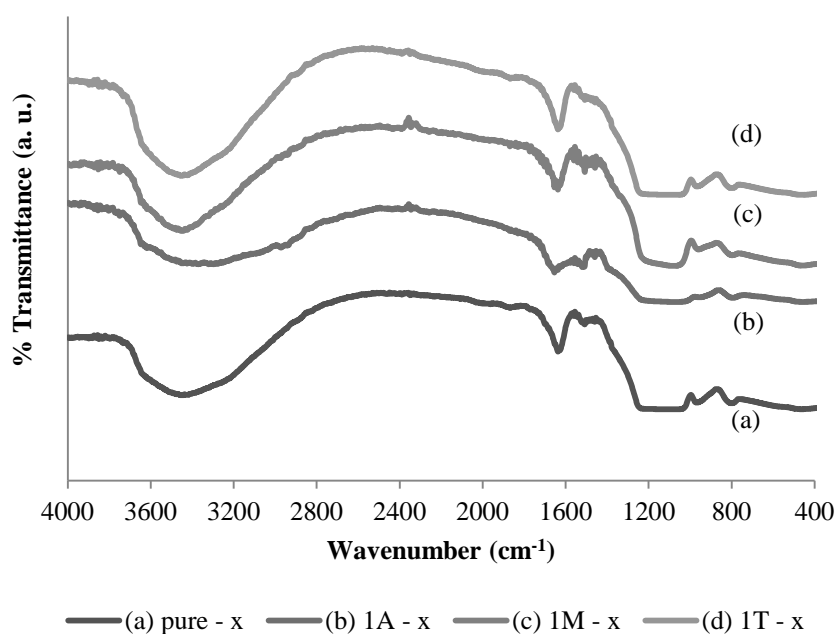


**Figure - 24: FTIR spectra of amoxicillin loaded and 1 ml functionalized SBA - 15 samples**

The FTIR spectrum of 1 ml functionalized samples is given in Figure - 24. As it could be observed in the graph, the samples show a similar spectrum as the pure silica sample. The only difference is the broadness of the peak at around  $3800 - 2800 \text{ cm}^{-1}$ . Also, there is a peak which is divided at around  $1600 \text{ cm}^{-1}$  indicating that an amine group is present in the structure of the samples which is due to the amoxicillin.

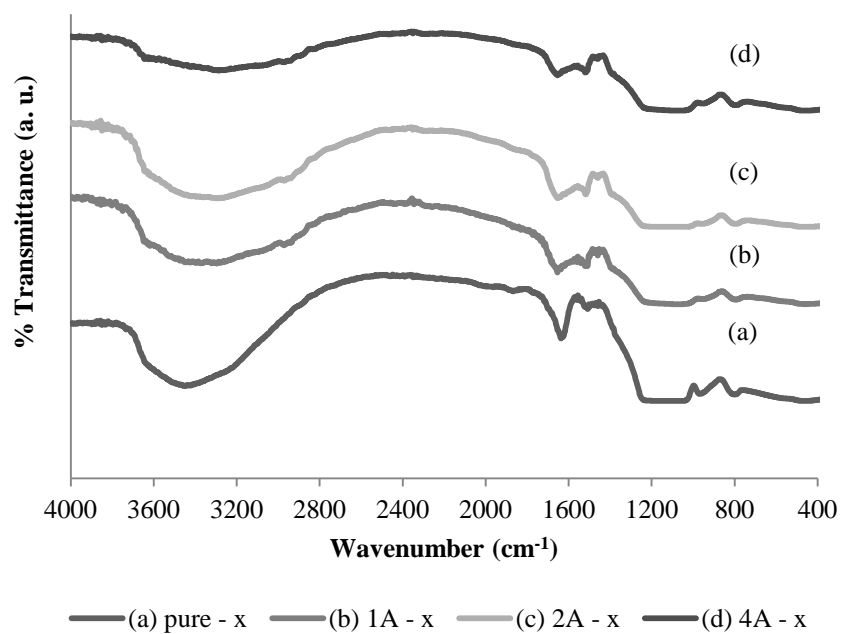


Figure - 25: FTIR spectra of amoxicillin loaded amine functionalized SBA - 15 samples

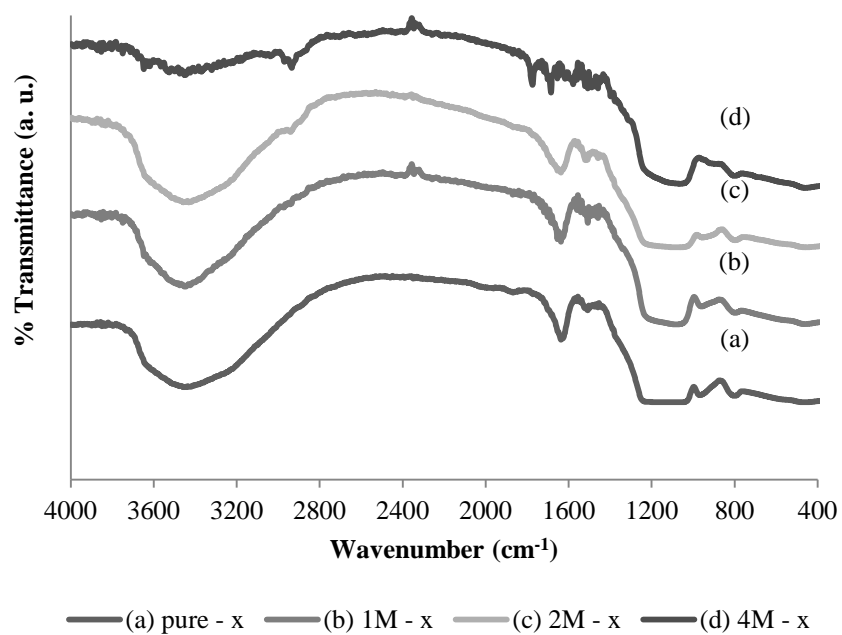
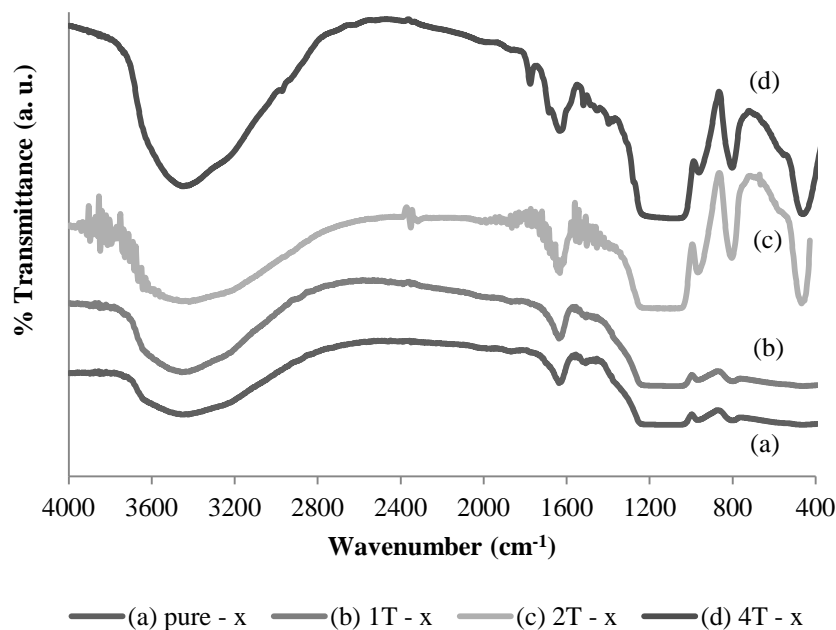


Figure - 26: FTIR spectra of amoxicillin loaded thiol functionalized SBA - 15 samples



**Figure - 27: FTIR spectra of amoxicillin loaded methyl functionalized SBA - 15 samples**

The peak at around  $1555\text{ cm}^{-1}$  could be attributed to the interaction between the carboxyl group ( $-\text{COOH}$ ) of amoxicillin and the amine group ( $-\text{NH}_2$ ) of the functionalized sample which reveals that the bond  $\text{COO}^- - \text{NH}_3^+$  is present after the drug loading. It is demonstrated that the bonding resulting from the silanol groups and the drug ( $\text{OH} - \text{COO}^-$ ) is weaker compared to the  $\text{COO}^- - \text{NH}_3^+$  bond [47, 50].

The broader band at around  $1100\text{ cm}^{-1}$  is attributed to the Si - O - Si asymmetric vibration while the peak at around  $800\text{ cm}^{-1}$  is present due to the symmetric vibration. The smaller peaks at around  $400\text{ cm}^{-1}$  could be related to the deformation modes of the Si - O - Si. Also, the band at around  $950\text{ cm}^{-1}$  could be assigned as the Si - OH bending [51]. It was established that all samples show a similar FTIR spectra after loading amoxicillin. The only difference in the spectra of each sample was the broadness of the similar peak. Therefore, it could be concluded that after the samples are loaded with the drug the linkages between the drug and silica are not quite different than the earlier bonds present.

## 5. 6. N<sub>2</sub> - ADSORPTION - DESORPTION ANALYSIS

### 5. 6. 1. SURFACE CHARACTERIZATION (BET ISOTHERMS)

In order to determine the pore size distribution gas adsorption is used to obtain adsorption and desorption isotherms. The volume of gas adsorbed or desorbed is measured at constant temperature and over a wide range of pressures. The calculation of the pore size distribution is based on the chosen model which might be cylindrical pores, wedge - shaped pores or ink - bottle pores. The type of isotherm branch (adsorption or desorption) which would be used for the calculation must also be decided. At the end of the desorption process, a residual layer is left due to the gas emptying from the cores of the pores. Thus, the thickness of the layer must be known in order to calculate the pore size distribution [52].

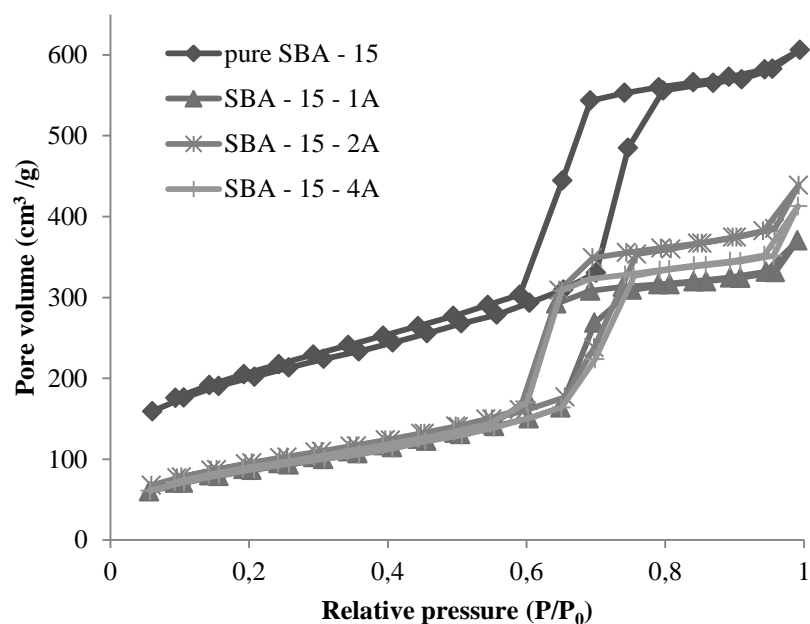


**Figure - 28: BET isotherms of pure and amine functionalized SBA - 15 samples**

In the figure above the BET isotherms of the pure sample and the amine functionalized samples are given. According to the graph, a large hysteresis loop is observed at  $(P/P_0) = 0.6$  which is also the pore - filling step. Also, it could be stated that it is similar to most of the isotherms given in the literature [40, 47, 53].

As a result of the difference in the radii curvature difference during adsorption and desorption a hysteresis loop occurs between the two branches of the isotherm. The desorption branch is thermodynamically more stable in comparison to the adsorption branch. Thus, it is more likely to use the desorption branch for the pore size determination [54]. SBA - 15 materials consist of pores as in the ink - bottle pore model.

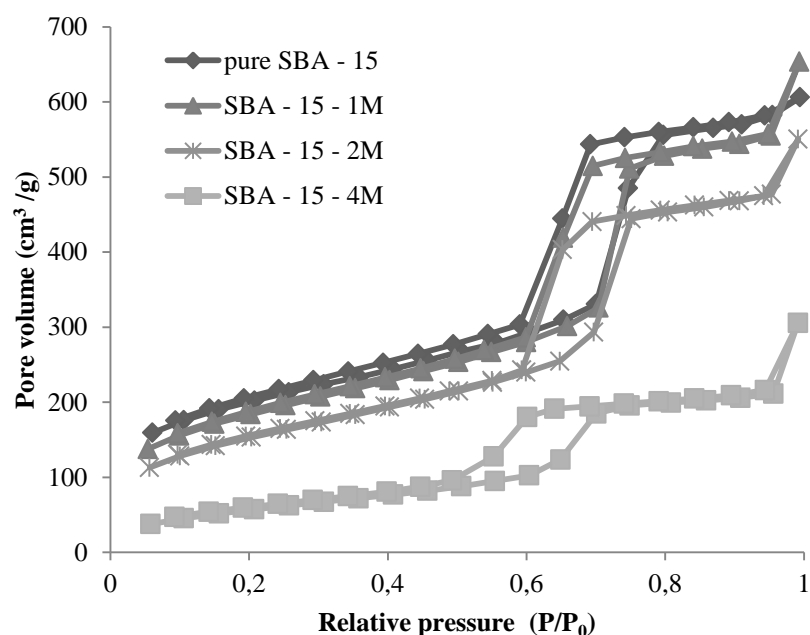


**Figure - 29: BET isotherms of pure and thiol functionalized SBA - 15 samples**

The large hysteresis loop of the isotherm in the figure above is at  $(P/P_0) = 0.6$ . The isotherms are type IV which is the characteristic of mesoporous materials. It has been reported that SBA - 15 materials synthesized by post-grafting method show a sharp increasing step with a typical H1 hysteresis loop. The sharpness is related to the narrow pore size distribution and highly ordered mesostructure [47]. As it could be seen in Figure - 29 the 4 ml MPTMS functionalized sample is not as sharp as expected which could be corresponded to the high efficiency of functionalization. Thus, the mesostructure might slightly be disrupted and so the broader isotherm is observed. Also, the broadness might be attributed to the lower volume of adsorption. The methyl functionalized samples show a similar trend with the pure sample. It could be observed in Figure - 30 that the isotherms of each of the samples are similar and have a sharp hysteresis loop at  $(P/P_0) = 0.6$ .

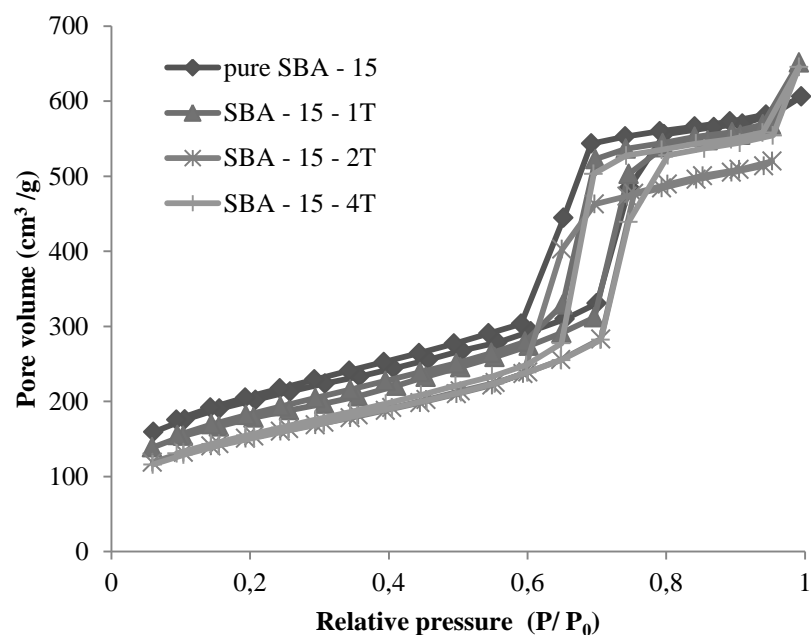


Figure - 30: BET isotherms of pure and methyl functionalized SBA - 15 samples

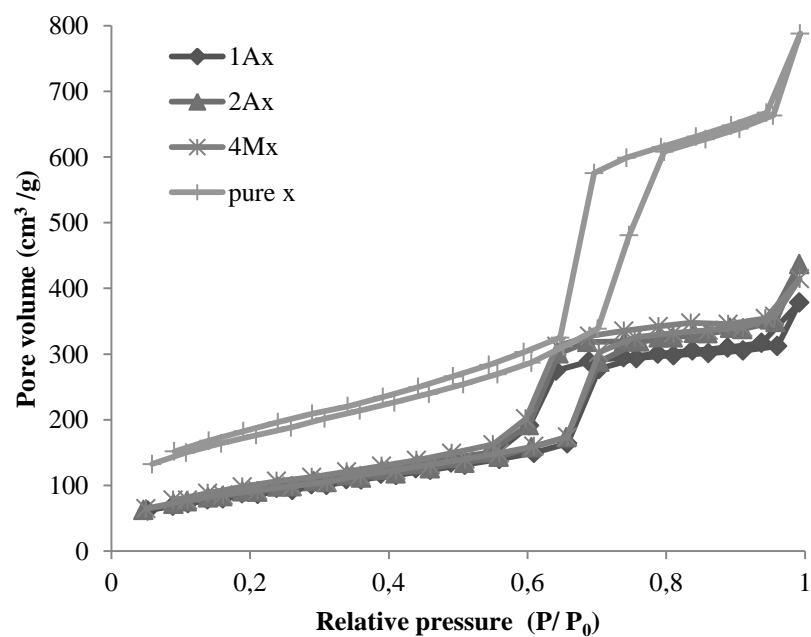
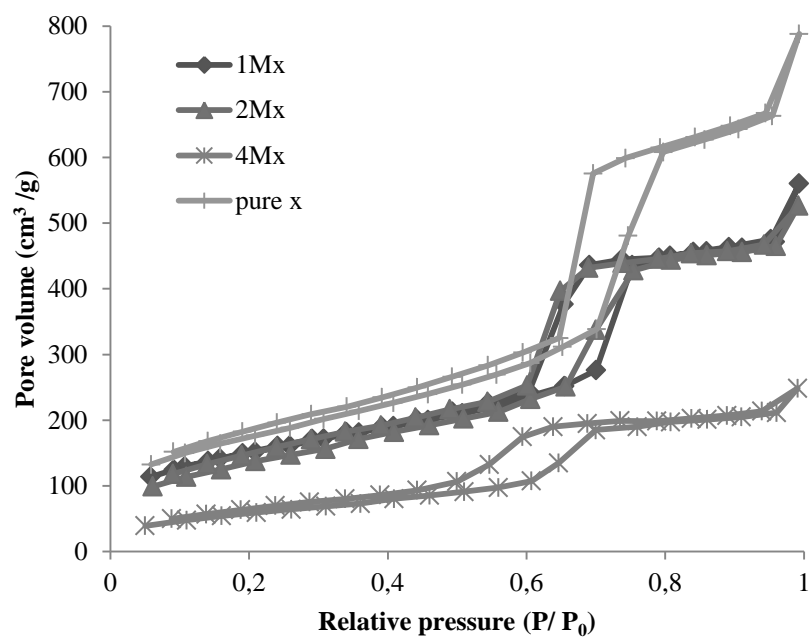
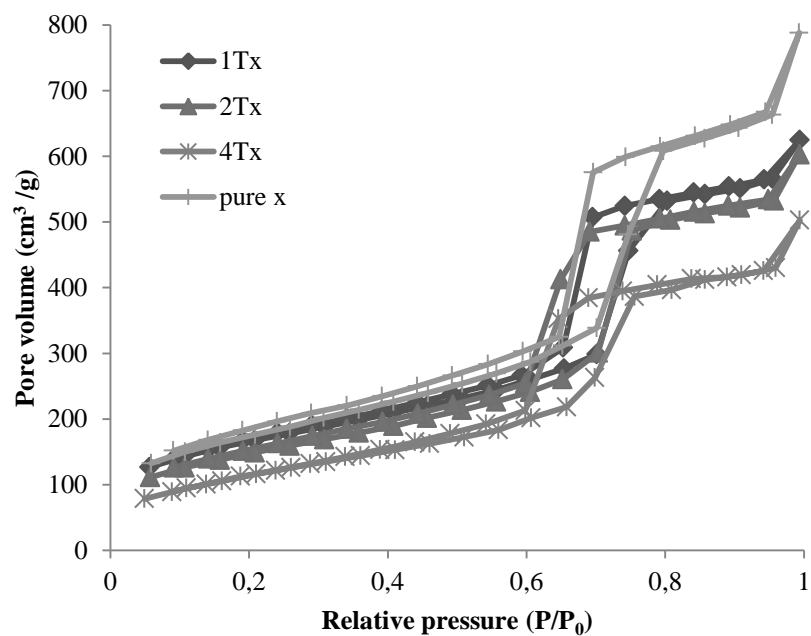


Figure - 31: BET isotherms of amoxicillin loaded pure and amine functionalized SBA - 15 samples



**Figure - 32: BET isotherms of amoxicillin loaded pure and thiol functionalized SBA - 15 samples**



**Figure - 33: BET isotherms of amoxicillin loaded pure and methyl functionalized SBA - 15 samples**

All of the isotherms of the amoxicillin loaded samples are similar to the unloaded samples. The only difference observed within the figures is related to desorption branch of the pure sample loaded with amoxicillin. In addition, the pore volumes have changed after the loading. Although, the relative pressure at which the pore - filling begins is remained.

In order to analyze each of the samples before and after functionalization and after the loading process; the pore size, pore volume and surface area are all indicated in Table - 10, Table- 11 and Table - 12 respectively.

**Table - 10: The pore size data of the pure and functionalized samples before and after amoxicillin loading**

<b>PORE SIZE DATA</b>	<b>Pure</b>	<b>1A</b>	<b>2A</b>	<b>4A</b>	<b>1M</b>	<b>2M</b>	<b>4M</b>	<b>1T</b>	<b>2T</b>	<b>4T</b>
BJH Method Adsorption Pore Diameter (nm)	7.824	7.161	6.581	7.881	7.834	7.790	6.559	7.696	7.942	7.806
<b>PORE SIZE DATA</b>	<b>Pure<sub>x</sub></b>	<b>1Ax</b>	<b>2Ax</b>	<b>4Ax</b>	<b>1Mx</b>	<b>2Mx</b>	<b>4Mx</b>	<b>1Tx</b>	<b>2Tx</b>	<b>4Tx</b>
BJH Method Adsorption Pore Diameter (nm)	7.768	6.669	6.666	6.674	7.858	6.623	6.528	7.772	7.884	7.888

The pore size data illustrates that due to the decrease in the pore size the functionalization is mostly completed by grafting the internal pores except for the samples 4A and 2T. The efficiency of the functionalization of these samples were rather low than the other samples. Thus, it might be due to the grafting of the outer surface of the pores [47].

After the amoxicillin is loaded within the mesoporous structures the pores get smaller than the unloaded samples except for the samples 1M, 1T and 4T. Thus, it might be a result of poor adsorption of the drug within the pores.

In comparison between the amoxicillin loaded functionalized samples and the amoxicillin loaded pure sample, the pore diameter is decreased for most of the samples. However, the methyl functionalized samples have larger pores. The reason of this could be also related to the attachment of the amine groups of amoxicillin onto the outer surface of the pores.

**Table - 11: The pore volume data of the pure and functionalized samples before and after amoxicillin loading**

<b>PORE VOLUME DATA</b>	<b>Pure</b>	<b>1A</b>	<b>2A</b>	<b>4A</b>	<b>1M</b>	<b>2M</b>	<b>4M</b>	<b>1T</b>	<b>2T</b>	<b>4T</b>
BJH Method Cumulative Adsorption Pore Volume (cm <sup>3</sup> /g)	1.037	0.601	0.702	0.664	0.996	0.853	0.501	0.973	0.782	0.986
<b>PORE VOLUME DATA</b>	<b>Pure<sub>x</sub></b>	<b>1Ax</b>	<b>2Ax</b>	<b>4Ax</b>	<b>1Mx</b>	<b>2Mx</b>	<b>4Mx</b>	<b>1Tx</b>	<b>2Tx</b>	<b>4Tx</b>
BJH Method Cumulative Adsorption Pore Volume (cm <sup>3</sup> /g)	1.216	0.599	0.694	0.660	0.856	0.835	0.407	0.949	0.931	0.806

The values given in Table - 11 reveal that after functionalization the pore volume is decreased. And so, this could be attributed to the successful grafting of the organic functional groups [53]. Although, the slight decrease in the pore volume of certain samples (1M, 1T and 4T) indicate less adsorption of the functional groups within the internal surface of the pores.

In comparison to the pure amoxicillin loaded sample, the functionalized and amoxicillin loaded samples possess a rather smaller pore volume. The decrease in the pore volume of the functionalized samples could be corresponded to the success in grafting and the anchoring of amoxicillin within the pores instead of the outer surface.

Also, it is established that the loading after functionalization results in lower pore volume. The pure sample and 1T are the only ones which the pore volume has increased after the drug loading. The reason of this might be due to the attachment of amoxicillin onto the outer surface of these samples. Therefore, the results are as expected. The pore volume must be lower after functionalization and drug loading.

**Table - 12: The surface area data of the pure and functionalized samples before and after amoxicillin loading**

<b>SURFACE AREA DATA</b>	<b>Pure</b>	<b>1A</b>	<b>2A</b>	<b>4A</b>	<b>1M</b>	<b>2M</b>	<b>4M</b>	<b>1T</b>	<b>2T</b>	<b>4T</b>
Multipoint BET (m <sup>2</sup> /g)	700.9	314.0	344.3	315.1	644.3	539.9	215.0	604.6	529.9	527.5
<b>SURFACE AREA DATA</b>	<b>Pure<sub>x</sub></b>	<b>1Ax</b>	<b>2Ax</b>	<b>4Ax</b>	<b>1Mx</b>	<b>2Mx</b>	<b>4Mx</b>	<b>1Tx</b>	<b>2Tx</b>	<b>4Tx</b>
Multipoint BET (m <sup>2</sup> /g)	621.3	309.9	325.9	325.4	528.9	486.9	216.1	578.3	522.1	421.4

The results reveal that after the functionalization the surface area is decreased and also after loading the samples with amoxicillin the surface area is decreased even more. Although, there are some exceptions such as the samples 4A and 4M which have a larger surface area in comparison to the unloaded samples. The reason of this might be either poor grafting on the internal surface or poor adsorption of amoxicillin within the pores.

As a result, the changes in pore size, pore volume and surface area are not quite different than expected. After the drug loading process, most of the samples result in smaller pore volume and surface area. Also, the samples have smaller pore sizes in comparison to their amoxicillin loaded versions. Therefore, the pore size distribution and the changes within the pore size, pore volume and surface area of the samples are as expected [40, 47, 53].

### 5. 6. 2. PORE SIZE DISTRIBUTION (BJH METHOD)

The pore size distribution was calculated using the desorption branch of the isotherms. SBA - 15 particles are highly ordered and possess a narrow pore size distribution. The figures of the pore size distribution establish the narrow size distribution. According to Figure - 34, the amine functionalized samples are distributed in the same range between 4.5 and 7.0 nm. Also, it could be observed that the pure sample has a broader distribution. This indicates that the grafting also narrowed the pore size distribution.

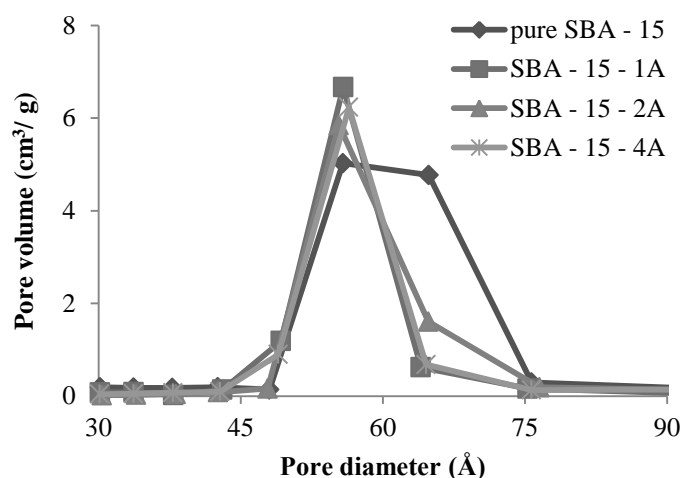


Figure - 34: Pore size distribution of pure and amine functionalized SBA - 15 samples

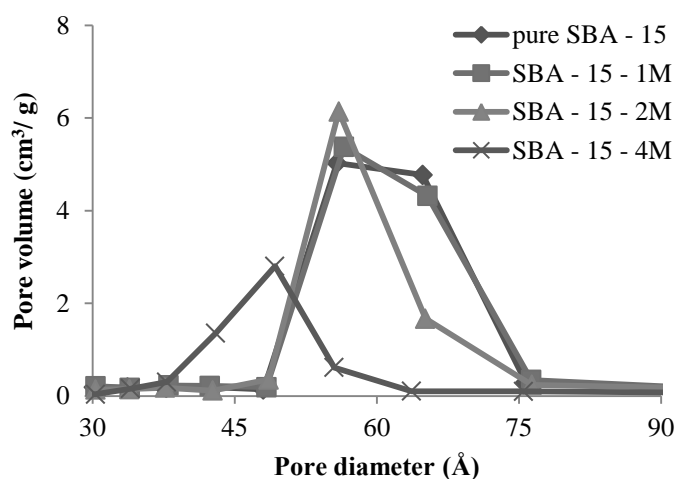
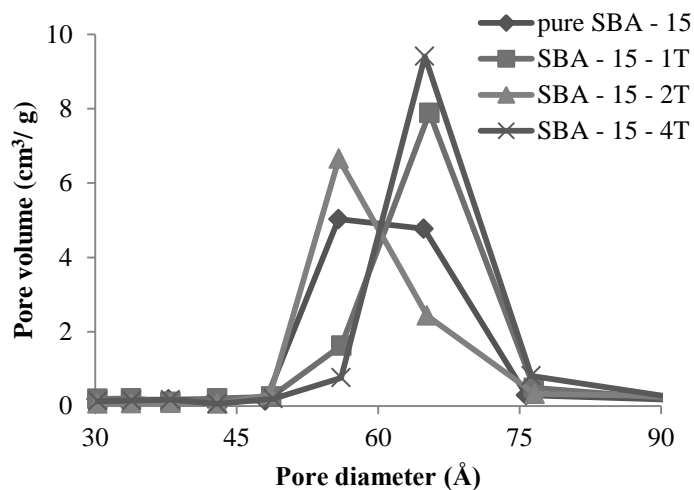


Figure - 35: Pore size distribution of pure and thiol functionalized SBA - 15 samples

The pore size distribution of the thiol functionalized samples reveals that the higher efficiency of functionalization results in narrower distribution at the range 4.5 - 7.0 nm. The distribution of the pore size of the sample 4M is broader and in the range 3.0 - 6.0 nm while the hysteresis loop of its isotherm is also broad.



**Figure - 36: Pore size distribution of pure and methyl functionalized SBA - 15 samples**

The pore size of the methyl functionalized samples is distributed in a narrow range 4.5 nm - 7.0 nm. The 2 ml TEMS functionalized sample is less ordered due to its broader distribution.

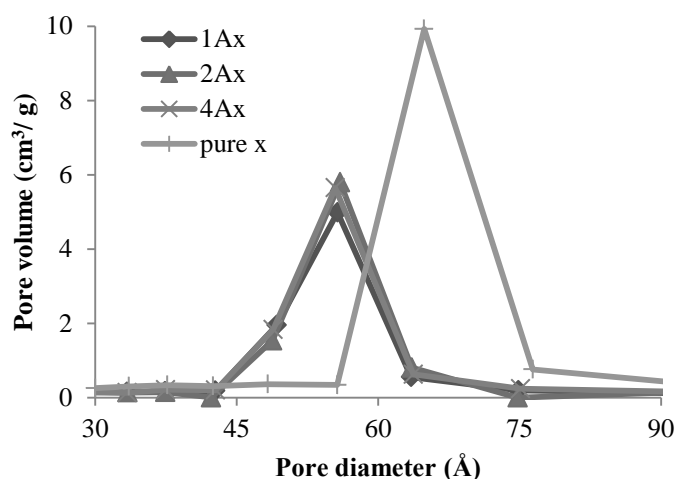


**Figure - 37: Pore size distribution of amoxicillin loaded pure and amine functionalized SBA - 15 samples**

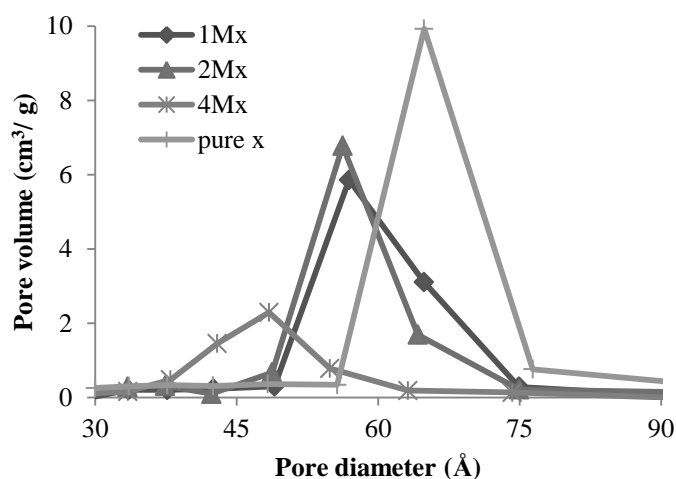


**Figure - 38: Pore size distribution of amoxicillin loaded pure and thiol functionalized SBA - 15 samples**

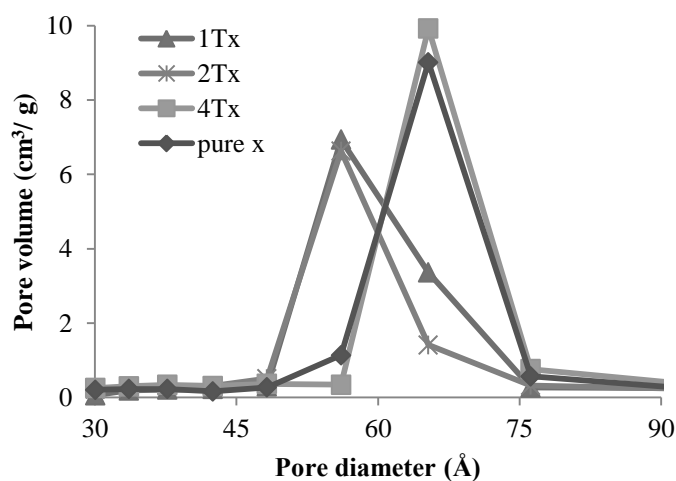


**Figure - 39: Pore size distribution of amoxicillin loaded pure and methyl functionalized SBA - 15 samples**

The amoxicillin loading of each sample has resulted in much narrower pore size distribution. All of the samples are in the same range of pore size even after the loading process.

## 5. 7. TEM MICROGRAPHS

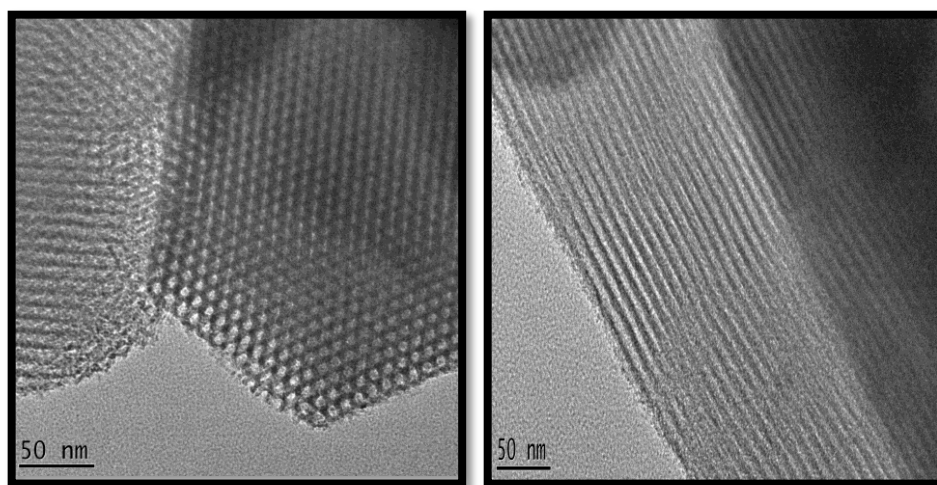


**Figure - 40: TEM micrographs of pure SBA - 15 sample**

The micrographs of the synthesized material prove that the highly ordered hexagonal mesoporous structure is present before any further application (functionalization). It is illustrated in several reports that the hexagonal array of these type of materials are highly ordered and stable [7, 47]. Thus, these micrographs also support this idea.

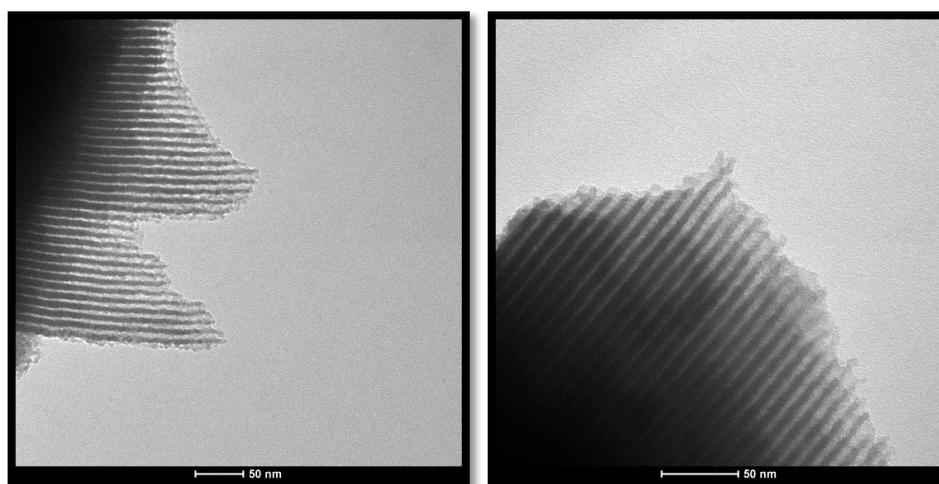


**Figure - 41: TEM images of SBA - 15 - 1A**

The TEM images of the 1 ml APTES functionalized samples still preserve the hexagonal mesostructure even after the functionalization. Also, the pore distances have been calculated and the average value is 7.9 nm. In addition, the scale bar of the micrographs is 50 nm.

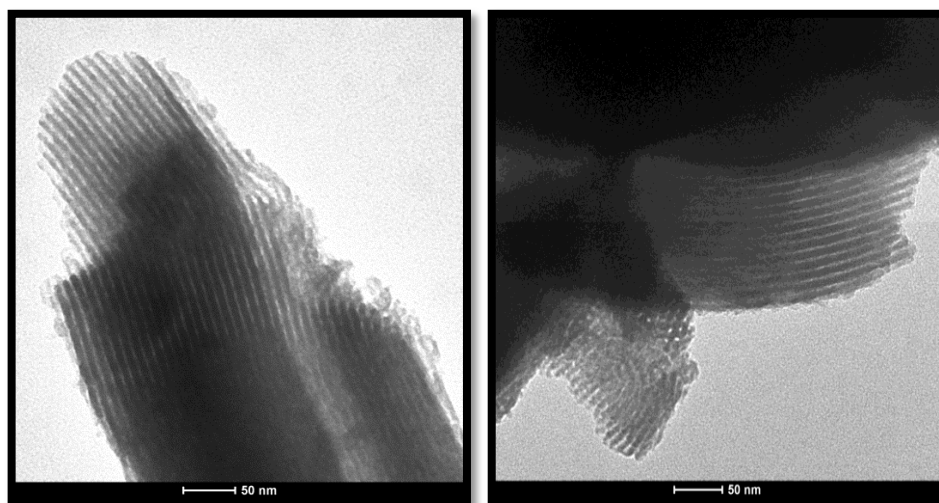


**Figure - 42: TEM images of SBA - 15 - 2A**

The micrographs reveal that the pore channels are still highly ordered. Although, the honeycomb structure present in the pure sample is slightly disrupted, the hexagonal array is observed. The calculated average pore distance is 9.1 nm.

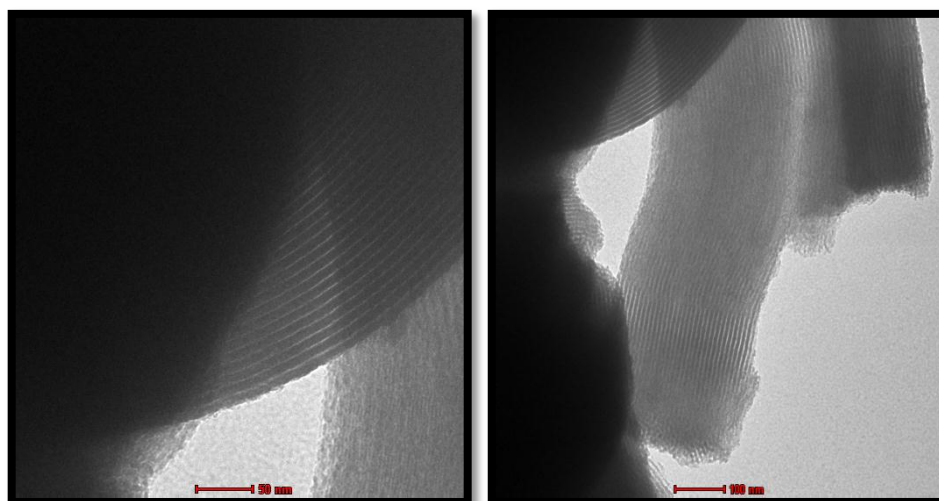


**Figure - 43: TEM micrographs of SBA - 15 - 4A**

According to the micrographs in Figure - 43, the sample contains mesoporous channels after the functionalization and the calculated pore distance is 9.2 nm which is similar to the value obtained for the other samples.

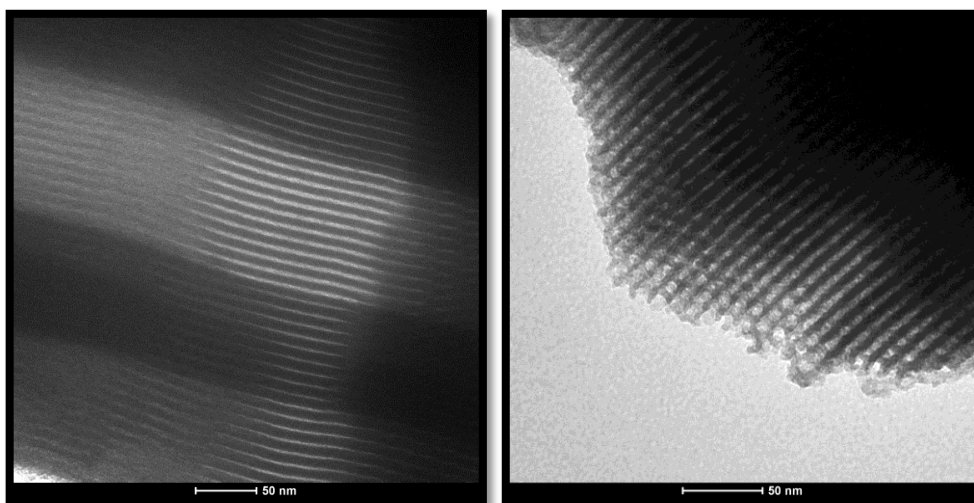


**Figure - 44:TEM micrographs of SBA - 15 - 1M**

The micrographs above show that the 1 ml MPTMS functionalized samples conserve the well - defined mesopores and honeycomb structure. In addition, the calculated pore distance value is 7.7 nm.

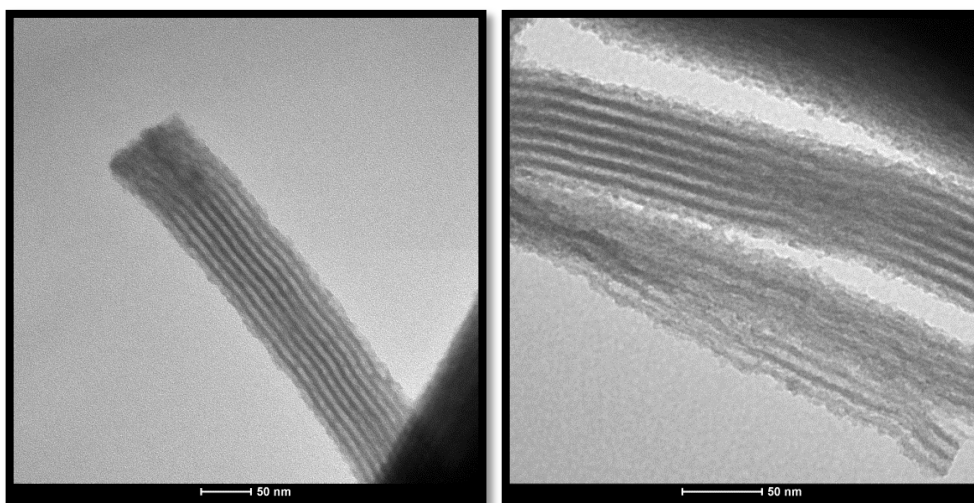


**Figure - 45:TEM micrographs of SBA - 15 - 2M**

The sample consists of mesoporous channels even after post - grafting the surface of the pores. According to the figure above, the average calculated pore distance is 10 nm and it is similar to the other calculated values.

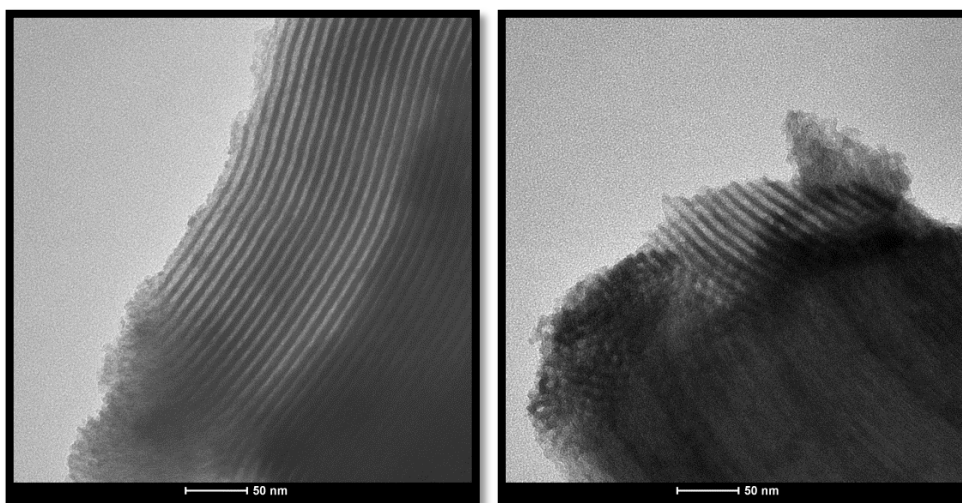


**Figure - 46:TEM micrographs of SBA - 15 - 4M**

The average calculated pore distance of the sample is 9.8 nm and it still exhibits the mesostructure after functionalization. Therefore, SBA - 15 samples are highly stable and their mesoporous channels are highly ordered.

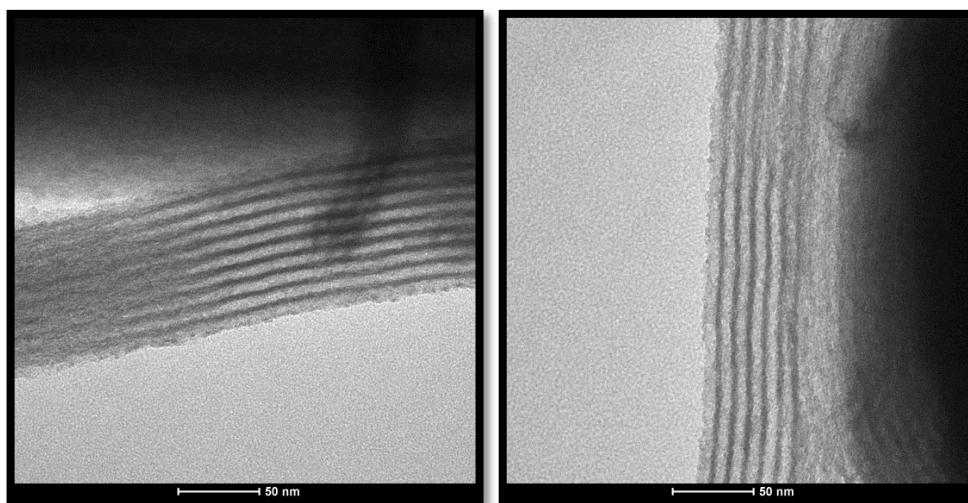


**Figure - 47:TEM micrographs of SBA - 15 - 1T**

The TEM images prove that the hexagonal array is highly stable and post grafting method is nearly a non - destructive method. The average pore distance is 8.7 nm which is similar to the values obtained from the other micrographs.

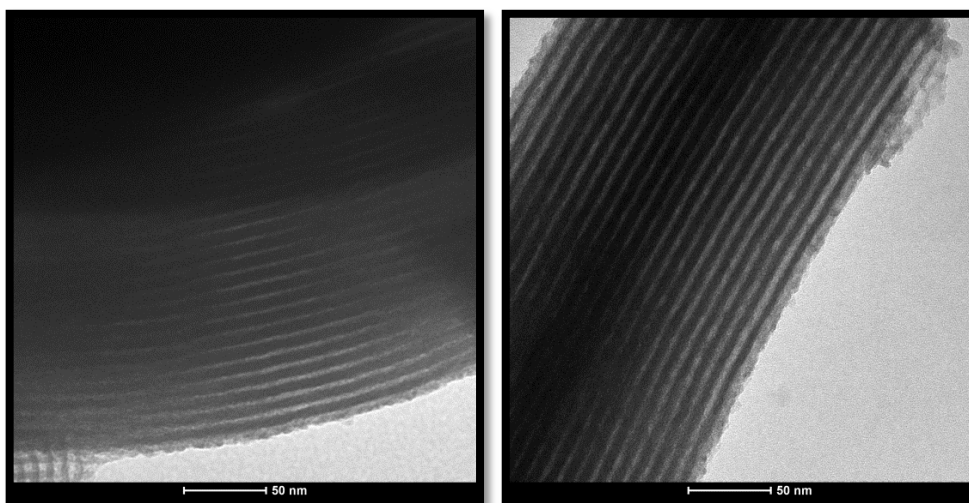


**Figure - 48:TEM micrographs of SBA - 15 - 2T**

The micrographs above indicate that the mesostructure is conserved after functionalization. The average pore distance is 9.7 nm which is also similar to the other calculated values using the micrographs.

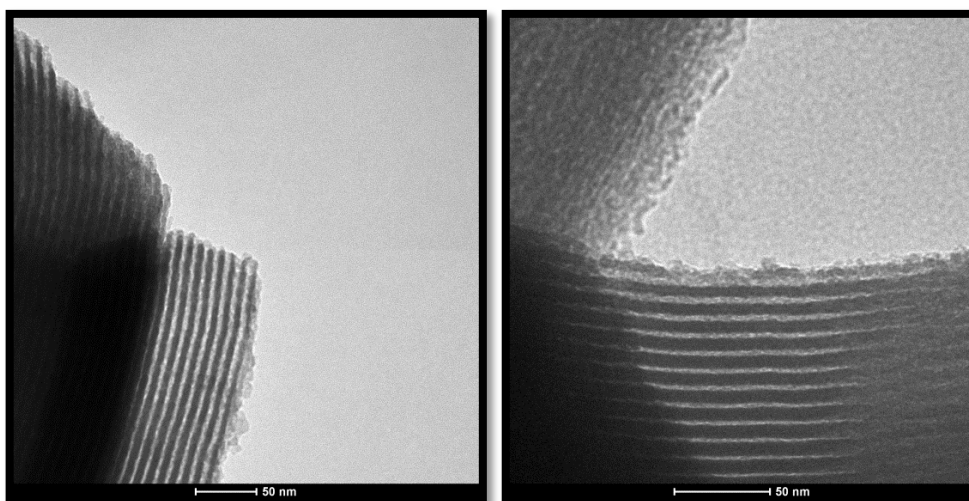


**Figure - 49:TEM micrographs of SBA - 15 - 4T**

The average measured pore distance of these functionalized materials is 8.6 nm. It is possible that the sample could possess the mesophase as in the pure sample even after it is functionalized. It is reported that SBA - 15 particles are highly stable and that these particles are potential hosts for guest molecules such as drugs [47].

## 5. 8. SOLID - STATE $^{29}\text{Si}$ - NMR SPECTRA

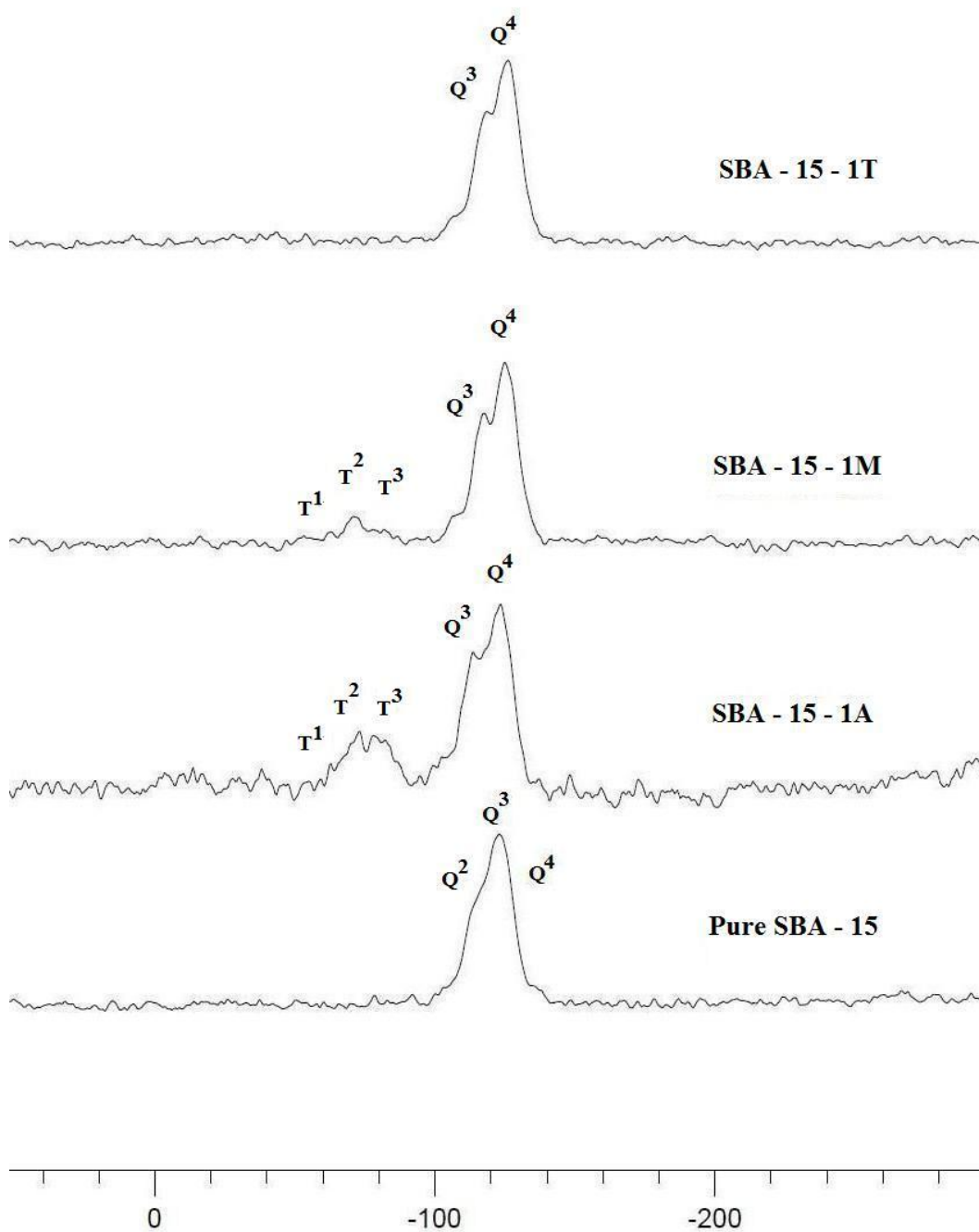


Figure - 50:  $^{29}\text{Si}$  - MAS - NMR spectra of the pure and 1 ml functionalized samples

The solid - state  $^{29}\text{Si}$  - MAS - NMR measurement has only been performed for the pure SBA - 15 sample and the 1 ml alkoxysilane functionalized samples. The obtained NMR spectra are given in Figure - 50. In order to characterize the chemistry and structural properties of the surface of the functionalized silicas, it is compulsory to find the best technique for the determination of certain properties and application areas. Therefore,  $^{29}\text{Si}$  - NMR would be a useful technique in order to obtain information about the surfaces of siliceous materials and the number of the silanols present on the surface [11].

The solid - state MAS - NMR analysis gives only information regarding qualitative analysis, while CP - NMR is both a quantitative and qualitative analysis. In comparison to the cross - polarization (CP) solid - state NMR analysis, magic - angle spinning (MAS) - NMR is less used. The main purpose of this technique is to eliminate the problems related to the chemical shift anisotropy and heteronuclear dipolar - coupling effects [55]. However, only the MAS technique is applied at the Central Laboratory for solid - state -  $^{29}\text{Si}$  - NMR.

It has been proven that high - resolution  $^{29}\text{Si}$  - NMR is an efficient technique to determine the structure of silicic acids and silicate anions in solutions.  $^{29}\text{Si}$  chemical shifts in silicate materials must be within the range of - 60 and - 120 ppm. The weak, overlapped and excess NMR lines are a result of the dipolar interactions and the anisotropy of the chemical shifts. There are several reports of solid silicates and aluminosilicates in the literature that also include the results of high - resolution  $^{29}\text{Si}$  NMR spectra [56].

The peak signals of a solid - state  $^{29}\text{Si}$  - MAS - NMR spectra could be assigned as M, D, T and Q (mono, di, tri and quartet). The M signal is observed as a result of the termination of the polymer. On the contrary, the D signals arise from the polymer backbone  $[\text{SiO}_2(\text{CH}_3)_2]_n$ . The T signals are due to the Si - C linkages  $[\text{T}^n = \text{RSi}(\text{OSi})_n(\text{OH})_{3-n}]$  while the Q signals are observed resulting from the Si - O bonds  $[\text{Q}^m = \text{Si}(\text{OSi})(\text{OH})_{4-m}, m = 2-4]$ . The indices n and m represent the number of oxo bridges. Trialkoxysilanes were used in the functionalization process and so the siloxane groups functionalized on the surface are classified as in the following: i)  $\text{T}^1$ : isolated groups ii)  $\text{T}^2$ : terminal groups and iii)  $\text{T}^3$ : crosslinked groups. The success of the grafting could be established by the presence of the crosslinked siloxane groups which also indicate that the coverage is close to monolayer. Furthermore, the silanol

groups could be attributed to the Q signals. Q<sup>2</sup> signals are observed in the presence of geminal silanols while Q<sup>3</sup> signals are due to the single silanol groups. Both of these signals arise from the silicons on the surface of the pore walls which result from incomplete condensation. In contrast, the Q<sup>4</sup> signals arise from the fully condensed siloxane groups present within the silica network of the interior mesoporous walls. Therefore, the presence of the signals T<sup>3</sup>, Q<sup>3</sup> and Q<sup>4</sup> reveal the success of the grafting process [57 - 61].

The pure sample shows a broad resonance over the range for Q<sup>2</sup>, Q<sup>3</sup> and Q<sup>4</sup> silicon atoms while the other three samples exhibit a resonance which could be differentiated. The intensity of the Q<sup>2</sup> silicon atoms of the functionalized samples are lower compared to the Q<sup>3</sup> silicon atoms as expected. The Q<sup>2</sup> silicon atoms which show very low intensity in the pure sample totally disappear after the functionalization process as expected. Therefore, the Q<sup>3</sup> and Q<sup>4</sup> silicon atoms could only be considered. The quantification related to the NMR spectra would not be useful to distinguish the silicon atoms on the surface of the micropores and mesopores. In comparison to the pure sample all of the functionalized samples exhibit a similar intensity [62]. In addition, T signals are observed in the NMR spectra of the modified samples. Although, the intensity of these signals are rather low compared to the Q signals. Besides, these are only observed in the amine and thiol functionalized samples. The T signals arise from the Si - C linkages of silicon atoms while the Q signals are present due to the silanol groups remaining on the surfaces of silica samples. Therefore, the pure sample contains a large amount of residual silanol groups. On the other hand, the amine and thiol functionalized samples possess Si - C bonds within their structure which are indicated by the broad T signals while the methyl functionalized sample only contains silanol groups. The presence of T and M signals indicate high organic loading. However, in this case, no M signals which are related to silicon atoms of the alkoxysilane [SiO(CH<sub>3</sub>)<sub>3</sub>] are present in the NMR spectra. In conclusion, it could be stated that the amine and thiol functionalization were successful [11].

## 5. 9. UV ANALYSIS

### 5. 9. 1. AMOXICILLIN LOADING

The calibration plot was plotted using the results obtained by the absorbance measurements of the prepared standard solutions (Table - 13). Thus, the percentage of the amoxicillin loading was calculated by using the equation obtained from the calibration plot. The slope of the graph is equal to the molar absorptivity coefficient ( $A=\epsilon.b.c$ ,  $b = 1\text{cm}$  {3}).

**Table - 13: Amount of amoxicillin used to prepare standard solutions**

Concentration	0.003125 M	0.00625 M	0.0125 M	0.025 M	0.05 M
Weight	0.0057 g	0.0114 g	0.0228 g	0.0457 g	0.0914 g
Volume	5 ml	5 ml	5 ml	5 ml	5 ml

1 ml of solution was taken from each sample for the UV analysis. Then, the sample solutions were diluted to 5 ml by using excess distilled water. The measurements were recorded between 200 - 800 nm. The absorbance values at 272 nm were used for the calculation of the concentration change of amoxicillin.

**Table - 14: % Weight of amoxicillin loaded to SBA - 15 samples**

Sample	Pure	1A	2A	4A	1M	2M	4M	1T	2T	4T
% Loaded amoxicillin	22.3	20.7	22.1	18.3	27.2	21.5	20.8	27.5	22.9	23.8

The UV analysis for the loading part was completed twice and the average values are given in Table - 14. According to the results, the maximum loading capacity is 27.5 % which is the 1 ml functionalized sample. However, it is reported in an article that the maximum loading capacity of amoxicillin using SBA - 15 materials is 24 % [40]. Thus, it could be stated that by functionalizing the surface of SBA - 15 materials, the loading capacity could also be enhanced. Therefore, the functionalization process is successful to increase the amount of the drug loaded within the SBA - 15 samples. The values given in Table - 14 indicate that by

grafting the surface with other functional groups the % loaded amoxicillin could either be hindered or enriched. The amine functionalized samples show a slightly lower capacity for amoxicillin which might be attributed to the possible loss of the amine groups from the surface during the loading process. The sample 1A with the highest efficiency of functionalization reveals that the amoxicillin is less attached to the pores of this material. Besides, it could be due to the blockage of the micropores with the amine groups after the functionalization process; and so the adsorption sites become inaccessible [50]. Also, the amoxicillin solution might not be concentrated high enough for better adsorption. Another reason could be the fact that the adsorption might be too low due to the pH and type of medium of the solution. It has been reported that the adsorption of amoxicillin could be enhanced by increasing the pH up to 7. In fact, the adsorption of amoxicillin through the pores of SBA - 15 materials is low in either powder or pellet form [40]. Thus, the pH plays an important role on the loading capacity. In the following figures the loading profile of amoxicillin is illustrated (Figure 51 - 53). The concentration of amoxicillin changes very much until the end of the process. As it could be observed from the plots there is an initial burst within the first four hours. The reason of the alterations is not clearly understood. However, it might be due to the physical attractions between the drug and sample in aqueous medium [28].

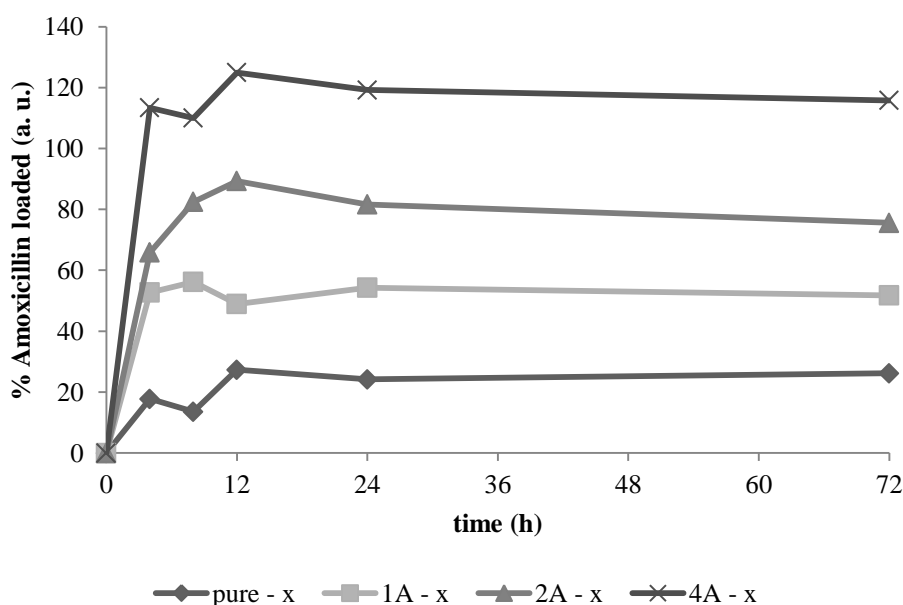


**Figure - 51: Profile of amoxicillin loaded amine functionalized samples**

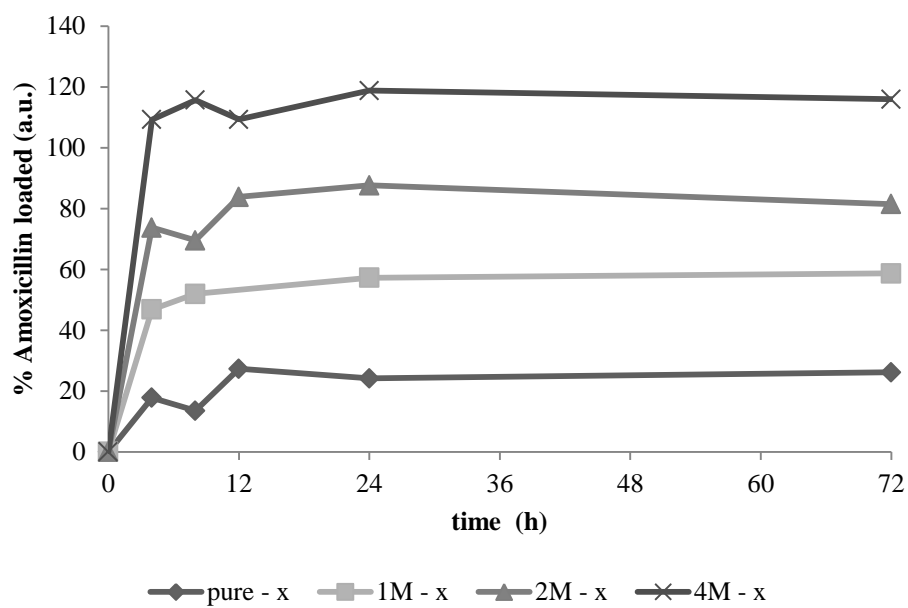


**Figure - 52: Profile of amoxicillin loaded thiol functionalized samples**

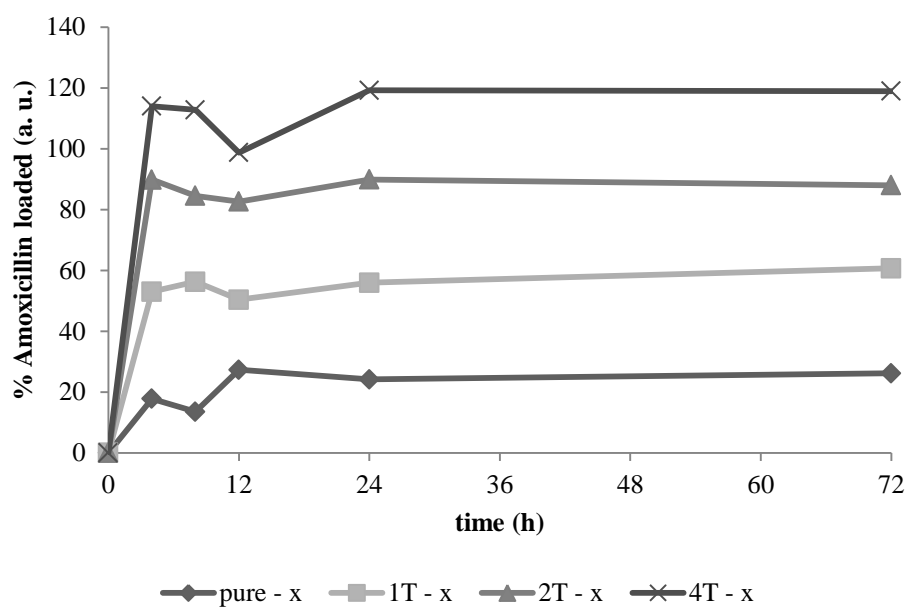


**Figure - 53: Profile of amoxicillin loaded methyl functionalized samples**

## 5. 9. 2. AMOXICILLIN RELEASE

The UV analysis for the release experiments were completed within six hours. For each measurement the same amount of the sample taken for the analysis (1 ml) was replaced with fresh medium of PBS. Therefore, the concentration of each sample was maintained and the analysis is much more adequate. The standard solutions of amoxicillin in PBS were prepared to plot a calibration plot. The slope of the plot was equal to the molar absorptivity coefficient. Thus, the calculations were made based on the value obtained as the slope.

The functional groups of the alkoxy silanes affect the drug delivery depending on their polarity. It is reported that the surface of silica becomes hydrophilic with the 3 - aminopropyl groups while the 3 - mercaptopropyl groups leave the surface slightly less hydrophilic. Therefore, the interactions between the mesoporous silica and amoxicillin would cause difference in terms of the loading capacity and the release rate [63]. According to Figure - 54, Figure - 55 and Figure – 56 the release of amoxicillin could be controlled by using a drug delivery system such as SBA - 15 particles. The maximum release (initial burst) is within the first half an hour and it could be sustained in the following six hours. Therefore, pure and functionalized SBA - 15 particles are a promising system for the control of amoxicillin release.

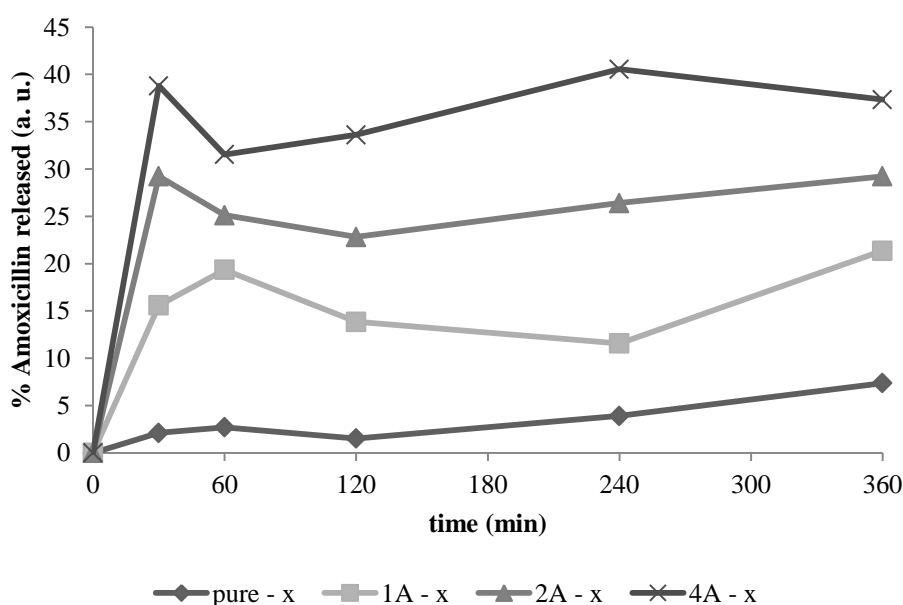


Figure - 54: Amoxicillin release profile of pure and amine functionalized samples

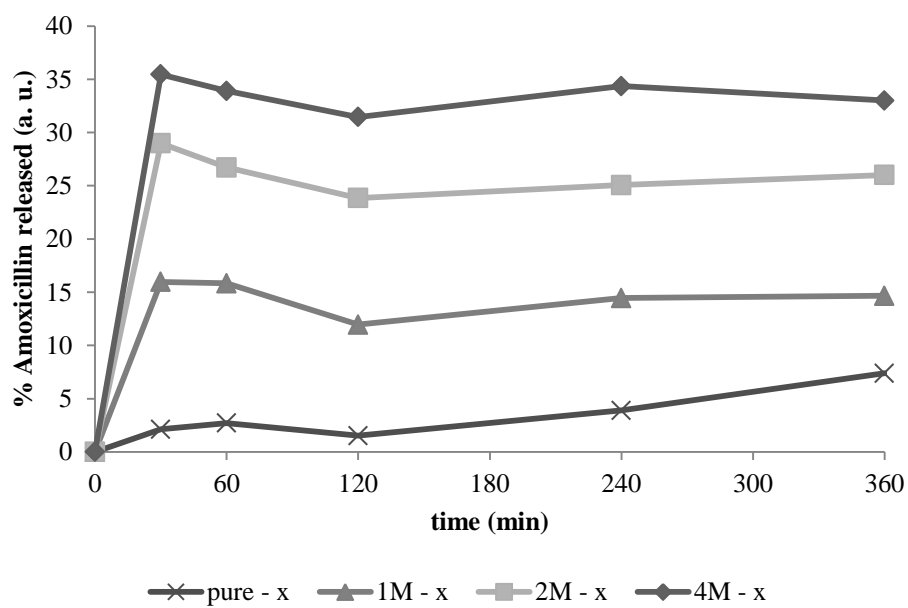


Figure - 55: Amoxicillin release profile of pure and thiol functionalized samples

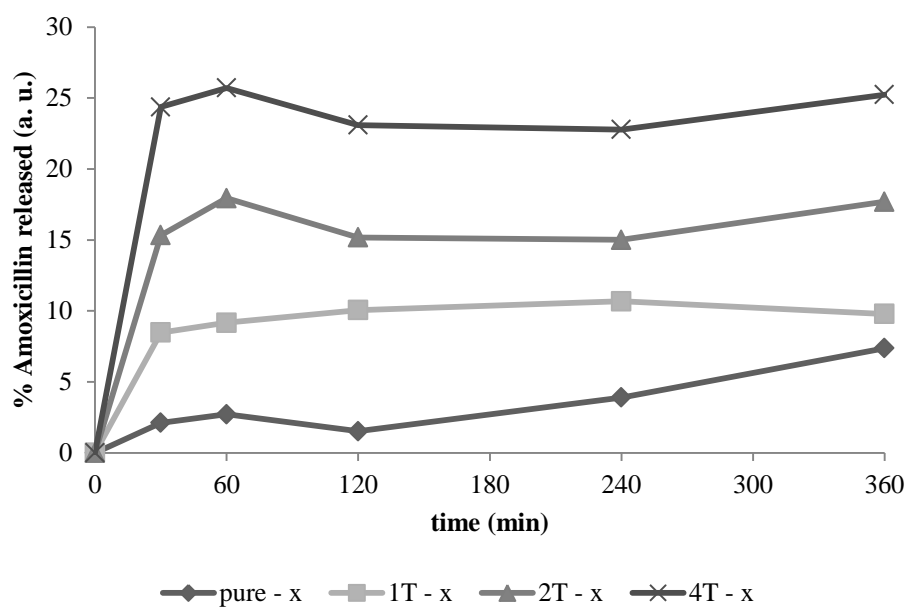
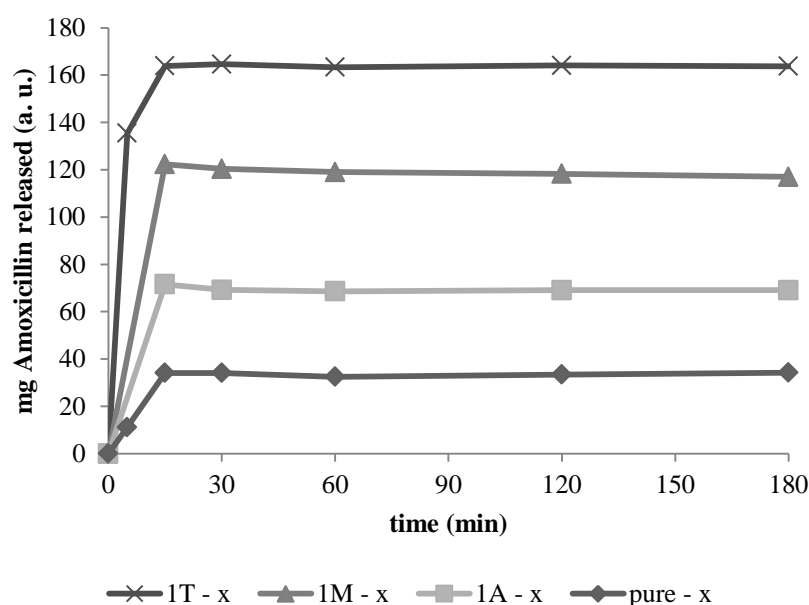


Figure - 56: Amoxicillin release profile of pure and methyl functionalized samples

## 5. 10. HPLC ANALYSIS

The retention time of each sample was between 1.5 and 1.8 minutes. Each of the samples were centrifuged at 11000 rpm for 5 minutes prior to the measurement. The peak heights of the chromatograms within the three hour measurement were similar to each other. Therefore, the peak area values obtained from the chromatograms were used to plot a graph indicating the release of amoxicillin (Figure - 57).



**Figure - 57: Amoxicillin release (in mg) from samples pure SBA - 15, 1A, 1M and 1T**

Table - 15 illustrates the retention times and peak areas obtained from the chromatograms within different time intervals while Table - 16 indicates the peak heights of each sample.

The HPLC method is very useful to obtain information about the release profile of amoxicillin. However, this characterization was only recorded for the pure and 1 ml functionalized samples. In addition, there are very few reports in the literature that have used HPLC method for the release measurements [40, 64]. In conclusion, it could be stated that the release of amoxicillin could be sustained and SBA - 15 particles are promising drug delivery systems to be used in controlled delivery.

**Table -15: The change in peak area of the chromatograms within 3 hours of amoxicillin release**

Samples	$t_{ret}$	Pure - x	$t_{ret}$	1A - x	$t_{ret}$	1M - x	$t_{ret}$	1T - x
5 min	1.823	6320.16	1.715	12531.97	1.580	11561.95	1.648	5379.26
15 min	1.540	10131.57	1.562	10540.26	1.568	10664.97	1.522	10085.96
30 min	1.552	10131.51	1.568	10146.46	1.568	10332.36	1.563	10215.60
60 min	1.540	9855.06	1.528	10049.33	1.548	10107.32	1.515	9999.99
120 min	1.528	10012.60	1.712	10119.46	1.528	9987.28	1.523	10126.72
180 min	1.530	10153.12	1.540	10119.89	1.523	9770.87	1.537	10061.11

**Table -16: The change in peak height of the chromatograms within 3 hours of amoxicillin release**

Samples	$t_{ret}$	Pure - x	$t_{ret}$	1A - x	$t_{ret}$	1M - x	$t_{ret}$	1T - x
5 min	1.823	983.925	1.715	1457.689	1.580	1453.158	1.648	1070.166
15 min	1.540	1348.457	1.562	1361.459	1.568	1379.156	1.522	1330.953
30 min	1.552	1344.233	1.568	1344.114	1.568	1364.735	1.563	1350.698
60 min	1.540	1336.526	1.528	1343.329	1.548	1353.854	1.515	1318.228
120 min	1.528	1353.533	1.712	1364.074	1.528	1349.914	1.523	1367.502
180 min	1.530	1326.403	1.540	1303.758	1.523	1317.184	1.537	1301.123

## CHAPTER 6

### CONCLUSION

The surfaces of the synthesized SBA - 15 samples were functionalized using different concentrations of different types of alkoxy silanes using post - grafting synthesis. The results of the analyses demonstrate that the synthesis route of the surface functionalization was successful. The samples were grafted with primary amine, organothiol and methyl groups by using APTES, MPTMS and TEMS, respectively.

The characterizations of the samples were completed both after the surface functionalization process and after the amoxicillin loading. The percent efficiency of the functionalization of each sample was calculated using the results of the elemental analysis. In addition, the percentage weight losses of the 1 ml functionalized samples were analyzed using TGA. The expected percentage weight losses were always higher than the obtained values which could be attributed to the functionalization process. The percent efficiency of functionalization of the samples differ depending on the type and concentration of the alkoxy silane being used. The sample SBA - 15 - 1A has the highest efficiency (85 %) among the amine functionalized samples while the sample SBA - 15 - 4M shows the highest efficiency (62.3 %) between the thiol functionalized ones. Although, the efficiency of the methyl functionalized samples are quite different than the other two groups. The sample 1T is the one with the highest efficiency (23 %) in comparison to the other samples. The reason of this could be due to the strong interaction of the amine groups while the methyl groups show a rather weak attraction towards silanol groups.

The powder patterns of the samples prove that the samples have a hexagonal crystal structure. Also, it reveals that neither the functionalization nor the amoxicillin loading could

disrupt the highly ordered structure. The expected diffraction peaks were observed in each SAXS pattern. Therefore, the chemical and thermal stability of the prepared samples are too high which is due to the thick pore walls. The diffraction peaks of the planes (100), (110) and (200) were present in the SAXS patterns. However, it was not possible to observe the diffraction peak with the highest intensity indexed as (100) in the powder XRD patterns. The only diffraction peaks that could be observed were the less intense peaks indexed as (110) and (200). The SAXS patterns gave information about the d - spacing values that were about 10.5 nm. Because the most intense peak (100) was not seen in the powder XRD patterns these values were not compared with the SAXS results. Therefore, the d - spacings related to the less intense peaks were compared. The d - spacings of the XRD results were between 4.9 and 5.4 nm while the values related to the SAXS results were between 5.8 and 6.3 nm. The d - spacing values were calculated according to the peaks at the plane (110). Also, these values were compared with amoxicillin loaded samples. The values of the peaks (200) were in the range of 4.4 and 4.6 nm. According to the values calculated from the powder XRD patterns, there was no significant change between the results.

The FTIR spectra of the samples are similar to each other therefore the effect of surface functionalization could not be explained using the slight differences. In comparison the pure SBA - 15 sample, the amine functionalized samples possess an additional peak at  $1555\text{ cm}^{-1}$  due to the  $\text{COO}^- - \text{NH}_3^+$  interaction. It is known that IR adsorption bands related to the stretching vibrational mode of the silanol groups present on the surface are observed in the range  $3740 - 3500\text{ cm}^{-1}$ . The remaining silanol groups on the pore surface (after the calcination process) appear in the spectrum as a broad band at  $3500 - 3000\text{ cm}^{-1}$  while the NH stretching bands are also observed at  $3380 - 3310\text{ cm}^{-1}$ . In all of the FTIR spectra related to the amoxicillin loaded samples a peak at  $1600\text{ cm}^{-1}$  is observed indicating the amine group of amoxicillin. Therefore, it is proven that the amoxicillin loading was successful.

The pore size, pore volume and surface area of each sample were characterized by  $\text{N}_2$  - adsorption - desorption analysis. In addition, the pore size distribution was calculated using BJH method. And so, the BET isotherms of the samples in the same group were plotted on the same graph for comparison. In fact, the effect of the concentration and the type of alkoxy silane were differentiated by comparing the pore size, pore volume and surface area

values. In contrast to the unmodified samples, generally after the functionalization and amoxicillin loading; the surface area, pore size and pore volume became smaller. In addition, the pore size distribution of the samples was between 4.5 and 7.0 nm. The pore size distribution became narrower even after the loading process.

The TEM images confirmed the hexagonal crystal structure composed of one - dimensional channels. Besides, it was verified that the porous structure was not disrupted after the post - grafting synthesis. Furthermore, the pore distances of the samples were roughly calculated using the TEM micrographs which vary between 7 and 10 nm.

The solid - state  $^{29}\text{Si}$  - MAS - NMR spectra gave information about the presence of silanol groups. The peaks have differed due to the type of functionalization. In comparison to the pure sample the main peak of interest is divided at - 120 ppm. The amine and thiol functionalized samples both have an additional peak at - 80 ppm due to the stronger interaction between silica and the alkoxy silane (Si - C linkages). Besides, this additional broader peak is not present in the NMR spectra of the methyl functionalized sample. According to the NMR spectrum, the amine and thiol functionalized samples are successfully grafted while the pure sample contains residual silanol groups.

The elemental analysis gave information about the loaded amount of amoxicillin within the samples 1A and 1M. Although, it was not possible to obtain information about the pure and 1T samples due to the very low amount of amoxicillin incorporation. Therefore, the amoxicillin loading has been monitored using a UV spectrophotometer. The UV absorbance spectra have been used to calculate the concentration change after three days and to identify the percentage of amoxicillin loaded within each sample. The elemental analysis results were similar to the values obtained from the UV analysis. In addition, the absorbance spectra recorded during the release in different time intervals was used to prepare a plot indicating the release profile. Furthermore, HPLC method was also used to plot the release profile. The results of both analyses established that the release of amoxicillin could be controlled. The release profiles indicate that the release is sustained rather than prolonged. Therefore, SBA - 15 particles are useful to encapsulate amoxicillin and sustain the release in a determined time interval. In fact, the surface functionalization is effective in the loading process. The main

outcome is that the amine functionalized samples show a similar percentage of amoxicillin loading while the other two groups of functionalized samples are not quite similar. In fact, the amount of amoxicillin loaded in the samples 4A and 4M is lower compared to the pure sample. In other words, amoxicillin loading is affected by the organic functional groups on the surface which have been substituted with the silanol groups. In addition, the results of the methyl functionalized samples are better than the other samples in terms of amoxicillin loading.

In conclusion, the loaded amount of amoxicillin is either enhanced or decreased depending on the type and concentration of alkoxy silane used for the post - grafting. Although, the release profiles of the samples are quite similar meaning that the functionalization does not affect the release of amoxicillin.

## REFERENCES

1. Allen, T. (1997). In *Particle size measurement* (Vol. 1, p. 114). London; New York: Chapman and Hall.
2. Meynen, V., Cool, P., & Vansant, E. F. (2009). Verified synthesis of mesoporous materials. *Microporous and Mesoporous Materials*, 125, 170 - 223.
3. Vallet - Regi, M., Balas, F., Colilla, M., & Manzano, M. (2007). Bioceramics and pharmaceuticals: A remarkable synergy. *Solid State Sciences*, 9, 768 - 776.
4. Kresge, C. T., Leonowicz, M. E., Roth, W. J., Vartuli, J. C., & Beck, J. S. (1992). *Nature*, 359, 710 - 712.
5. Vallet - Regi, M., Balas, F., & Arcos, D. (2007). Mesoporous Materials for Drug Delivery. *Angew. Chem. Int. Ed.*, 46, 7548 - 7558.
6. Izquierdo-Barba, I., Martinez, A., Doadrio, A. L., Perez-Pariente, J., & Vallet-Regi, M. (2005). Release evaluation of drugs from ordered three-dimensional silica structures. *European Journal of Pharmaceutical Sciences* , 26, 365 - 373.
7. Zeng, W., Qian, X. - F., Zhang, Y. - B., Yin, J., & Zhu, Z. - K. (2005). Organic modified mesopores MCM - 41 through solvothermal process as drug delivery system. *Materials Research Bulletin*, 40, 766 - 772.

8. Wright, H. H. (2005). Enzymes supported on ordered mesoporous solids: a special case of an inorganic - organic hybrid. *J. Mater. Chem.*, 15, 3690 - 3700.
9. Vallet-Regi, M., Ruiz-Gonzalez, L., Izquierdo-Barba, I., & Gonzalez-Calbet, J. M. (2006). Revisiting silica based ordered mesoporous materials: medical applications. *J. Mater. Chem.*, 16, 26 - 31.
10. Vallet - Regi, M., Balas, F., Colilla, M., & Manzano, M. (2008). Bone - regenerative bioceramic implants with drug and protein controlled capability. *Progress in Solid State Chemistry*, 36, 163 - 191.
11. Garcia, N., Benito, E., Guzman, J., Tiemblo, P., Morales, V., & Garcia, R. A. (2007). Functionalization of SBA-15 by an acid-catalyzed approach: A surface characterization study. *Microporous and Mesoporous Materials*, 106 , 129 - 139.
12. He, Q., Shi, J. C., Wei, C., Zhang, L., Wu, W., Bu, W., et al. (2011). Synthesis of oxygen deficient luminescent mesoporous silica nanoparticles for synchronous drug delivery and imaging. *Chem. Commun.*, 47, 7947 - 7949.
13. He, Q., & Shi, J. (2011). Mesoporous silica nanoparticle based nano drug delivery systems: synthesis, controlled drug release and delivery, pharmacokinetics and biocompatibility. *J. Mater. Chem.*, 21, 5845 - 5855.
14. Rosenholm, J. M., & Lindén, M. (2008). Towards establishing structure - activity relationships for mesoporous silica in drug delivery applications. *Journal of Controlled Release*, 128, 157 - 164

15. Shi, X., Wang, Y., Ren, L., & N., Z. (2009). Novel mesoporous silica - based antibiotic releasing scaffold for bone repair. *Acta Biomaterialia*, 5, 1697 - 1707.
16. Izquierdo-Barba, I., Colilla, M., Manzano, M., & Vallet-Regí, M. (2010). In vitro stability of SBA-15 under physiological conditions. *Microporous and Mesoporous Materials*, 132 , 442 - 452.
17. de Sousa, A., Maria, D. A., de Sousa, R. G., & de Sousa, E. M. (2010). Synthesis and characterization of mesoporous silica/poly(N-isopropylacrylamide) functional hybrid useful for drug delivery. *J Mater Sci*, 45, 1478 - 1486.
18. Lebeau, B., Gaslain, F., Fernandez - Martin, C., & Babonneau, F. (2009). In *Ordered Porous Solids* (p. 286). Elsevier B. V.
19. Lebeau, B., Gaslain, F., Fernandez - Martin, C., & Babonneau, F. (2009). In *Ordered Porous Solids* (p. 285). Elsevier B. V.
20. Lebeau, B. G.-M. (2009). In *Ordered Porous Solids* (pp. 287 - 288). Elsevier B. V.
21. Vallet - Regi, M., Colilla, M., & Gonzalez, B. (2011). Medical applications of organic – inorganic hybrid materials within the field of silica - based bioceramics. *Chem. Soc. Rev.*, 40, 596 - 607.
22. Robinson, J. R. (1978). In *Sustained and controlled release drug delivery systems* (p. 3). New York: Marcel Dekker Inc.

23. Santini, J. (2000). Microchips as Controlled Drug Delivery Devices. *Angew. Chem. Int. Ed.*, 39, 2396-2047.
24. Katzung, B. G. (1995). In *Basic and Clinical Pharmacology* (6th ed., p. 66). Norwalk, Conn: Appleton & Lange.
25. Katzung, B. G. (1995). In *Basic and Clinical Pahrmacology* (6th ed., pp. 69 - 71). Norwalk, Conn: Appleton & Lange.
26. Katzung, B. G. (1995). In *Basic and Clinical Pharmacology* (6th ed., pp. 3 - 5). Norwalk, Conn: Appleton & Lange.
27. Shi, Z. G., Guo, Q. Z., Liu, Y. T., Xiao, Y. X., & Xu, L. (2011). Drug delivery devices based on macroporous silica spheres. *Materials Chemistry and Physics*, 126, 826–831.
28. Li, Z., Su, K., Cheng, B., & Deng, Y. (2010). Organically modified MCM-type material preparation and its usage in controlled amoxicillin delivery. *Journal of Colloid and Interface Science*, 342, 607 - 613.
29. Robinson, J. R. (1978). In *Sustained and controlled release drug delivery systems* (pp. 72 - 82). New York: Marcel Dekker Inc.
30. Robinson, J. R. (1978). In *Sustained and controlled release drug delivery systems* (p. 127). New York: Marcel Dekker Inc.

31. Hwang, D. H., Lee, D., Lee, H., Choe, D., Lee, S. H., & Lee, K. (2010). Surface functionalization of SBA-15 particles for ibuprofen delivery. *Korean J. Chem. Eng.*, 27 (4), 1087-1092.
32. Yang, P., Quan, Z., Li, C., Lian, H., Huang, S., & Lin, J. (2008). Fabrication, characterization of spherical CaWO<sub>4</sub>:Ln @MCM-41(Ln = Eu<sup>3+</sup>, Dy<sup>3+</sup>, Sm<sup>3+</sup>, Er<sup>3+</sup>) composites and their applications as drug release systems. *Microporous and Mesoporous Materials*, 116 , 524 - 531.
33. Aerts, C. A., Verraedt, E., Depla, A., Follens, L., Froyen, L., Humbeeck, J. V., et al. (2010). Potential of amorphous microporous silica for ibuprofen controlled release. *International Journal of Pharmaceutics*, 397, 84 - 91.
34. Zhao, Y., Trewyn, B. G., Slowing, I. I., & Lin, V. S.-Y. (2009). Mesoporous Silica Nanoparticle-Based Double Drug Delivery System for Glucose-Responsive Controlled Release of Insulin and Cyclic AMP. *J. Am. Chem. Soc.*, 131, 8398 - 8400.
35. Liu, J., Jiang, X., Ashley, C., & Brinker, C. J. (2009). Electrostatically Mediated Liposome Fusion and Lipid Exchange with a Nanoparticle-Supported Bilayer for Control of Surface Charge, Drug Containment, and Delivery. *J. Am. Chem. Soc.*, 131, 7567 - 7569.
36. Wang, L. -S., Wu, L. -C., Lu, S. -Y., Chang, L. -L., Teng, I. -T., Yang, C. M., et al. (2010). Biofunctionalized Phospholipid - Capped Mesoporous Silica Nanoshuttles for Targeted Drug Delivery: Improved Water Suspensibility and Decreased Nonspecific Protein Binding. *ACS Nano*, 4 (8), 4371 - 4379.

37. Piscitelli, S. C., & Rodvold, K. (2005). In *Drug interactions in infectious diseases* (2nd ed., p. 151) Totowa: Humana Press.
38. Egorov, N. S. (1985). In *Antibiotics: a scientific approach* (p. 12). Moscow: Mir Publishers.
39. Franklin, T. J., & Snow, G. A. (2005). In *Biochemistry and molecular biology of antimicrobial drug action* (p. 23). New York: Springer.
40. Vallet-Regí, M., Doadrio, J. C., Doadrio, A. L., Izquierdo-Barba, I., & Pérez-Pariante, J. (2004). Hexagonal ordered mesoporous material as a matrix for the controlled release of amoxicillin. *Solid State Ionics*, 172, 435 - 439.
41. Katzung, B. G. (1995). In *Basic and Clinical Pharmacology* (6th ed., p. 35). Norwalk, Conn: Appleton & Lange.
42. Joshy, M. I., Elayaraja, K., Suganthi, R. V., Veerla, S. C., & Kalkura, S. N. (2011). In vitro sustained release of amoxicillin from lanthanum hydroxyapatite nano rods. *Current Applied Physics*, 11 (4), 1100-1106.
43. Gallagher, J. C. (2008). In *Antibiotics: simplified* (pp. 34-38). Jones and Bartlett Publishers.
44. Wang, J., Liu, Q., Zhang, G., Li, Z., Yang, P., Jing, X., et al. (2009). Synthesis, sustained release properties of magnetically functionalized organic-inorganic materials: Amoxicillin anions intercalated magnetic layered double hydroxides via calcined precursors at room temperature. *Solid State Sciences*, 11 , 1597 - 1601.

45. Zhao, D., Huo, Q., Feng, J., Chmelka, B. F., & Stucky, G. D. (1998). Nonionic Triblock and Star Diblock Copolymer and Oligomeric Surfactant Syntheses of Highly Ordered, Hydrothermally Stable, Mesoporous Silica Structures. *J. Am. Chem. Soc.*, *120*, 6024-6036.
46. Lee, K., Lee, D., Lee, H., Kim, C. K., Wu, Z., & Lee, K. (2010). Comparison of amine - functionalized mesoporous silica particles for ibuprofen delivery. *Korean J. Chem. Eng.*, *27* (4), 1333-1337.
47. Song, S. W., Hidajat, K., & Kawi, S. (2005). Functionalized SBA-15 Materials as Carriers for Controlled Drug Delivery: Influence of Surface Properties on Matrix-Drug Interactions. *Langmuir*, *21*, 9568-9575.
48. Cullity, B. D. (1956). In *Elements of X-ray diffraction* (pp. 303 - 304). Reading, Mass.: Addison-Wesley Pub. Co.
49. Glatter, O., & Kratky, O. (1982). In *Small Angle X-ray Scattering*. London: Academic Press Inc.
50. Szegedi, A., Popova, M., Goshev, I., Mihály, J., (2011). Effect of amine functionalization of spherical MCM - 41 and SBA - 15 on controlled release. *Journal of Solid State Chemistry*, *184*, 1201 – 1207
51. Y. Xu, et al., Improving adsorption and activation of the lipase immobilized in amino-functionalized ordered mesoporous SBA-15, *Solid State Sciences* (2011), doi:10.1016/j.solidstatesciences.2011.03.003

52. Allen, T. (1997). In *Particle size measurement* (Vol. 1, pp. 104 - 105). London; New York: Chapman and Hall.
53. Rosenholm, J. M., Penninkangas, A., & Linden, M. (2006). Amino-functionalization of large-pore mesoscopically ordered silica by a one-step hyperbranching polymerization of a surface-grown polyethyleneimine. *Chem. Commun.* , 3909 - 3911.
54. Allen, T. (1997). In *Particle size measurement* (Vol. 1, pp. 108 - 109). London, New York: Chapman and Hall.
55. Duer, M. J. (2002). In *Solid-state NMR spectroscopy: principles and applications*. Malden, MA: Blackwell Science.
56. Lippma, E., Magi, M., Samoson, A., Engelhardt, G., & Grimmer, A. R. (1980). Structural Studies of Silicates by Solid-state High-Resolution  $^{29}\text{Si}$  NMR. *J. Am. Chem. Soc.*, 102 (15), 4889-4893.
57. Yang, L. M., Wang, Y. J., Luo, G. S. & Dai, Y. Y. (2005). Functionalization of SBA-15 mesoporous silica with thiol or sulfonic acid groups under the crystallization conditions. *Microporous and Mesoporous Materials*, 84, 275 - 282
58. Luan, Z., Fournier, J. A., Wooten, J. B., Miser, D. E. & Chang, M. J. (2005). Functionalized mesoporous SBA-15 silica molecular sieves with mercaptopropyl groups: Preparation, characterization and application as adsorbents. *Studies in Surface Science and Catalysis*, 156, 897 - 906
59. Guzmán-Castillo, M.L., Pérez-Romo, P., Armendáriz-Herrera, H., Hernández-Beltrán, F., Tobón-Cervantes, A., López, C., Fripiat, J. & Pérez-Pariente, J. (2005).  $^{29}\text{Si}$  MAS-NMR study of the silica condensation in the synthesis of mesoporous materials. *Studies in Surface Science and Catalysis*, 158, 455 - 460

60. Liu, Y.- H., Lin, H. - P., Mou, C. - Y. (2004). Direct Method for Surface Silyl Functionalization of Mesoporous Silica. *Langmuir*, 20, 3231 - 3239
61. Herledan-Semmer, V., Dakhlaoui, S., Guenneau, F., Haddad, E. & Gedeon, A. (2004). SPECTROSCOPIC EVIDENCE OF SBA-15 MESOPOROUS SOLIDS FUNCTIONALIZATION. *Studies in Surface Science and Catalysis*, 154, 1519 - 1524
62. Palkovits, R., Yang, C. -M., Olejnik, S., & Schüth, F. (2006). Active sites on SBA-15 in the Beckmann rearrangement of cyclohexanone oxime to  $\epsilon$ -caprolactam. *Journal of Catalysis*, 243, 93 - 98.
63. Vathyam, R., Wondimu, E., Das, S., Zhang, C. Hayes, S., Tao, Z., Asefa, T. (2011). Improving the Adsorption and Release Capacity of Organic - Functionalized Mesoporous Materials to Drug Molecules with Temperature and Synthetic methods. *J.Phys.Chem. C.*, 115, 13135 - 13150
64. Doadrio, A. L., Sousa, E. M., Doadrio, J. C., Pariente, J. P., Izquierdo-Barba, I., & M., V.-R. (2004). Mesoporous SBA-15 HPLC evaluation for controlled gentamicin drug delivery. *Journal of Controlled Release*, 97, 125 - 132.

## APPENDIX A

### CHROMATOGRAMS (HPLC ANALYSIS)

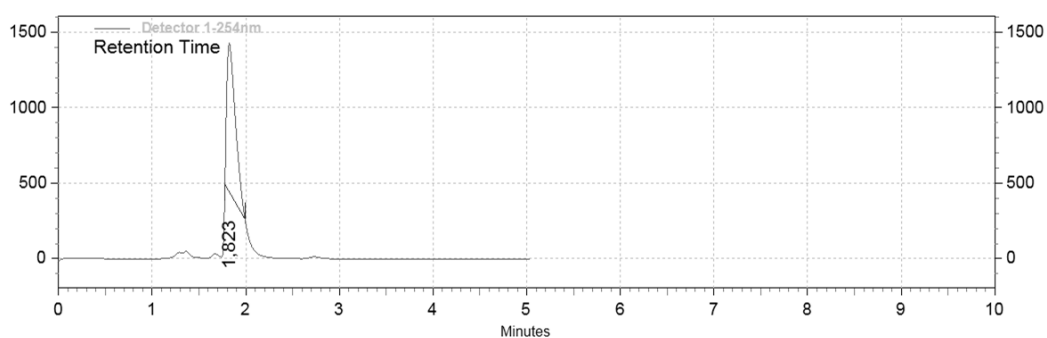


**Figure - 59: Amoxicillin release of pure SBA - 15 after 5 minutes**

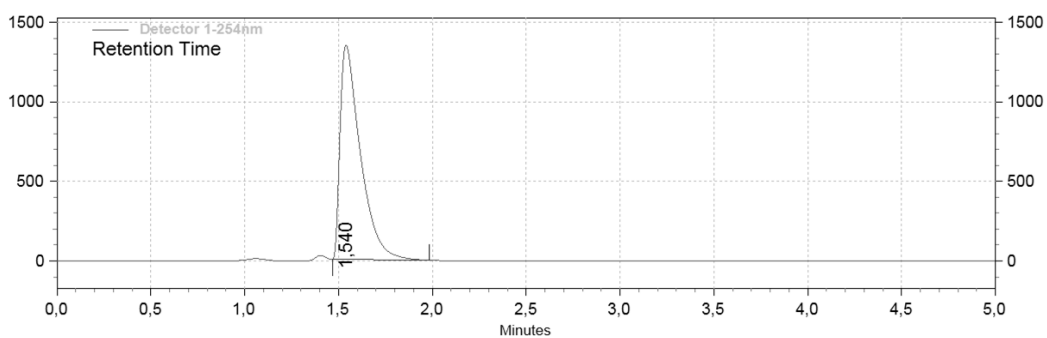


**Figure - 60: Amoxicillin release of pure SBA - 15 after 15 minutes**

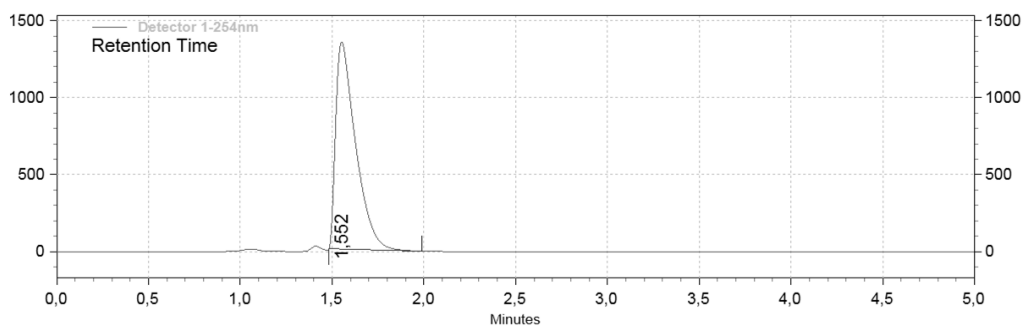


**Figure - 61: Amoxicillin release of pure SBA - 15 after 30 minutes**

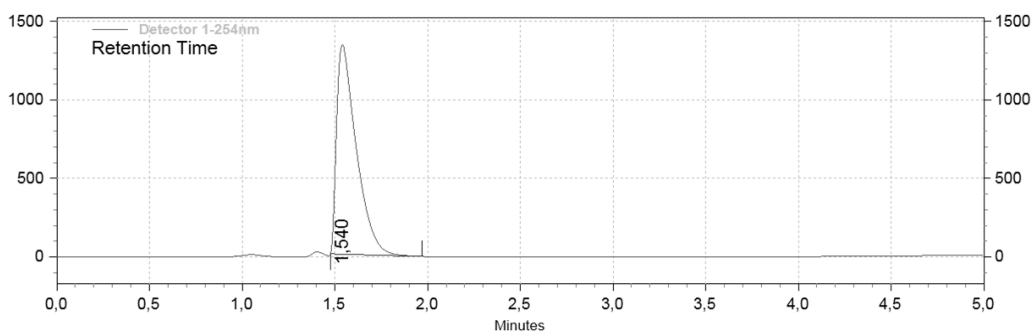


**Figure - 62: Amoxicillin release of pure SBA -15 after 60 minutes**

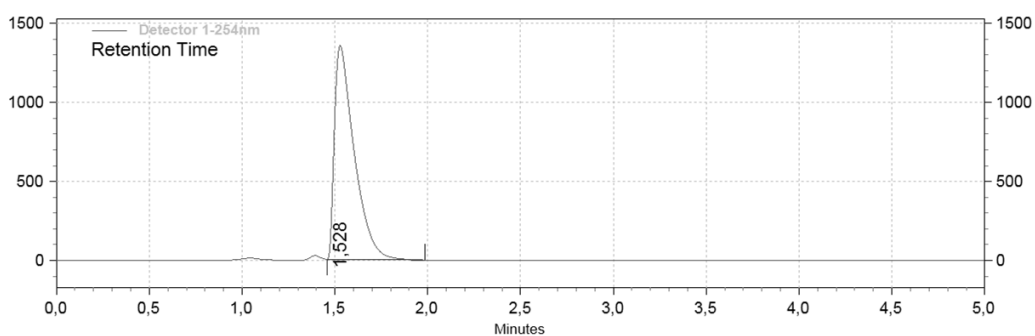


**Figure - 63: Amoxicillin release of pure SBA - 15 after 120 minutes**

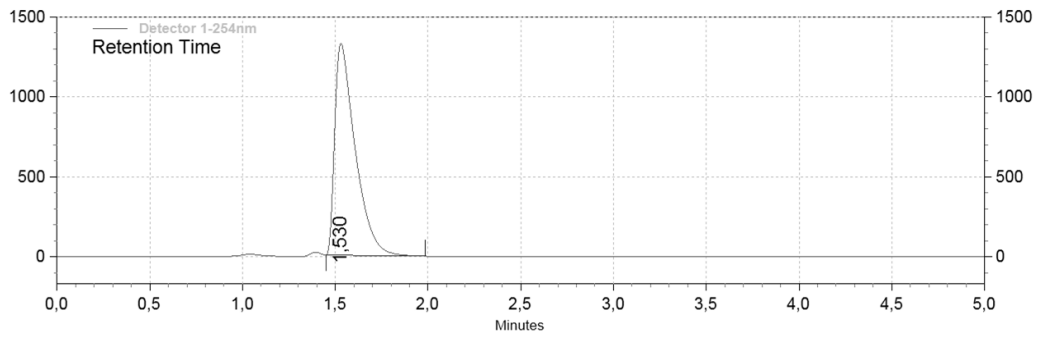


**Figure - 64: Amoxicillin release of pure SBA - 15 after 180 minutes**

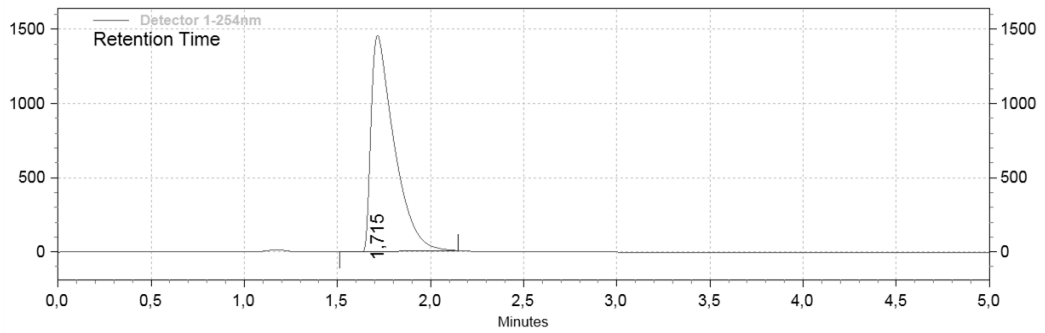


**Figure - 65: Amoxicillin release of SBA - 15 - 1A after 5 minutes**

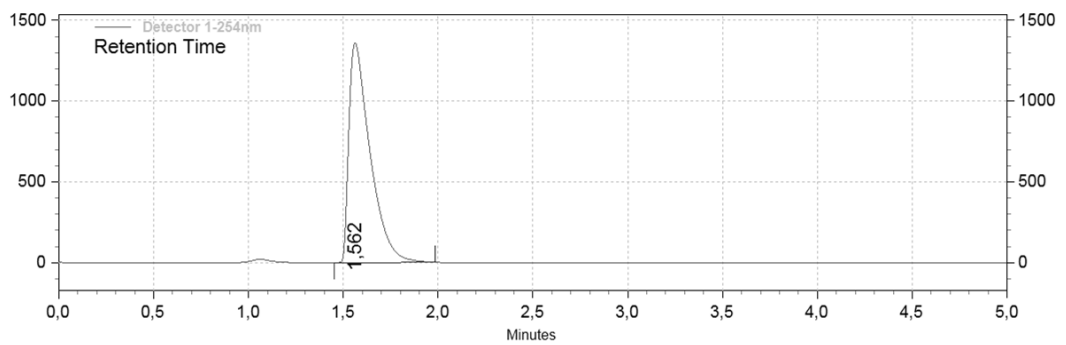


**Figure - 66: Amoxicillin release of SBA - 15 - 1A after 15 minutes**

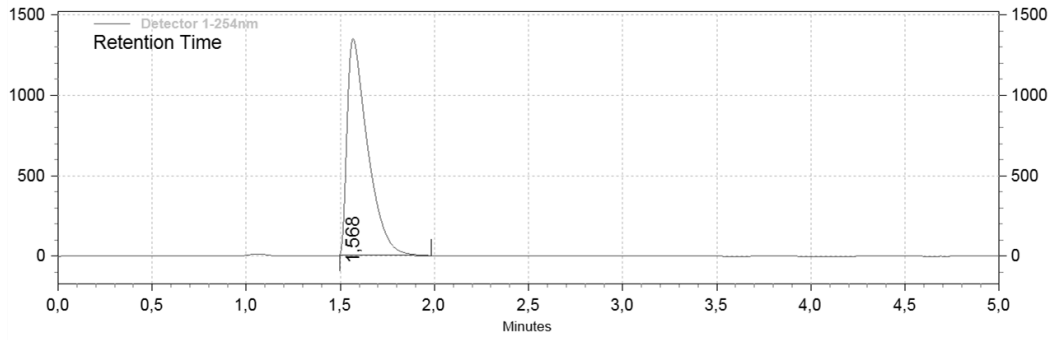


**Figure - 67: Amoxicillin release of SBA - 15 - 1A after 30 minutes**

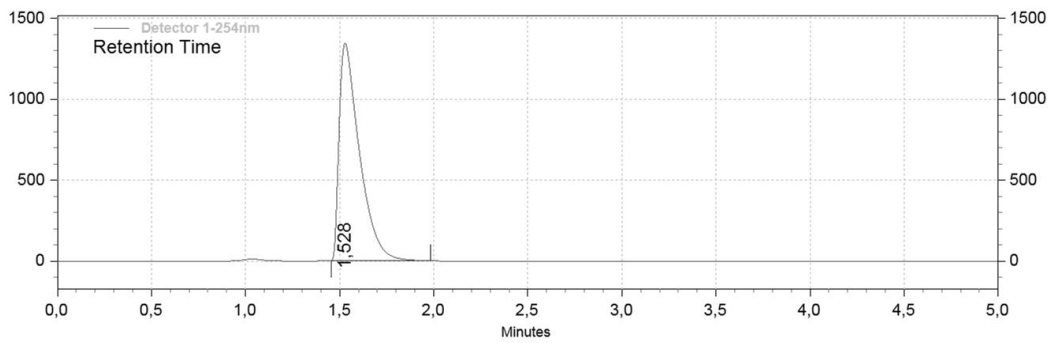


**Figure - 68: Amoxicillin release of SBA - 15 - 1A after 60 minutes**

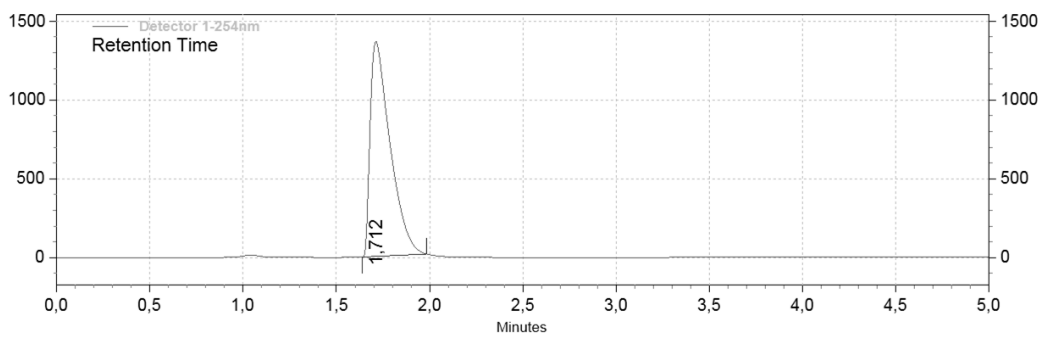


**Figure - 69: Amoxicillin release of SBA - 15 - 1A after 120 minutes**

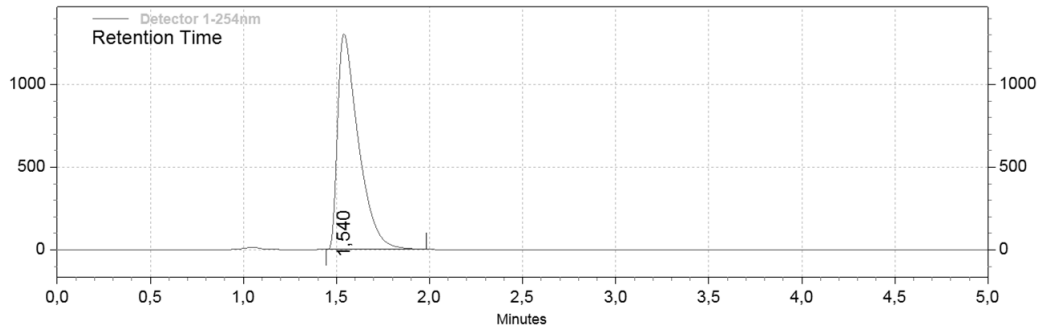


**Figure - 70: Amoxicillin release of SBA - 15 - 1A after 180 minutes**

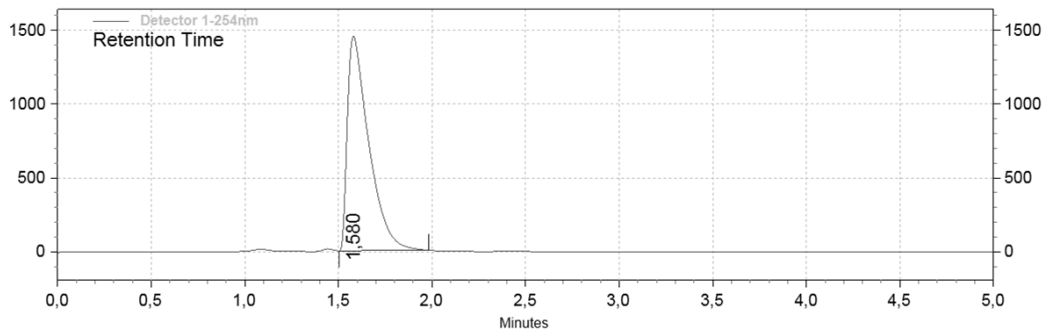


**Figure - 71: Amoxicillin release of SBA - 15 - 1M after 5 minutes**

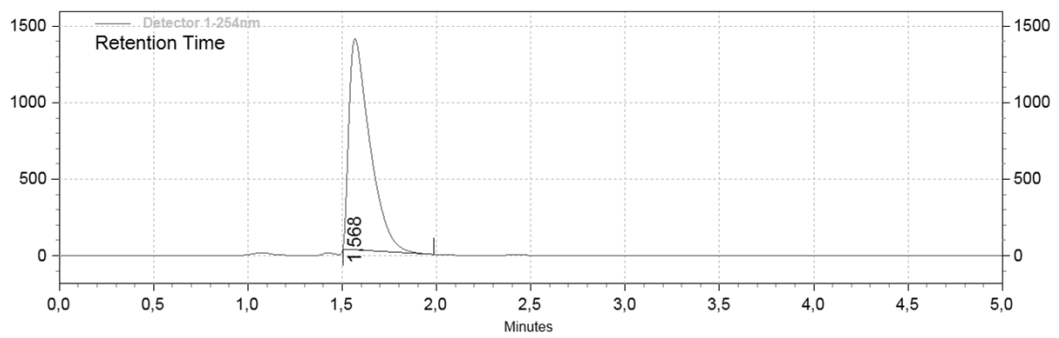


**Figure - 72: Amoxicillin release of SBA - 15 - 1M after 15 minutes**

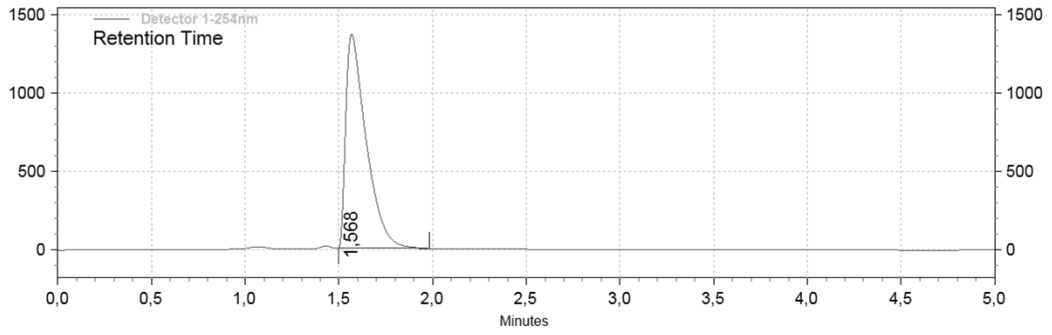


**Figure - 73: Amoxicillin release of SBA - 15 - 1M after 30 minutes**

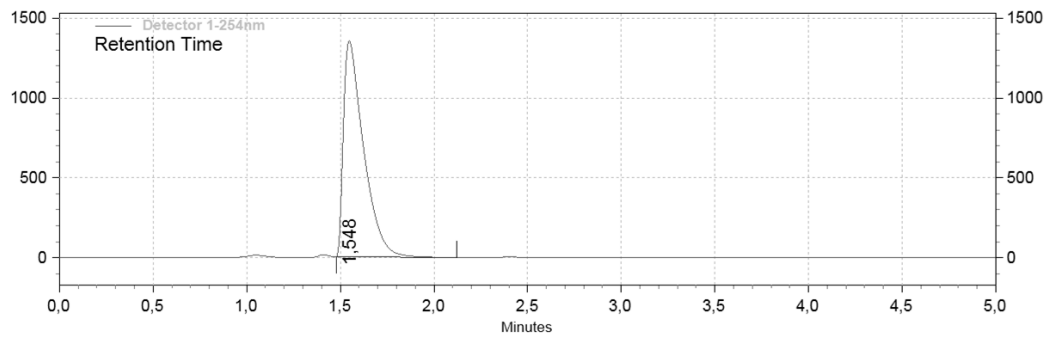


**Figure - 74: Amoxicillin release of SBA - 15 - 1M after 60 minutes**

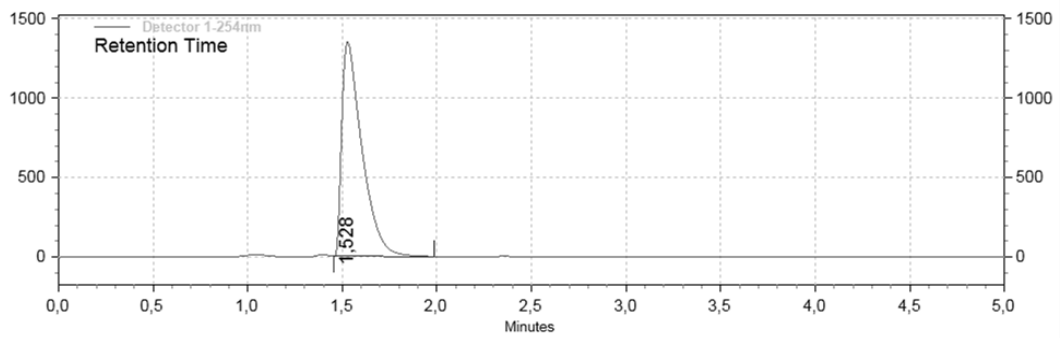


**Figure - 75: Amoxicillin release of SBA - 15 - 1M after 120 minutes**

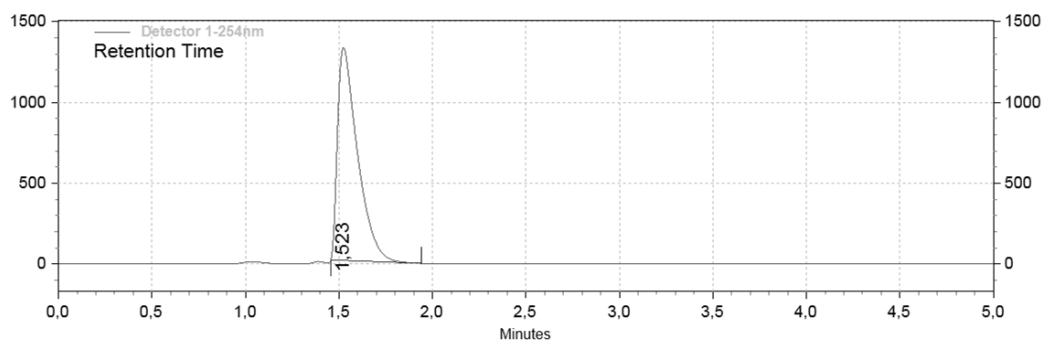


**Figure - 76: Amoxicillin release of SBA - 15 - 1M after 180 minutes**

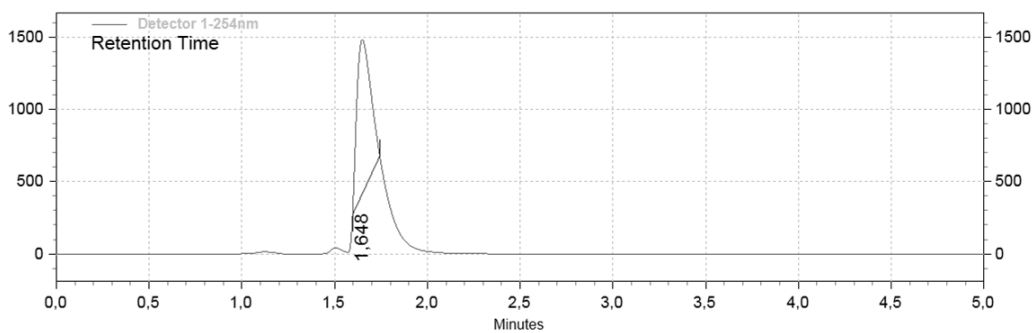


**Figure - 77: Amoxicillin release of SBA - 15 - 1T after 5 minutes**

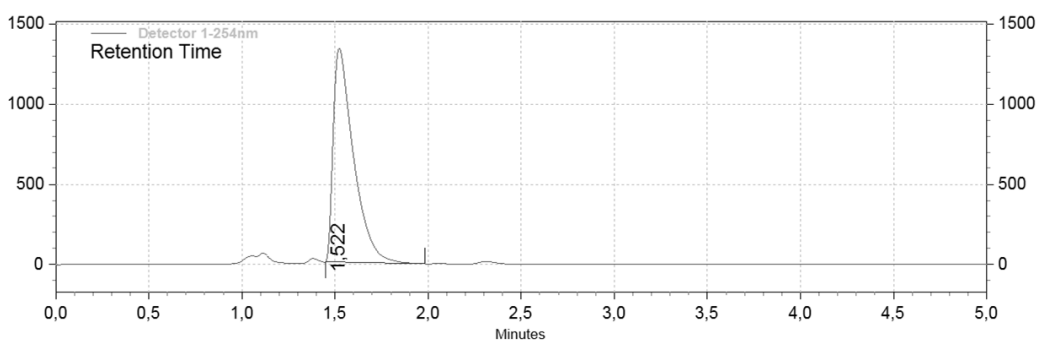


**Figure - 78: Amoxicillin release of SBA - 15 - 1T after 15 minutes**

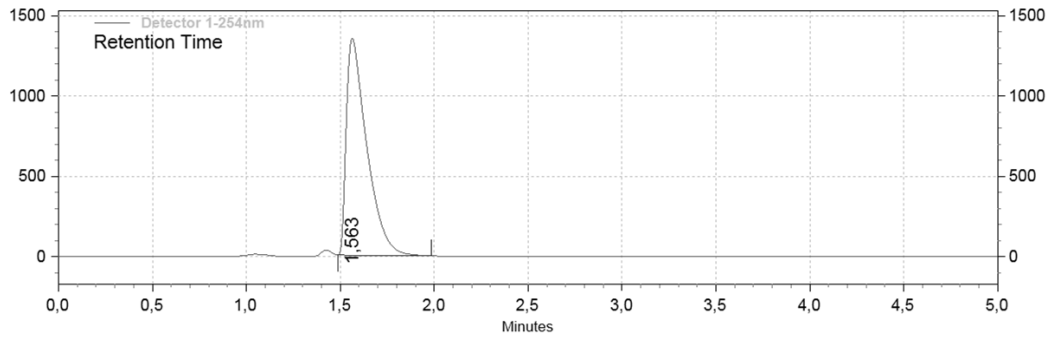


**Figure - 79: Amoxicillin release of SBA - 15 - 1T after 30 minutes**

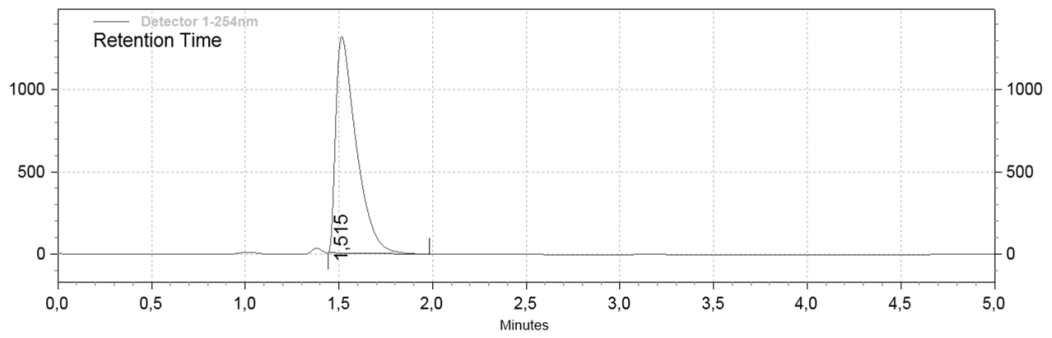


**Figure - 80: Amoxicillin release of SBA - 15 - 1T after 60 minutes**

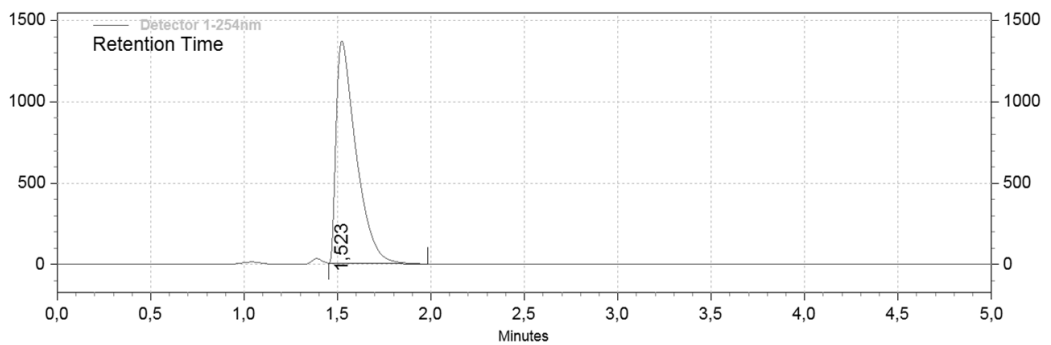


**Figure - 81: Amoxicillin release of SBA - 15 - 1T after 120 minutes**

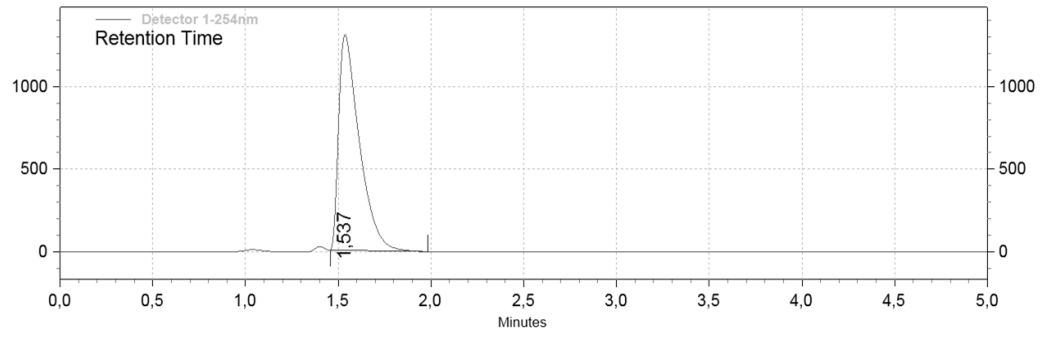


**Figure - 82: Amoxicillin release of SBA - 15 - 1T after 180 minutes**